AD-A058 637 OKLAHOMA STATE UNIV STILLWATER COLL OF ENGINEERING F/G 21/7
IMPROVED ENGINE PERFORMANCE THROUGH HEAT TRANSFER CONTROL.(U)
JUL 78 R G MURRAY DAAG29-76-G-0263
UNCLASSIFIED ARO-14099.2-EX NL

1 OF 2
AD
A058637

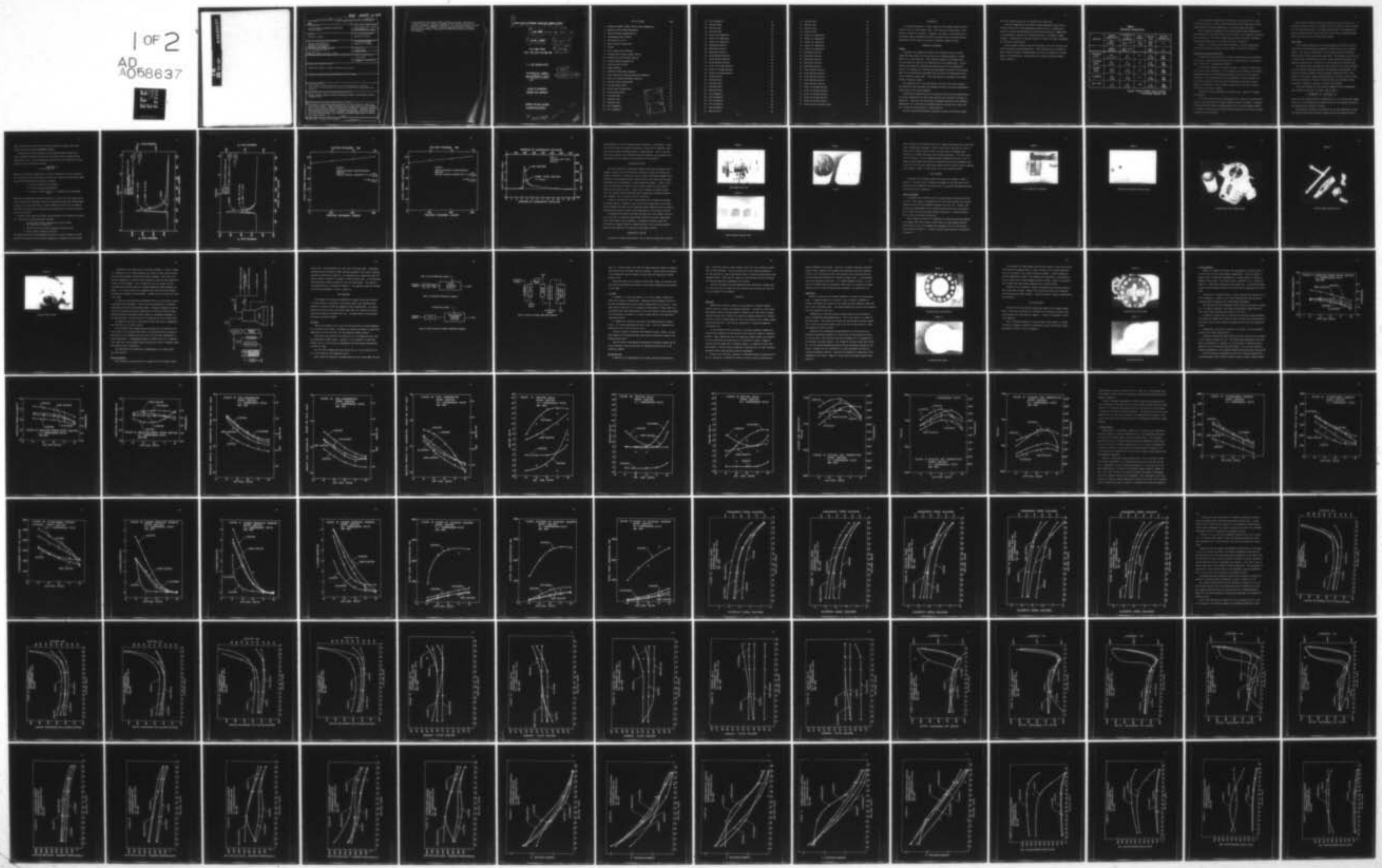

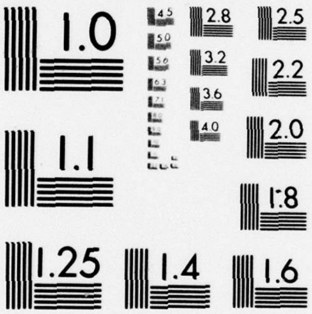

MICROCOPY RESOLUTION TEST CHART
NATIONAL BUREAU OF STANDARDS-1963-A

ARO 14099.2-EX

REPORT DOCUMENTATION PAGE

RUCTIONS
BEFORE COMPLETING FORM

1. REPORT NUMBER
~~1001~~

2. GOVT ACCESSION NO.

3. RECIPIENT'S CATALOG NUMBER

4. TITLE (and Subtitle)
Improved Engine Performance Through Heat Transfer Control

5. TYPE OF REPORT & PERIOD COVERED
Final Report from 1 June 76 to 30 June 78

6. PERFORMING ORG. REPORT NUMBER

7. AUTHOR(s)
Richard G. Murray

8. CONTRACT OR GRANT NUMBER(s)
DAA G29-76-G-0263

9. PERFORMING ORGANIZATION NAME AND ADDRESS
College of Engineering ✓
Oklahoma State University
Stillwater, OK 74074

10. PROGRAM ELEMENT, PROJECT, TASK AREA & WORK UNIT NUMBERS
Project No. P-14099-E

11. CONTROLLING OFFICE NAME AND ADDRESS
U. S. Army Research Office
P. O. Box 12211
Research Triangle Park, NC 27709

12. REPORT DATE
28 July 1978

13. NUMBER OF PAGES

14. MONITORING AGENCY NAME & ADDRESS (if different from Controlling Office)

15. SECURITY CLASS. (of this report)
unclassified

15a. DECLASSIFICATION/DOWNGRADING SCHEDULE

16. DISTRIBUTION STATEMENT (of this Report)

Approved for public release; distribution unlimited.

17. DISTRIBUTION STATEMENT (of the abstract entered in Block 20, if different from Report)

18. SUPPLEMENTARY NOTES

The findings in this report are not to be construed as an official Department of the Army position, unless so designated by other authorized documents.

19. KEY WORDS (Continue on reverse side if necessary and identify by block number)

Ceramic coating, engine, insulated combustion chamber, semi-adiabatic engine, zirconium oxide

20. ABSTRACT (Continue on reverse side if necessary and identify by block number)

The advance of technology requires engines to be more efficient, weight less, and be more reliable. Common materials used for engine parts are not designed close to their thermal limit for strength and lubrication. Additional component loading necessarily will demand a corresponding increase in component cooling. This increased cooling not only represents a thermodynamic loss that detracts from cycle efficiency but it also consumes additional engine power to operate the cooling system.

-over-

DD FORM 1 JAN 73 1473 EDITION OF 1 NOV 65 IS OBSOLETE

Unclassified

A new approach to the thermal loading problem is to apply a thin layer of a ceramic insulator to combustion chamber surfaces thereby reducing heat transfer and metallic component temperature. The following document describes the results of a test program to evaluate engine performance for engines having ceramic coatings. Both spark and compression ignition performance was examined.

⑥

IMPROVED ENGINE PERFORMANCE THROUGH HEAT TRANSFER CONTROL.

⑨

FINAL REPORT. 1 Jun 76 - 30 Jun 78,

⑩ RICHARD G. MURRAY

⑪ 28 Jul 78

⑫ 111 p.

FOR A GRANT PERIOD
FROM 1 JUNE 1976 TO 30 JUNE 1978

U. S. ARMY RESEARCH OFFICE

⑱ ARO

ARO PROJECT NO. P-14099-E
GRANT NO. DAAG29-76-G-0263
⑮

⑲ 14099.2-EX

COLLEGE OF ENGINEERING
OKLAHOMA STATE UNIVERSITY

APPROVED FOR PUBLIC RELEASE;
DISTRIBUTION UNLIMITED.

78 09 05 137

391 931

LIST OF FIGURES

Page

INTRODUCTION

The following document is a final report for Grant Number DAAG29-76-G-0263 funded by the U.S. Army reserve office. This Project was started June 1, 1976 and had a duration of two years. In general, the scope of this Project was to investigate engine performance and emission characteristics resulting from the application of both ceramic and catalytic combustion chamber surfaces.

THEORETICAL BACKGROUND

Purpose

In general, heat engines are devices that transform a portion of high temperature heat energy into work and reject the remaining energy as a waste product at a lower temerature. Most theoretical engine cycles employ adiabatic processes for expansion and compression of the contained gases. Typical analyses for simplified reciprocating spark-ignition (S-I) and compression ignition (C-I) engines will indicate that approximately two-thirds of the energy input can be theoretically transformed into work while the remaining one-third will be rejected as waste heat. This wasted energy is contained in the exhaust products leaving the engine.

Real engines not only lose approximately one-third of the input energy in the exhaust but they also employ non adiabatic processes that waste approximately another third of the energy supplied.

Since metallic engine parts are in continuous contact with the working fluid at elevated temperature they absorb heat from the fluid and tend to increase in temperature. Structural and lubrication requirements necessitate that component temperature can be controlled to reasonable values by cooling with a heat transfer to either the cooling jacket or lubricating oil.

This heat transfer theoretically represents an energy loss from the engine that could otherwise partially be converted into useful work.

Since the temperature of the metallic engine components results from an intimate contact with a high temperature working fluid it is theoretically possible to control and decrease heat transfer and thus metallic temperatures by incorporating a coating of an insulating material on combustion chamber surfaces. Theoretically if the heat transfer is reduced the engine performance and efficiency should improve.

Several ceramic substances have been developed in the last few years that exhibit excellent insulating properties. These substances can be sprayed on metal surfaces by flame or plasma methods and also can be applied by a device known as a detonation gun. Some properties of various coatings and metals follow in Table 1.

Table I
PHYSICAL PROPERTIES

MATERIAL	THERMAL CONDUCTIVITY	COEFFICIENT OF EXPANSION	BULK DENSITY	SPECIFIC HEAT	MELTING TEMPERATURE
	$\frac{BTU}{hr\ ft\ {}^oF}$	$\frac{in}{in\ {}^oF} \times 10^{-6}$	$\frac{gm}{cm\ 3}$	$\frac{BTU}{\#{}^oF}$	^oF
	$(\frac{cal}{Sec\ cm\ C})$	$(\frac{cm}{cm\ C} \times 10^{-6})$		$(\frac{cal}{cm\ C})$	$({}^oC)$
ZIRCONIUM OXIDE	0.67 (2.77×10^{-3})	5.4 (3 . 0)	5.2	0.175 (6 . 018)	4500 (2482)
ALUMINUM OXIDE	1.58 (0 . 01)	4.1 (2 . 28)	3.3	0.28 (0 . 028)	3600 (1982)
CHROME OXIDE	1.50 (0 . 01)	5.0 (2 . 78)	4.6	0.20 (0 . 020)	3000 (1649)
ALUMINUM	120 (0 . 50)	13.0 (7 . 22)	2.7	0.22 (0 . 022)	1220 (660)
CAST IRON	27 (0 . 11)	6.5 (3 . 61)	7.88	0.11 (0 . 011)	2800 (1538)

SOURCE: "ROKIDE CERAMIC SPRAY COATING",
THE NORTON COMPANY, 1961.

It can therefore be stated that theoretically the application of a relatively thin layer of a ceramic insulating material should reduce heat transfer, reduce metallic structural temperature, and increase engine efficiency.

From a combustion standpoint, the elevated ceramic surface temperature in conjunction with an expected catalytic effect should assist combustion especially for lean mixtures. This factor should enhance preflame reactions and promote better engine performance on low grade fuels for C-I operation.

Finally, it is expected that decreased metallic structural temperatures should allow component redesign to reduce weight and increase reliability.

Coating Selection and Application

As previously mentioned several insulating coatings have been developed in recent years. Among these are aluminum oxide, zirconium oxide, zirconium silicate, chrome oxide, and magnesium aluminate.

To reduce heat transfer in an engine cylinder, two physical coating properties are of prime importance. First, the material must adhere to the metallic subsurface without any significant intersurface stress over a wide range of temperature. This necessitates that the coefficient of thermal expansion of the coating should be of the same order of magnitude as the base structure. Second, it should have as low a thermal conductivity as possible in order to effectively control heat transfer.

Properties of lesser importance are specific heat, compressive strength, and adherence.

Of all the coating materials investigated yttria stabilized zirconium oxide best fits the requirements for engine combustion chamber insulation. Adherence of plasma and flame sprayed zirconium oxide to cast iron and aluminum surfaces is, however, in some cases not good and coating separations will occur if proper techniques are not observed.

Before coating metallic surfaces they should be clean and free of oil. In some cases it may be necessary to preheat cast iron surfaces to expel residual oil from machining processes. To promote good bonding, it is suggested that metallic surfaces be grit blasted and given a flash coat of nickel aluminate before application of the zirconium oxide coating.

Engine Model

A more indepth theoretical study was performed by the author in 1976 to quantify the expected performance changes of insulated versus non-insulated engines. This study was undertaken at the National Aeronautics and Space Administration--Johnson Space Center (NASA-JSC). The outcome of this study was a computer model to predict heat transfer, engine operation parameters, and component temperatures as a function of coating conductivity and thickness.

The model utilized a modified otto cycle analysis with variable specific heats and variable polytropic exponents for compression and expansion. The quantity of exhaust residual, intake properties, compression ratio, bore, stroke, air fuel ratio, engine speed and percent of throttle could be varied. Processes considered in the model included residual gas expansion, intake, compression, combustion, expansion, blowdown, and scavenge.

Cyclic heat transfer was calculated by summation of the instantaneous heat transfer for each unit of engine rotation, (dΘ) or

$$Q = \oint \frac{T_g - T_w}{R} \, d\Theta + 2 \oint \frac{T_g - T_o}{R} \, d\Theta$$

Where T_g is the working fluid bulk temperature, T_w is the cooling water temperature, T_o is the lubricating oil temperature and R is the combined convective and conductive heat transfer resistance.

The convective resistance is controlled by the film coefficient (h) and the exposed surface area (A) which includes the circular cylinder head and

and piston surfaces as well as the variable cylindrical surface area of the engine cylinder Θ is cyclic crankshaft rotation.

Recent work by several authorities has yielded valuable insight into engine combustion processes and the resulting values for the convective film coefficient (1,2,3). The relationships chosen for the film coefficient in this model are those by Woschni as follows:

$$h = 0.035 \left(\frac{K}{B}\right)\left(\frac{B \rho V}{\mu}\right)^{0.8}$$

Where K is the thermal conductivity, B is the cylinder bore, μ is the viscosity, ρ is the density and V represents gas velocity as a function of mean piston speed V_p and varies from process to process as follows:

$$V = 2.28\ V_p \text{ (compression and intake)}$$

$$V = 6.18\ V_p \text{ (scavenge and blowdown)}$$

$$V = 2.28\ V_p + 0.00324\ \frac{V_s\ T_1}{P_1\ V_1}\ \Delta P \quad \text{(combustion and scavenging)}$$

Where V_s is instantaneous cylinder volume P_1, T_1, and V_1 are inlet closure properties and ΔP is the difference between instantaneous pressure and unfired engine pressure at the same crank angle. Neither combustion kinetics nor an expected reduction in lubricating oil temperature with reduced heat transfer were accounted for in the model.

Results of this model for various coating thickness are displayed in Figures 1-3. Note that as coating thickness increases:

1. Exposed coated surface temperature increases rapidly for combustion and expansion,
2. Metallic piston intersurface temperature decreases and
3. Overall cyclic efficiency increases.

One important outcome of the mathematical analysis as shown in Figure 4 is that convective resistance to heat transfer predominates throughout the cycle except

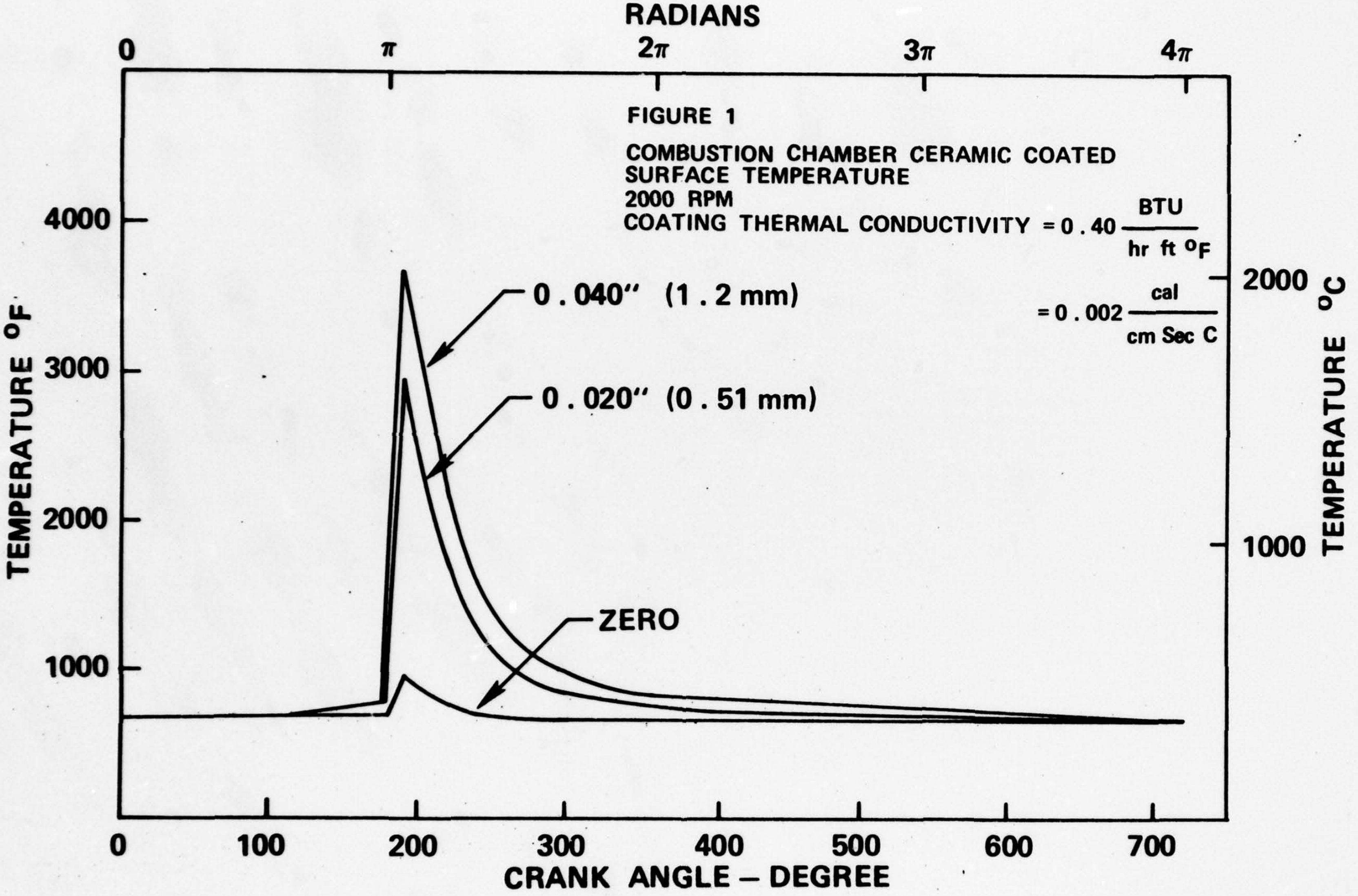

FIGURE 1

COMBUSTION CHAMBER CERAMIC COATED SURFACE TEMPERATURE
2000 RPM
COATING THERMAL CONDUCTIVITY $= 0.40 \frac{\text{BTU}}{\text{hr ft }^{\circ}\text{F}}$
$= 0.002 \frac{\text{cal}}{\text{cm Sec C}}$

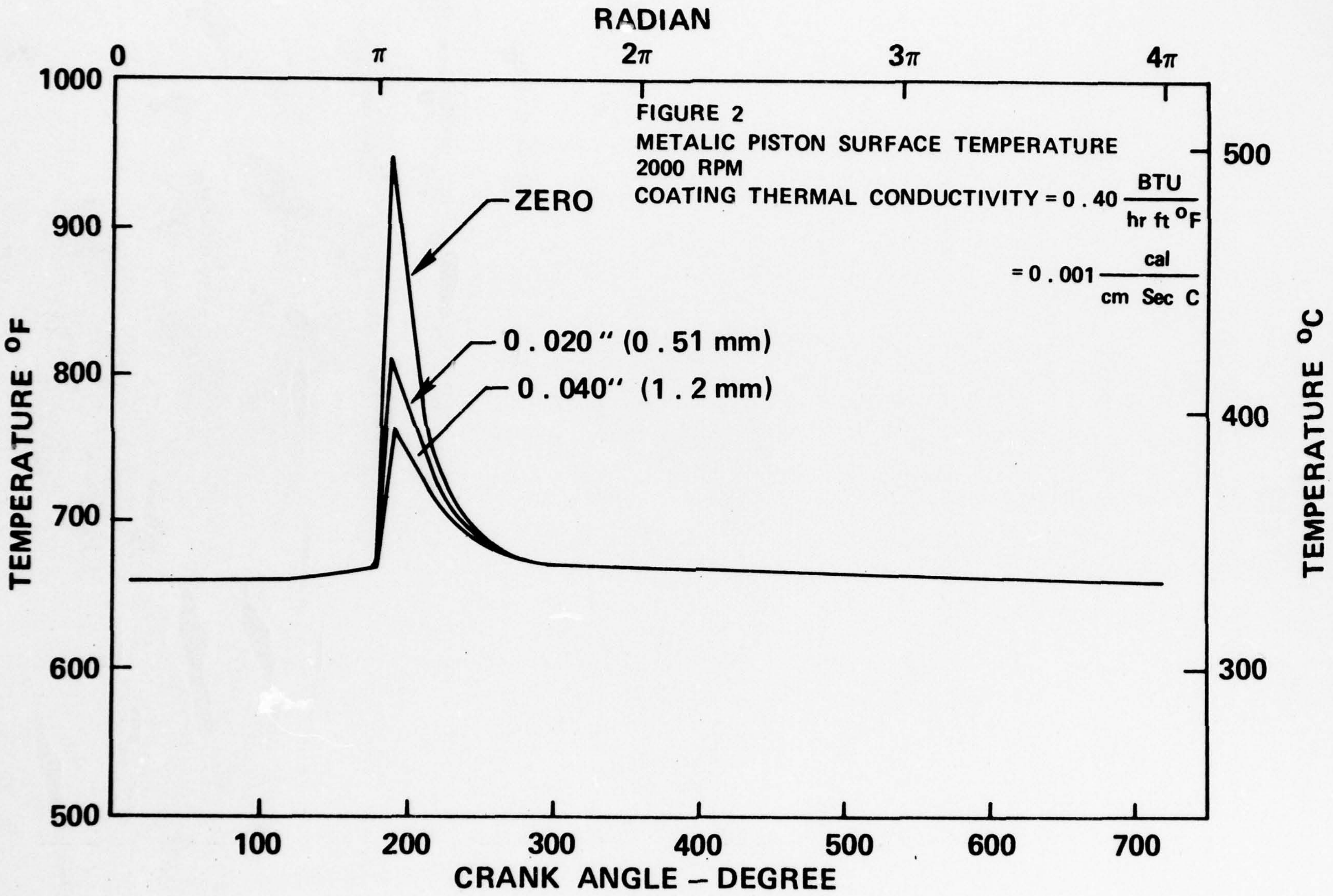

FIGURE 2
METALIC PISTON SURFACE TEMPERATURE
2000 RPM
COATING THERMAL CONDUCTIVITY $= 0.40 \frac{\text{BTU}}{\text{hr ft } ^{\circ}\text{F}}$

$= 0.001 \frac{\text{cal}}{\text{cm Sec C}}$

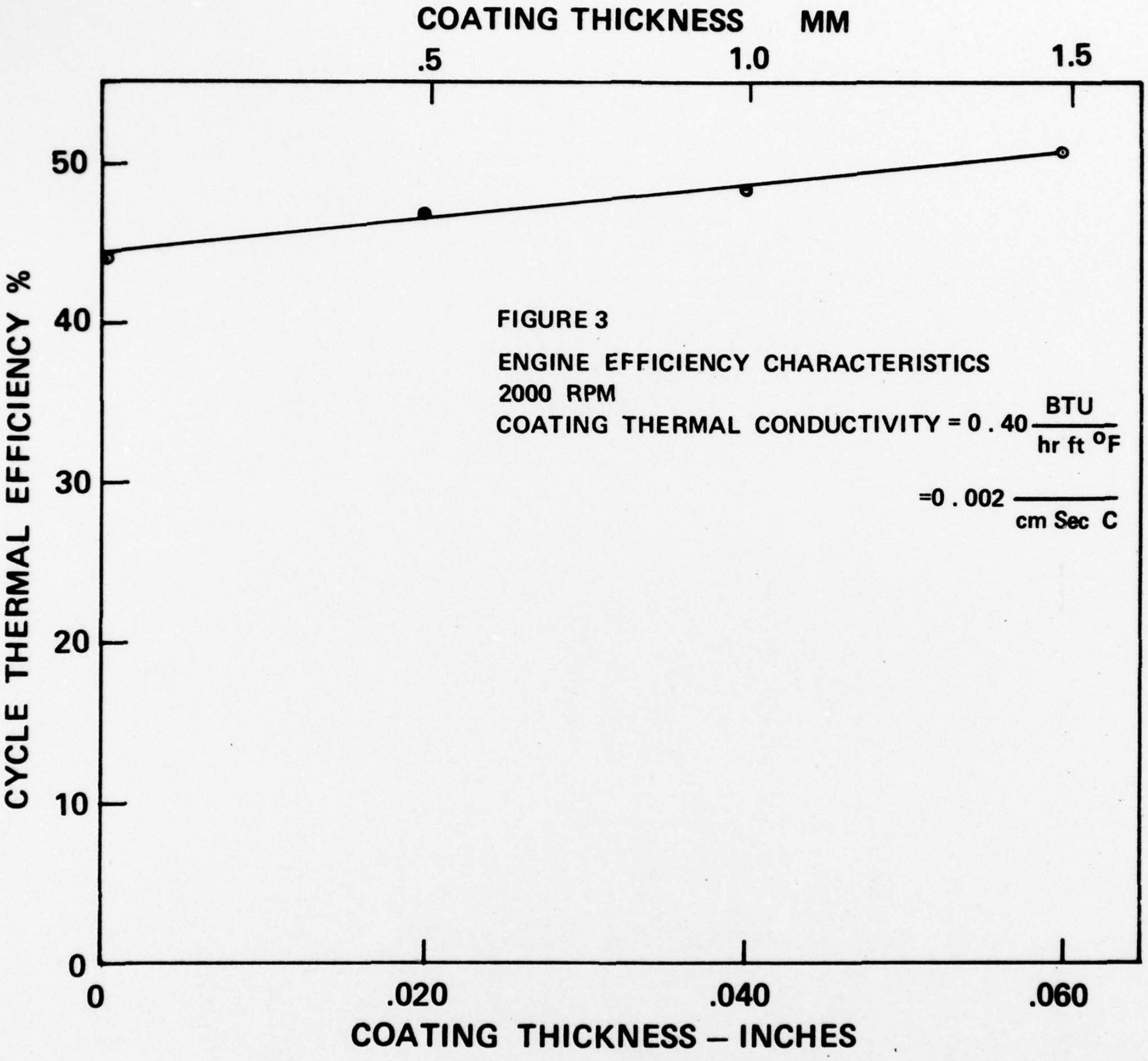

FIGURE 3

ENGINE EFFICIENCY CHARACTERISTICS
2000 RPM
COATING THERMAL CONDUCTIVITY $= 0.40 \frac{\text{BTU}}{\text{hr ft }^{\circ}\text{F}}$

$= 0.002 \frac{}{\text{cm Sec C}}$

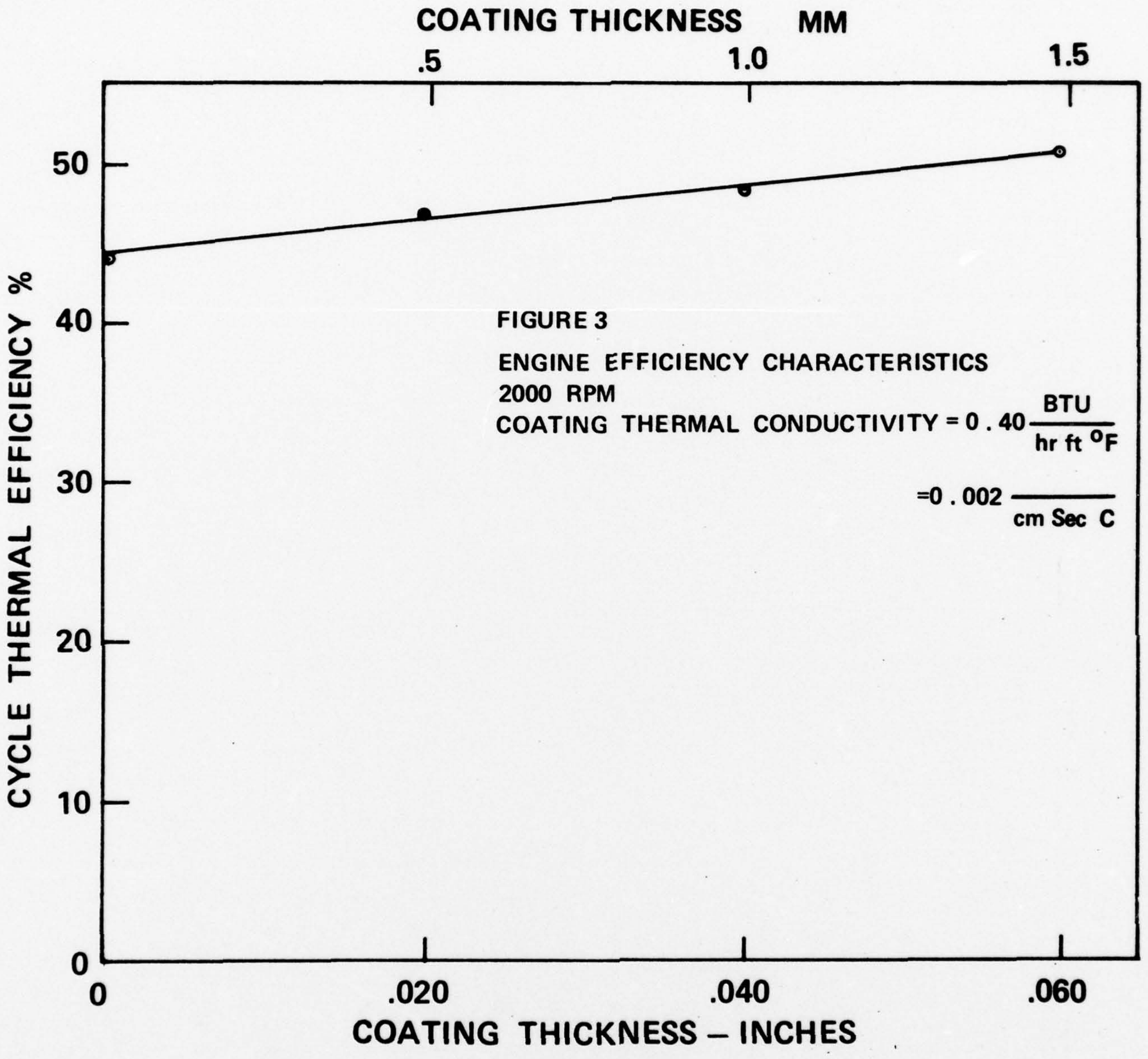

FIGURE 3

ENGINE EFFICIENCY CHARACTERISTICS
2000 RPM
COATING THERMAL CONDUCTIVITY = $0.40 \frac{\text{BTU}}{\text{hr ft } ^{\circ}\text{F}}$

$= 0.002 \frac{}{\text{cm Sec C}}$

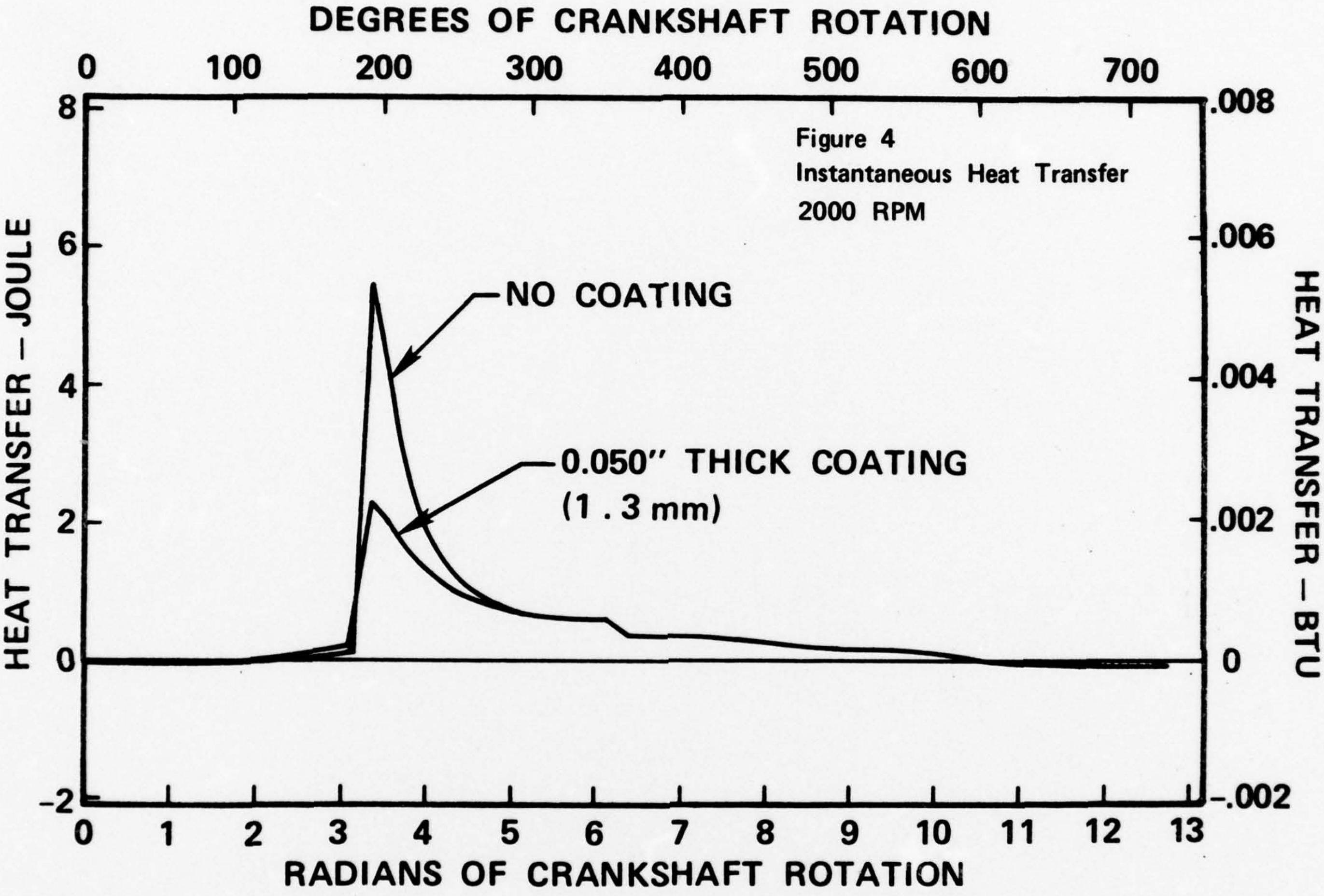

Figure 4
Instantaneous Heat Transfer
2000 RPM

during combustion and early expansion where turbulence is significant. During this critical time the convective resistance is lost and the conductive resistance of an insulating coating becomes a sizeable benefit. This is also the time of high working fluid temperature where the greatest power production can be expected if heat transfer can be minimized by the insulation.

PRELIMINARY TESTING

The above theoretical expectations appeared sufficiently optimistic that a sequence of engine test were performed by NASA-JSC in which the author participated. Objectives of these tests were to identify performance changes and to establish if flame sprayed ceramic coatings could in fact endure the torturous environment of a reciprocating I-C engine combustion chamber. Figure 5 illustrates the NASA-JSC test facility with the four cylinder 153 cubic inch S-I Chevrolet test engine in place. Figure 6 and 7 portray the ceramic coated cast iron cylinder head and aluminum pistons respectively coating thicknesses were a nominal 0.51 to 0.76 mm (0.020 to 0.030 inch).

Results of the NASA-JSC tests indicated that yttria stabilized zirconium oxide would adhere to aluminum, steel, and cast iron engine parts for at least the one hundred plus hours of test operation without separation from the metallic subsurface and would not display visible degradation of the ceramic structure.

Performance observations resulting from these tests were somewhat inconclusive, some areas of operation showed slight efficiency and power improvements while others showed a small sacrifice. In general non-knocking power and efficiency was somewhat higher but combustion knock, and the resulting performance decrease appeared to be promoted by the ceramic surface.

COMPREHENSIVE TESTING

As previously stated the preliminary test at NASA-JSC proved that zirconium

Figure 5

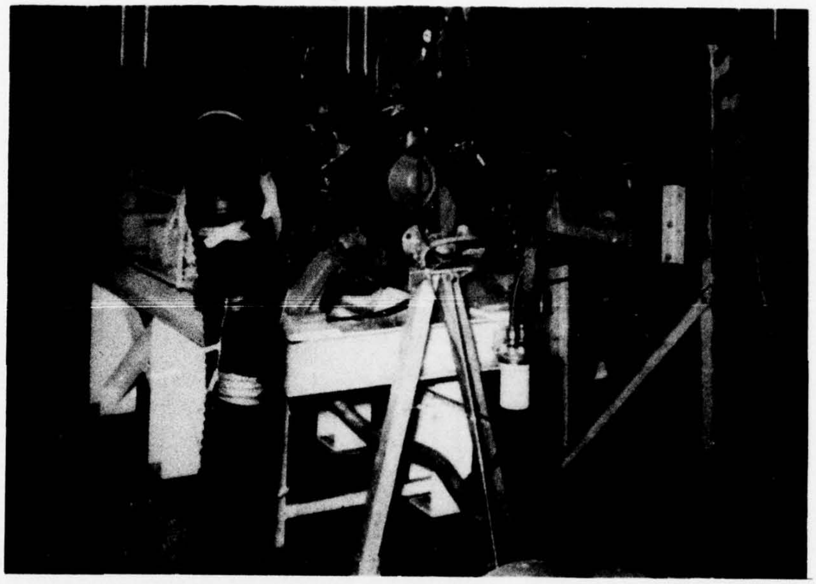

NASA Engine Test Cell

Figure 6

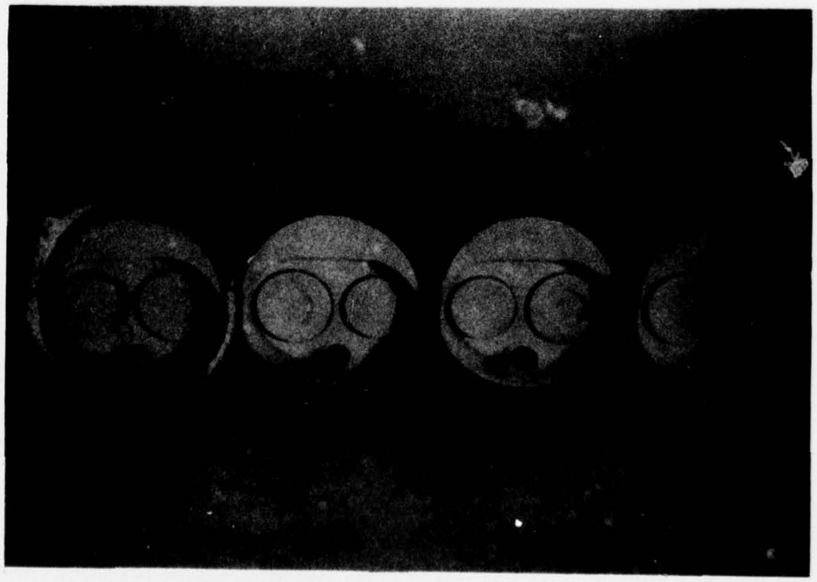

Multi-Cylinder Cylinder Head

Figure 7

Pistons

oxide coatings could withstand the harsh S-I engine environment and in some cases yield a performance improvement. Based on these early tests the U.S. Army research office issued a grant to fund a two year effort at Oklahoma State University to further investigate coated engine performance. This work consisted of two phases. First to document engine performance for both S-I and C-I ceramic coated engines and second to investigate emission and performance characteristics for zirconium oxide coated engines with and without catalysts applied to the exposed ceramic, in other words, an in situ catalytic reactor.

TEST APPARATUS

The engine test laboratory used for the above test program is shown in Figure 8. Principle items of laboratory equipment for the OSU project can be divided into two categories, the engine with its associated instrumentation and the emission analysis apparatus.

Analysis Apparatus

A Cooperative Fuel Research (CFR) low speed crankcase engine was used for all tests. This engine was equipped with the split head cylinder that allowed compression ratio testing capability between 4 and 18 to one. Figures 9 and 10 show the configuration of this cylinder head and piston with and without a yttria stabilized zirconium oxide coating, respectively. Coating thickness for all tests was 0.64 mm (0.025 inch).

Note in Figure 10 that for C-I operation the spark plug has been replaced by an adapter that holds a pencil type injector for open chamber operation. This injector as well as the adaptor were designed solely for this project and are shown in Figure 11. A typical injection spray pattern is illustrated in Figure 12.

Figure 8

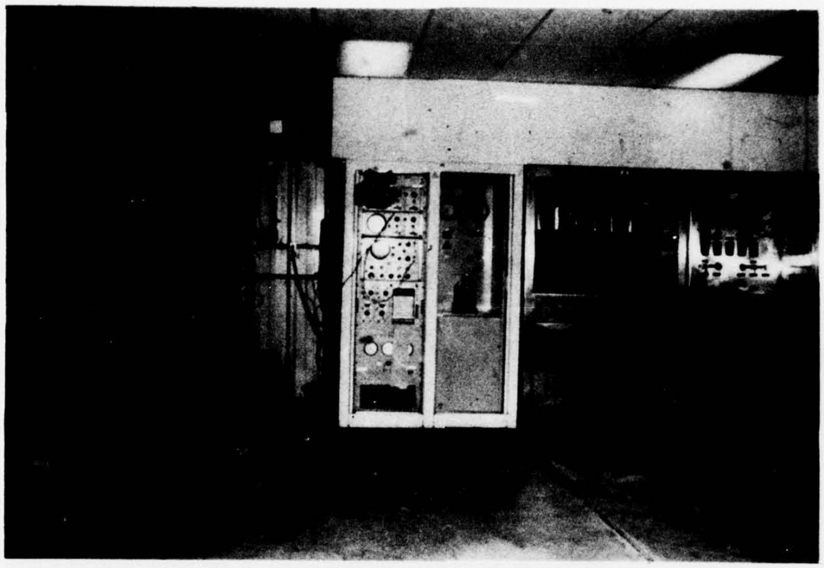

O.S.U. Engine Test Laboratory

Figure 9

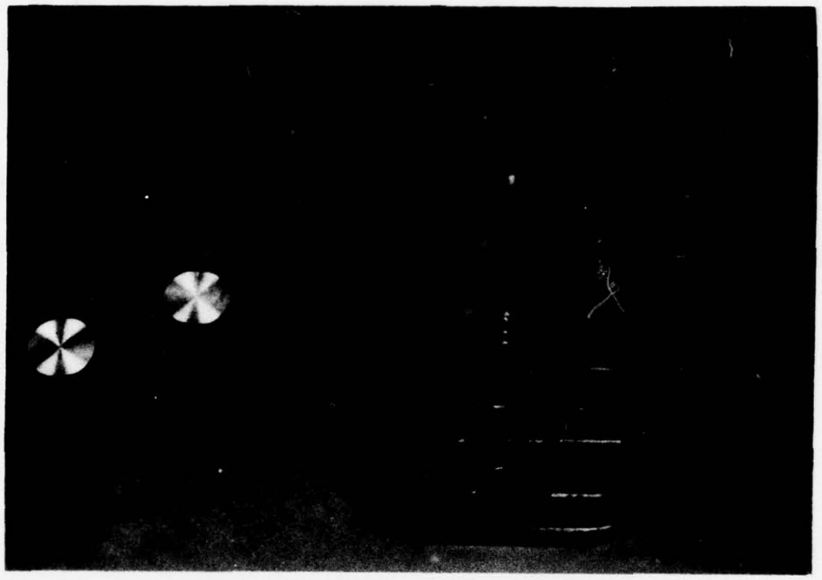

Cylinder Parts Without Ceramic Coating

Figure 10

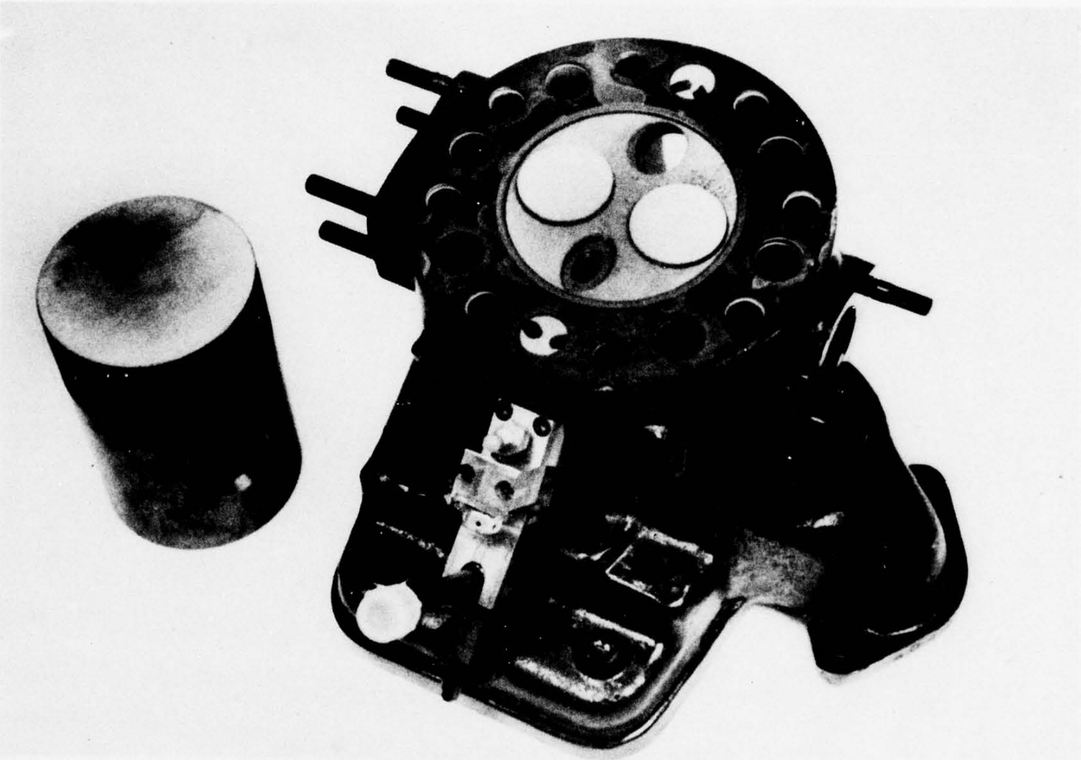

Cylinder Parts With Ceramic Coating

Figure 11

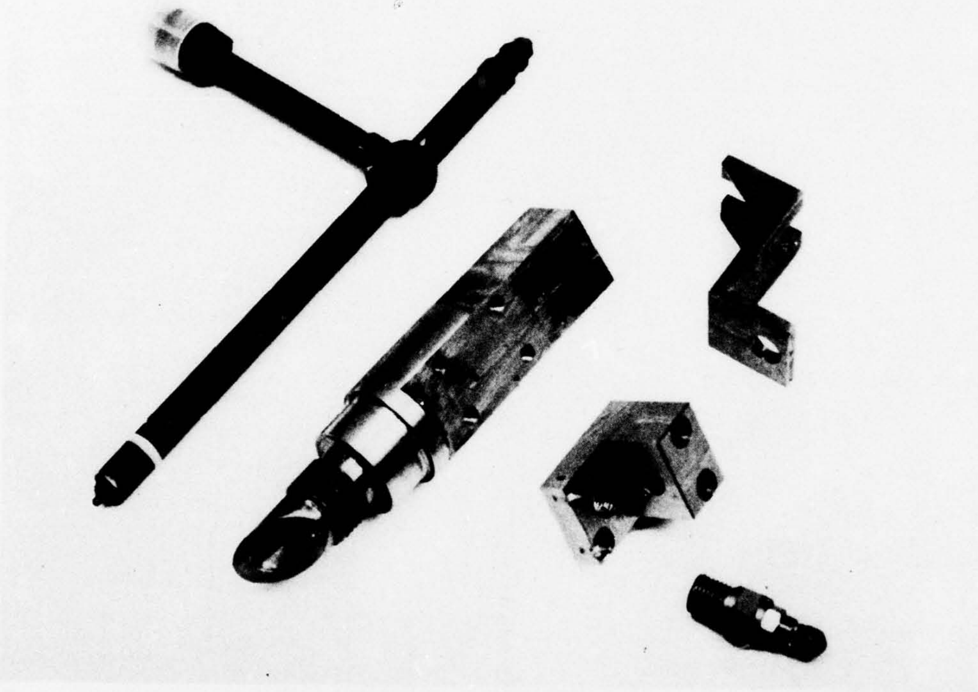

Injector Adaptor Exploded View

Figure 12

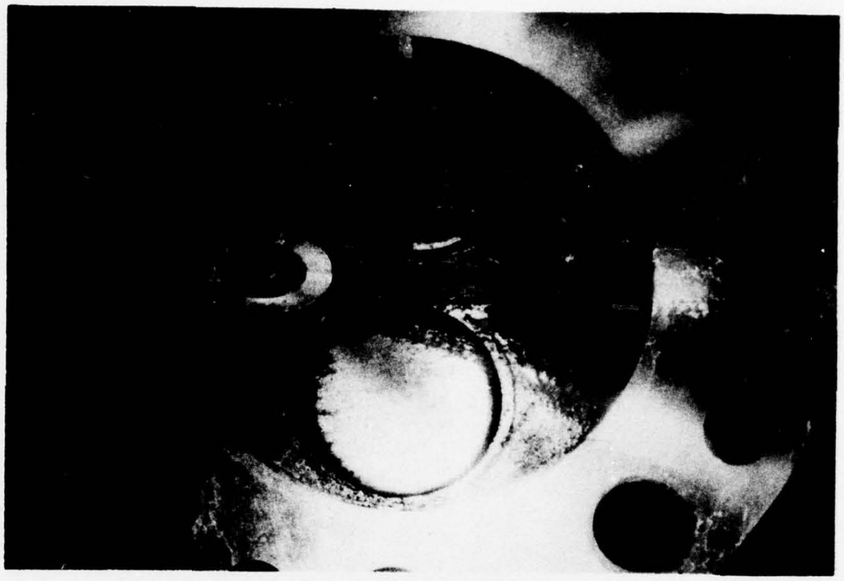

Injection Spray Pattern

A schematic of the engine and its associated equipment is shown in Figure 13. Combustion air was forced through an ice tower to remove excess moisture and then flowed through a laminar flow element flowmeter. Mass rate of air flow was regulated by a throttle valve preceding a surge tank that reduced pulsations for the flowmeter. For S-I operation, fuel was sprayed into the airstream and the mixture heated to standard temperature before entering the engine. S-I fuel was drawn from a graduated flask and then flowed through a rotameter for redundant flow measurement. Indolene clear (98 octane) was used as S-I fuel.

C-I fuel was also drawn from a graduated flask for a known time to establish primary flow measurement. Back up flow was determined by a micrometer controlled rack on the Bosch injection pump. A pressure transducer on the injection line produced an electric signal used to establish injection timing. Injection timing was adjustable within limits by a micrometer adjustment on the injection pump. The fuel used for C-I operation was I-H cat diesel fuel.

The engine was cooled by a boiling water jacket and lube oil temperature was controlled by an electric heater.

An AVL 14DP240C strain gauge pressure transducer and two photocells provided signals to an indicated power meter of the modified Phillips design (4). The output of this transducer was also used for oscilloscope observation of engine performance. A photographic display of pressure time (P-T), injection time, spark time, and crankshaft angular position were taken to document timing and combustion delay information.

Gas temperatures were monitored by thermocouples in the exhaust pipe and intake manifold.

Emission Apparatus

Three substances were analyzed in the exhaust of the test engine, hydro-

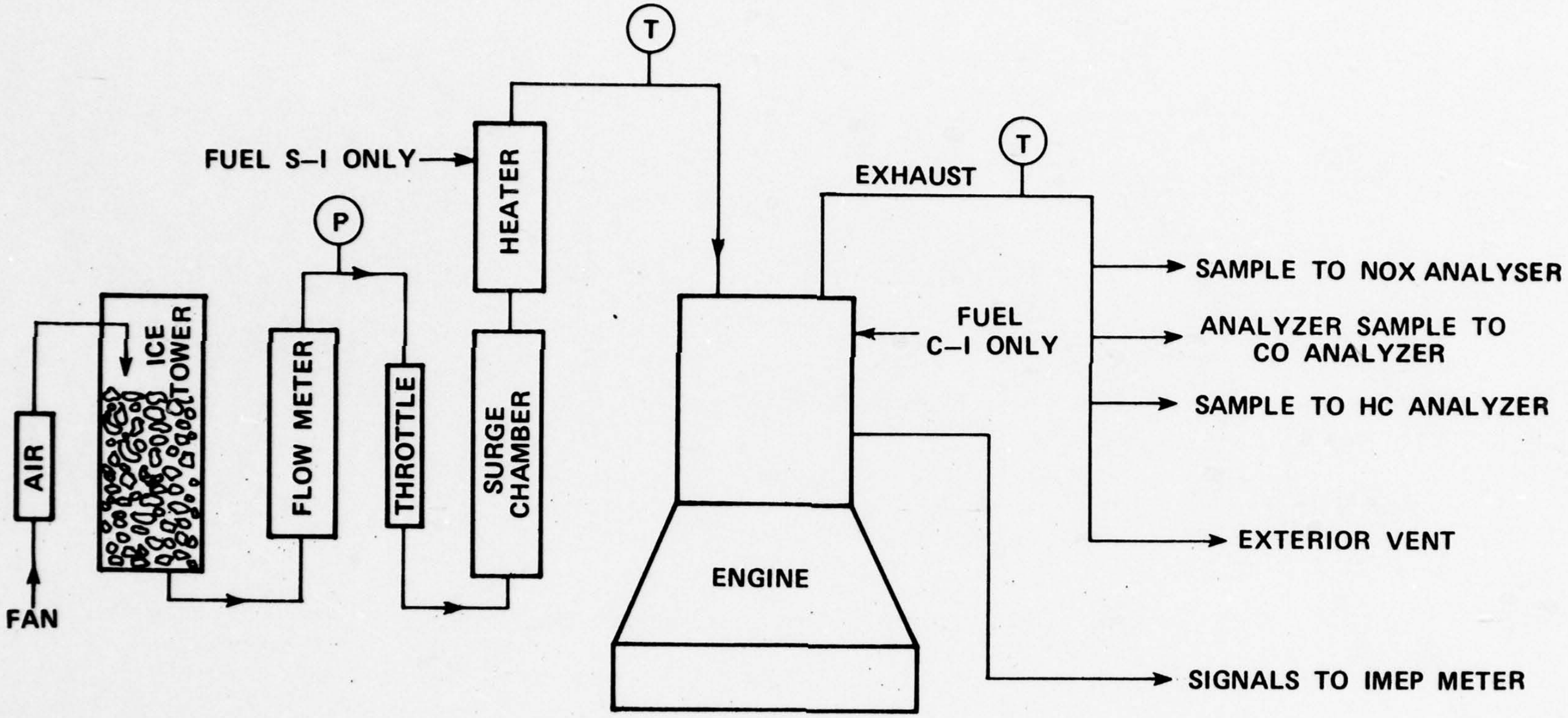

Figure 13. Engine Schematic

carbons (HC), carbon monoxide (CO), and oxides of nitrogen (NOX). Hydrocarbon concentration was observed by flame ionization detection (FID) using a sampling apparatus illustrated in Figure 14. HC concentration was reported as parts per million carbon as related to a propane ($C_3 H_8$) calibration gas. A non-dispersive infrared analyzer (NDIR) was used as a back up HC instrument. This same device monitored CO as illustrated in Figure 15. The sampling system and the NDIR used for NOX measurement is shown in Figure 16.

TEST PROCEDURE

Each sequence of testing was preceded by an engine tune-up that included a cylinder deglaze, installation of new piston rings, valve lapping and measurement of clearance volume for compression ratio determination. All instrumentation was given a major calibration before each test sequence and a minor calibration periodically between test runs. An engine break in was performed following each engine assembly.

S-I Tests

Before each sequence of S-I tests the fuel and ignition system performance and calibration was verified. The engine was started and brought to operational temperature on natural gas fuel to avoid combustion chamber deposits.

Engine runs were started at low values (6 to 1) of compression ratio (CR) and progressed to higher values. Initially, it was intended to secure data between 4 and 14 to one CR but low performance and violent knock necessitated a smaller CR range.

Air fuel ratios ranging from lean misfire (18 to 1) and rich misfire (14 to 1) were tested for each compression ratio.

Spark timing was adjusted to minimum advance for best torque (MBT) for each

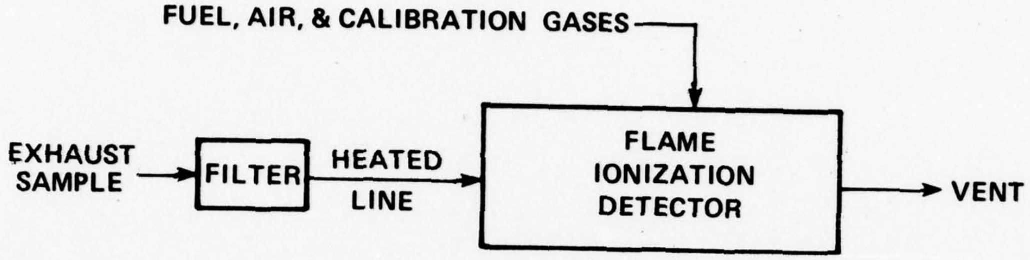

Figure 14 Hydrocarbon Measurement Apparatus

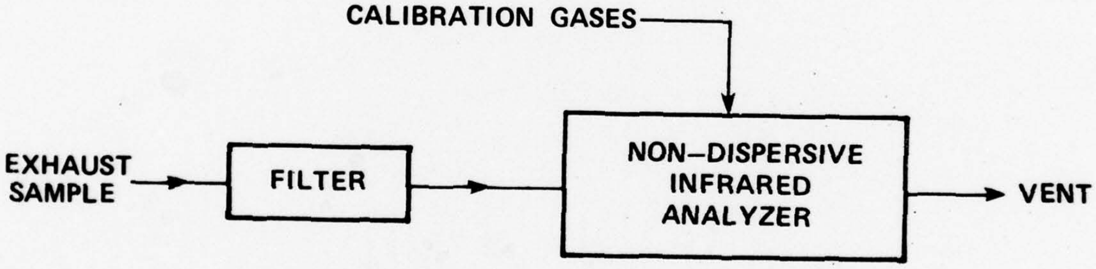

Figure 15 Carbon Monoxide & Backup Hydrocarbon Apparatus

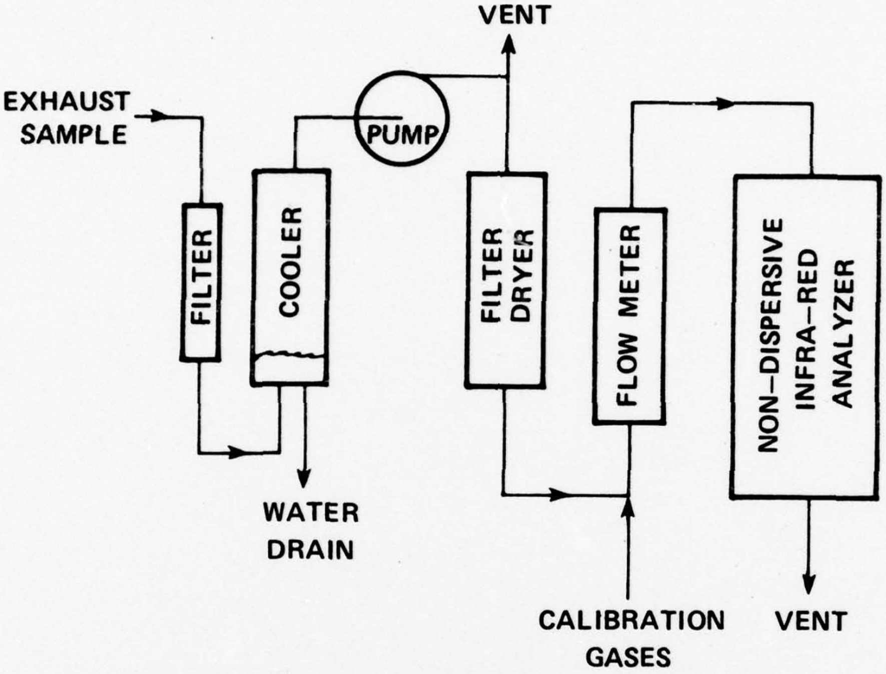

Figure 16 Oxides of Nitrogen Measurement Apparatus

data run. Several minutes (5 or more) of engine operation elapsed to establish equilibrium on each run before data was recorded. Ignition delay was measured as the crankshaft rotation between the spark pulse and significant cylinder pressure rise.

Before each data run all emission filters were changed, air and fuel flow rates were re-established and intake air fuel mixture temperature was adjusted to 305K (85F).

C-I Tests

In general, C-I tests were similar to S-I tests, however, natural gas could not be used as a warm-up fuel. Compression ratios between 14 and 18 to one were investigated for air fuel ratios ranging from 19 to 34 to one. It was found that CR lower than 14 to 1 resulted in misfire and A-F richer than 19 to one produced such high concentrations of soot that emission filters were plugged in a few seconds of operation. A-F ratios leaner than 34 to one resulted in significant misfire.

C-I engine tests started at low values of CR and progressed to higher values. A-F ratios progressed from rich to lean. Inlet air temperature was regulated to 322K (120F) for all C-I tests.

Injection timing was adjusted to MBT whenever possible, however, the maximum advance was 53 degrees and many tests had not reached best torque at the maximum advance limit.

Ignition delay was determined by measuring the difference between the injector transducer pulse and the point of significant pressure rise in the combustion chamber.

Preliminary Test

A complete set of performance data was taken during the projects first year. No emission data was taken, however, since the in situ catalytic project had not been formulated. Once the second year in situ study was approved it was realized that all tests would need be rerun to include emission profiles and combustion delay. These last two items are a key indicator of how the catalyst is effecting combustion, performance, and emission.

Since test procedures and instrumentation were significantly changed after the first year and since some first year data had wide variation this data will not be included in this document.

CATALYSTS

Selection

Theoretically catalytic surfaces can be expected to influence chemical kinetics prior to, during, and following combustion. Catalysts by their nature form chemical bonds of varying degrees of stability with other atoms or groups. Although one must hope ultimately to explain the chemical behavior of a metallic catalyst in purely quantum mechanical terms, this objective still remains largely beyond reach and one is left with the construction of essentially emperical correlations (5).

It can be expected that the material of an engine combustion chamber must catalytically influence the rate and path of the reactions leading to combustion products. When aluminum and cast iron combustion chamber surfaces are replaced by yttria stabilized zirconium oxide it is reasonable to expect a change in reaction time and composition of exhaust products. An expansion of this idea would predict a further change in combustion characteristics if active catalytic substances such as platinum and cerium were introduced.

To pursue this principle a program was undertaken during the second year of the U.S. Army grant to identify the affect of various catalytic substances on engine performance and emission. Initially, six metals (platinum, palladium, cerium, nickel, tungstan, and titanium) were selected as possible candidates. Of these, two, platinum and cerium, were applied to the zirconium oxide combustion surface and subjected to a sequence of engine tests. It was expected that these substances would yield: 1) a reduced tendency to knock, 2) a decrease in preflame chemical and physical delay time, 3) a reduction in exhaust emissions, and 4) a more favorable engine tolerance to low grade fuel (6).

Application

Metallic catalysts are not usually applied to a surface in the pure metal state. A common procedure is to dissolve a salt or metallic compound in a solvent, distribute this solution on the surface and then chemically reduce the dried film to the parent metal. This above procedure was used for both catalysts that were applied for this test.

Preparation of a platinum catalyst solution consisted of dissolving 1.2 grams of dihydrogen hexachloroplatinate IV ($H_2 Pt Cl_6 . 6H_2O$) in 2.0 grams of distilled water. This solution was spread over the polished zirconium surfaces with a glass rod and then allowed to dry in air for 24 hours prior to a final oven drying at 422K for 12 hours.

Reduction of the dihydrogen hexachloroplatinate to platinum black was achieved by placing the surfaces in a sealed steel box and placing the box in an electric oven. Before heating, the box was purged of air by flushing with dry nitrogen for several minutes. The nitrogen in turn was forced from the box by a flow of gaseous hydrogen entering at the top and pushing nitrogen out the bottom. Hydrogen flow was controlled to 17 cubic centimeters per hour and continued throughout reduction. Reduction was completed by maintaining a 533K temperature for 24 hours. Figures 17 and 18 show the platinum surfaces after reduction.

Figure 17

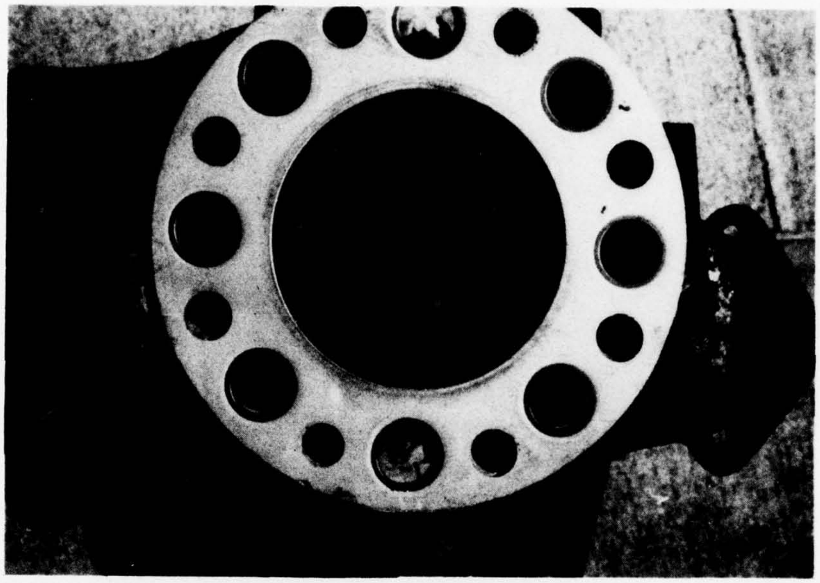

Platinum Coated Cylinder Head

Figure 18

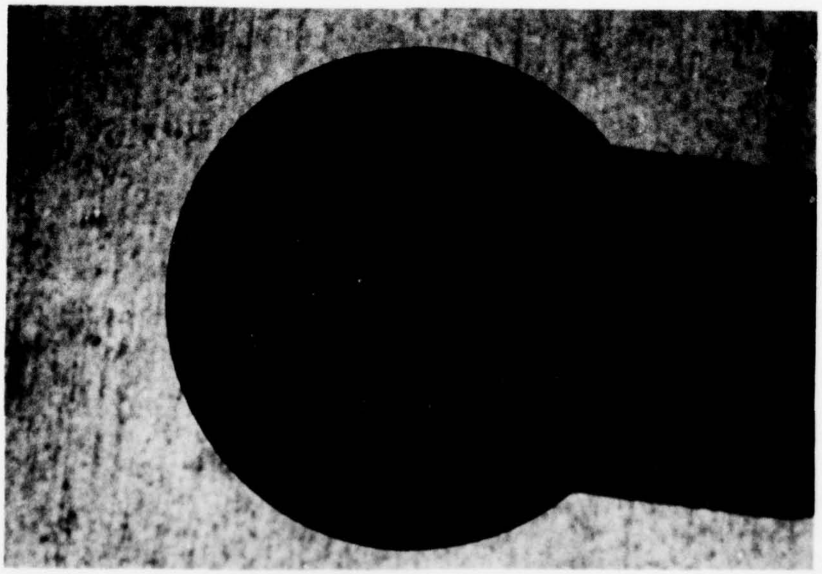

Platinum Coated Piston

The procedure for cerium application was quite similar to that for platinum. The solution was prepared with 15.1 grams of cerium (III) 2,4 pent-anedionate Ce $(C_5H_7O_2)_3 \cdot XH_2O$ in 59.1 grams of absolute alchohol. Initial hydrogen reduction temperature was 450K. This reduction was followed by a second application of solution and a final hydrogen reduction at 589K. Figure 19 illustrates the cylinder head surface after reduction with a cerium catalyst.

Production of a satisfactory surface and reduction was much more difficult with cerium than platinum. Refusal of the coating to reduce, poor adherence, and blistering were common problems. Figure 20 portrays a typical unsatisfactory cerium surface.

DATA AND ANALYSIS

Raw data was recorded manually during each engine run on computer format forms. After data acquisition all information was transferred to punch cards and processed in an IBM system 370 computer. A copy of the program is listed in the appendix.

Table 2 following tabulates all reported data, while Figures 21 through 76 display the graphical behavior of non-coated, coated, and catalytic engine performance for both S-I and C-I operation.

Figure 19

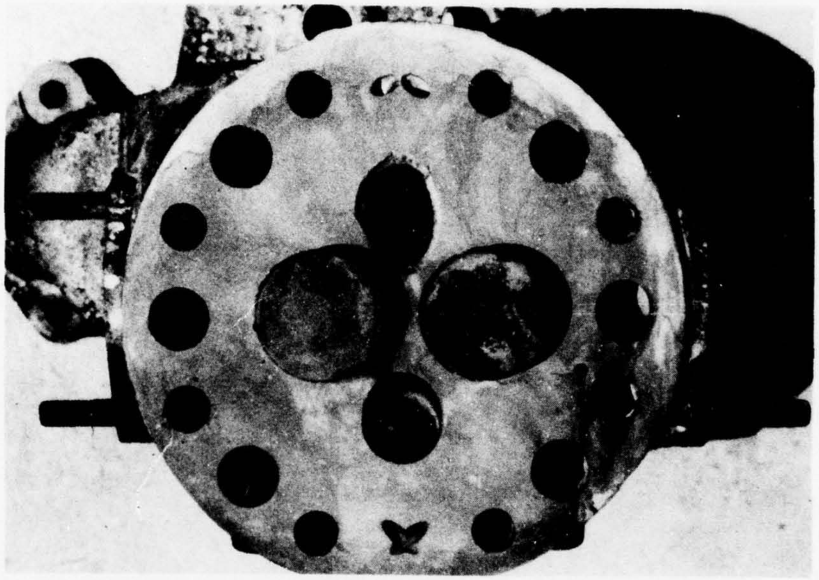

Cerium Coated Cylinder Head

Figure 20

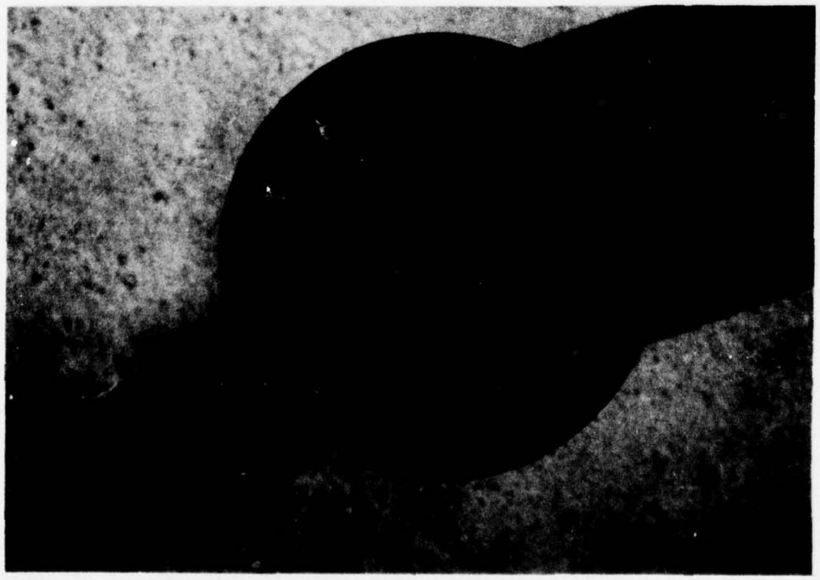

Cerium Coated Piston

S-I Data Analysis

Figures 21 through 23 illustrate the relationship of indicated power to air fuel ratio for the various engine configurations. Note, that power in general shows a significant improvement for zirconium coated S-I engines as compared to non-coated. This trend, however, reversed at 10 to 1 CR for mid range A-F. Severe knock accounted for this power loss. The uncoated surfaces resisted knock presumably because of the lower surface temperature of the bare metal.

In opposition to expected results, a power sacrifice was observed for catalytic operation. In general, all S-I data indicated that both cerium and platinum inhibited combustion and reduced engine performance.

Indicated specific fuel consumption (ISFC) trends are portrayed in Figures 24 to 26, where as expected, the zirconium coated engine showed superiority until severe knock destroyed power output at a CR of 10.

As expected, ignition delay is much less for zirconium coated performance (see Figures 27 through 29) no doubt caused by the fuel-air mixture having contact with a hotter surface during its residence on the intake and compression strokes.

Unexpectedly, the catalytic coatings do not appear to initiate preflame reactions that reduce ignition delay.

Exhaust gas temperature (EGT) portrays the usual decline with an increase of CR as shown in Figures 30 to 32. The typical peak temperature on the lean side of stoichiometric is present, as is the increase in temperature with a reduction in heat transfer for the coated engine. Note that the combustion inhibiting phenomenon of the catalytic surfaces delays and reduces the peak EGT.

HC and CO emissions are generally similar for zirconium coated and non-coated performance while catalytic surfaces tended to produce somewhat higher

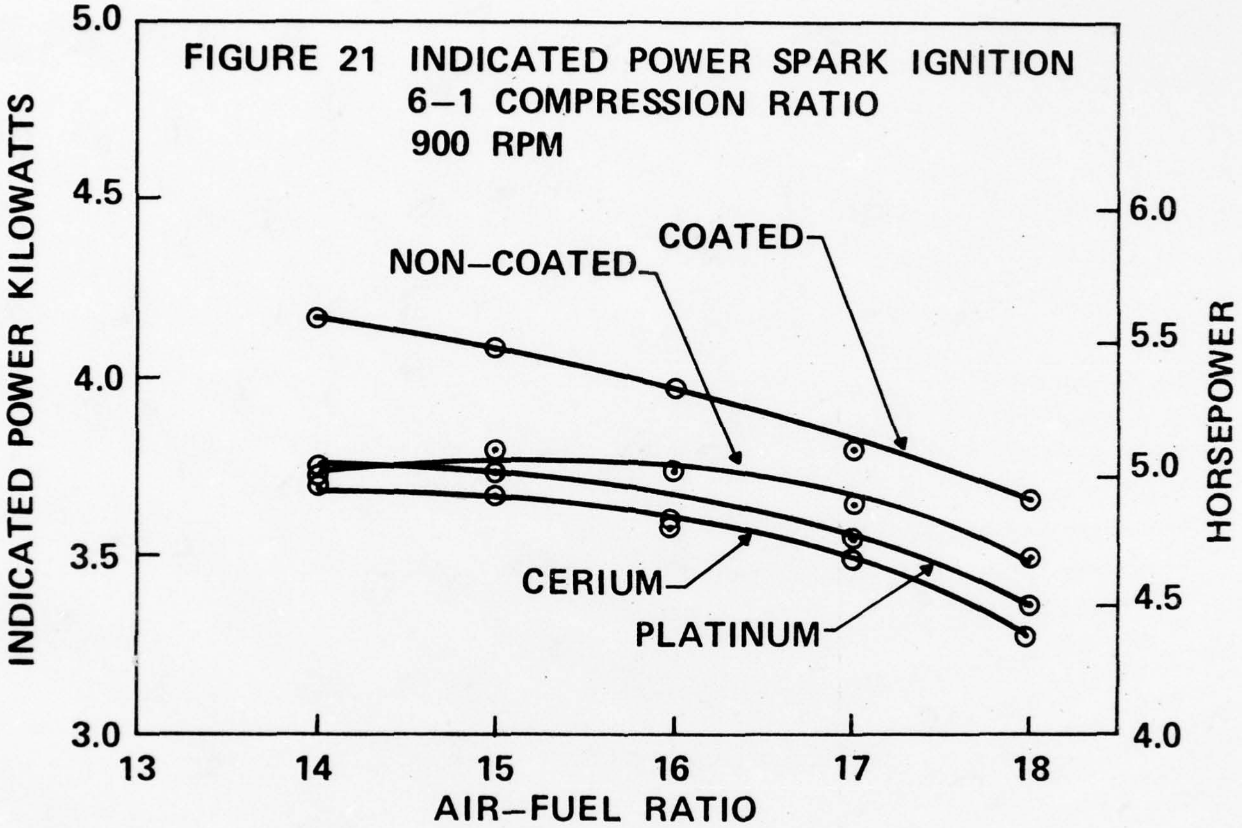
FIGURE 21 INDICATED POWER SPARK IGNITION
6-1 COMPRESSION RATIO
900 RPM
INDICATED POWER KILOWATTS
HORSEPOWER
AIR-FUEL RATIO
5.0
4.5
4.0
3.5
3.0
6.0
5.5
5.0
4.5
4.0
13
14
15
16
17
18
COATED
NON-COATED
CERIUM
PLATINUM

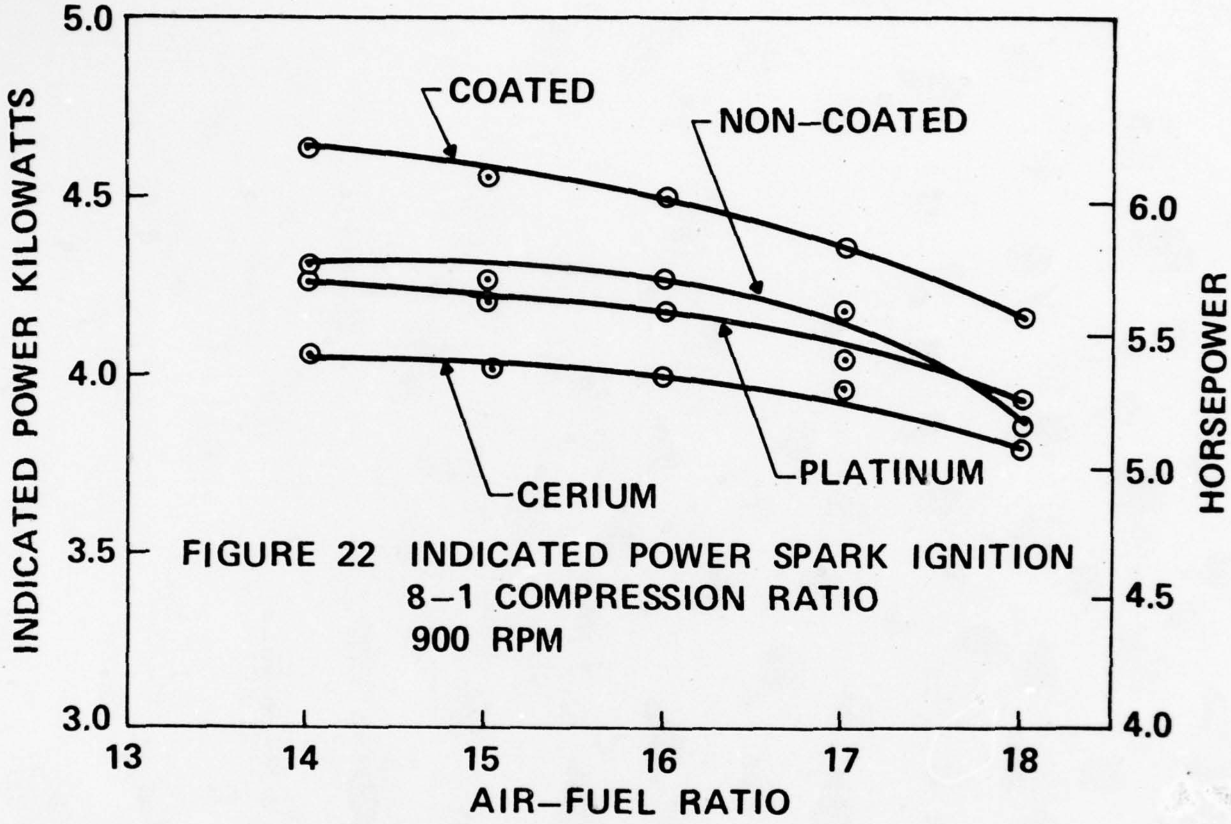

FIGURE 22 INDICATED POWER SPARK IGNITION
8-1 COMPRESSION RATIO
900 RPM

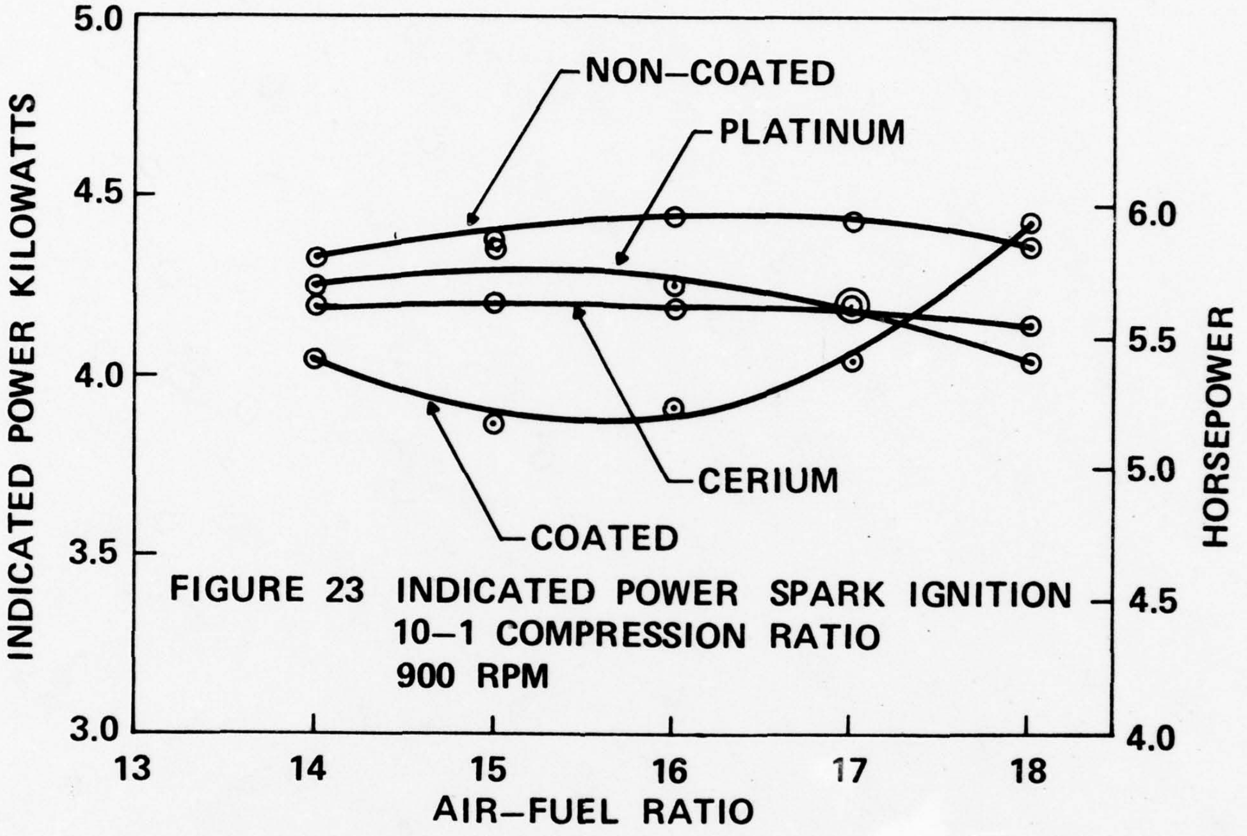

FIGURE 23 INDICATED POWER SPARK IGNITION
10–1 COMPRESSION RATIO
900 RPM

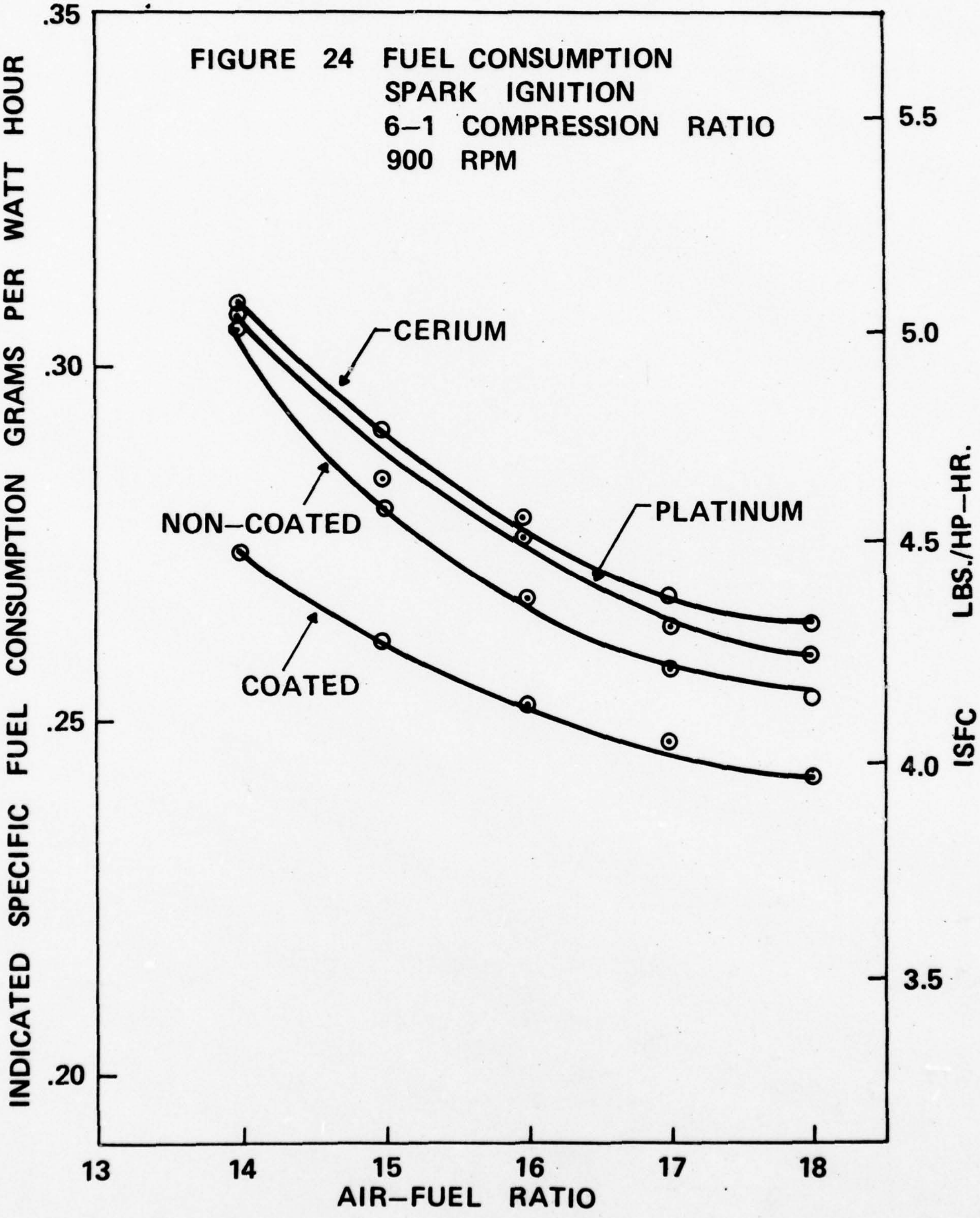

FIGURE 24 FUEL CONSUMPTION
SPARK IGNITION
6–1 COMPRESSION RATIO
900 RPM

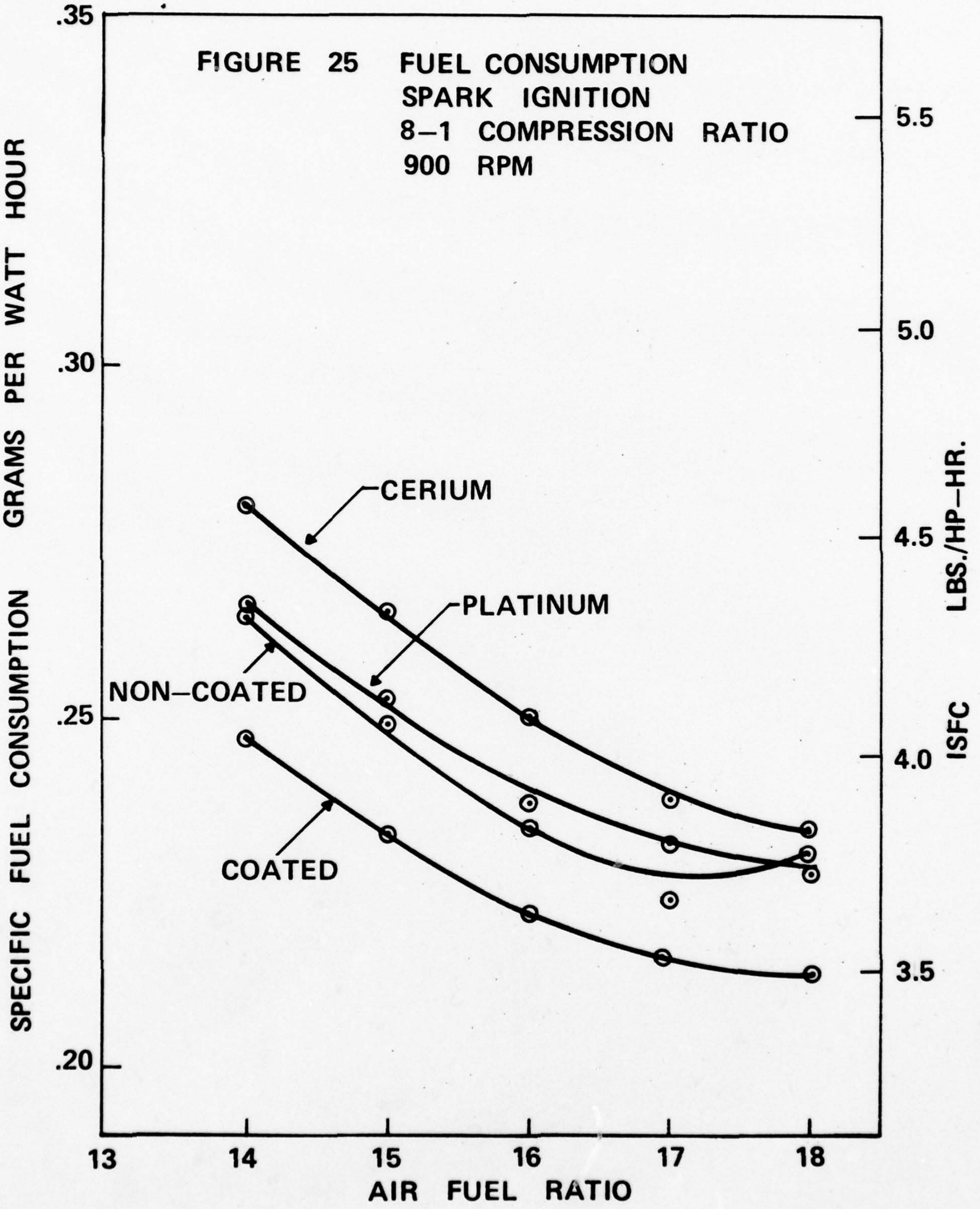
FIGURE 25 FUEL CONSUMPTION
SPARK IGNITION
8–1 COMPRESSION RATIO
900 RPM

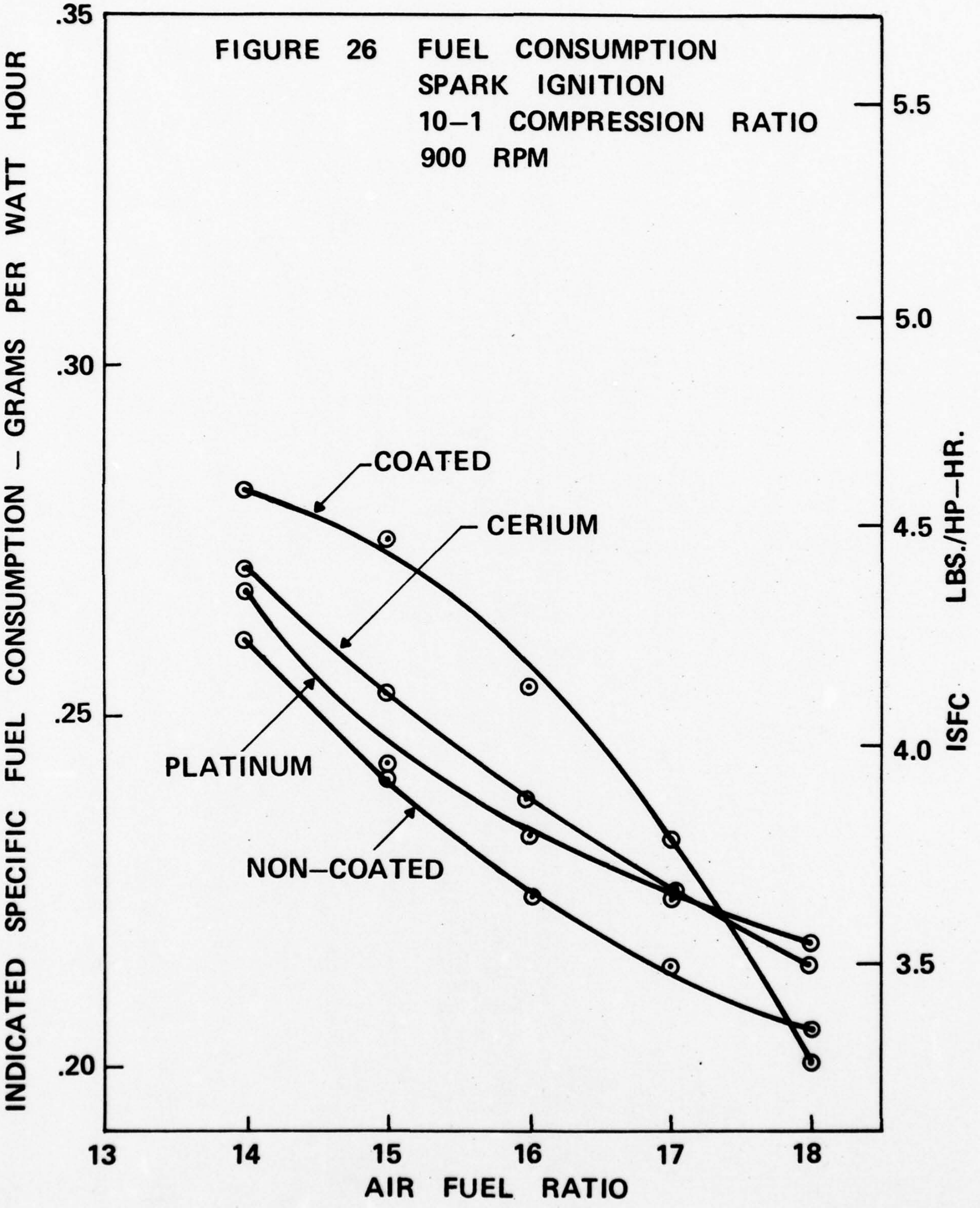

FIGURE 26 FUEL CONSUMPTION
SPARK IGNITION
10–1 COMPRESSION RATIO
900 RPM

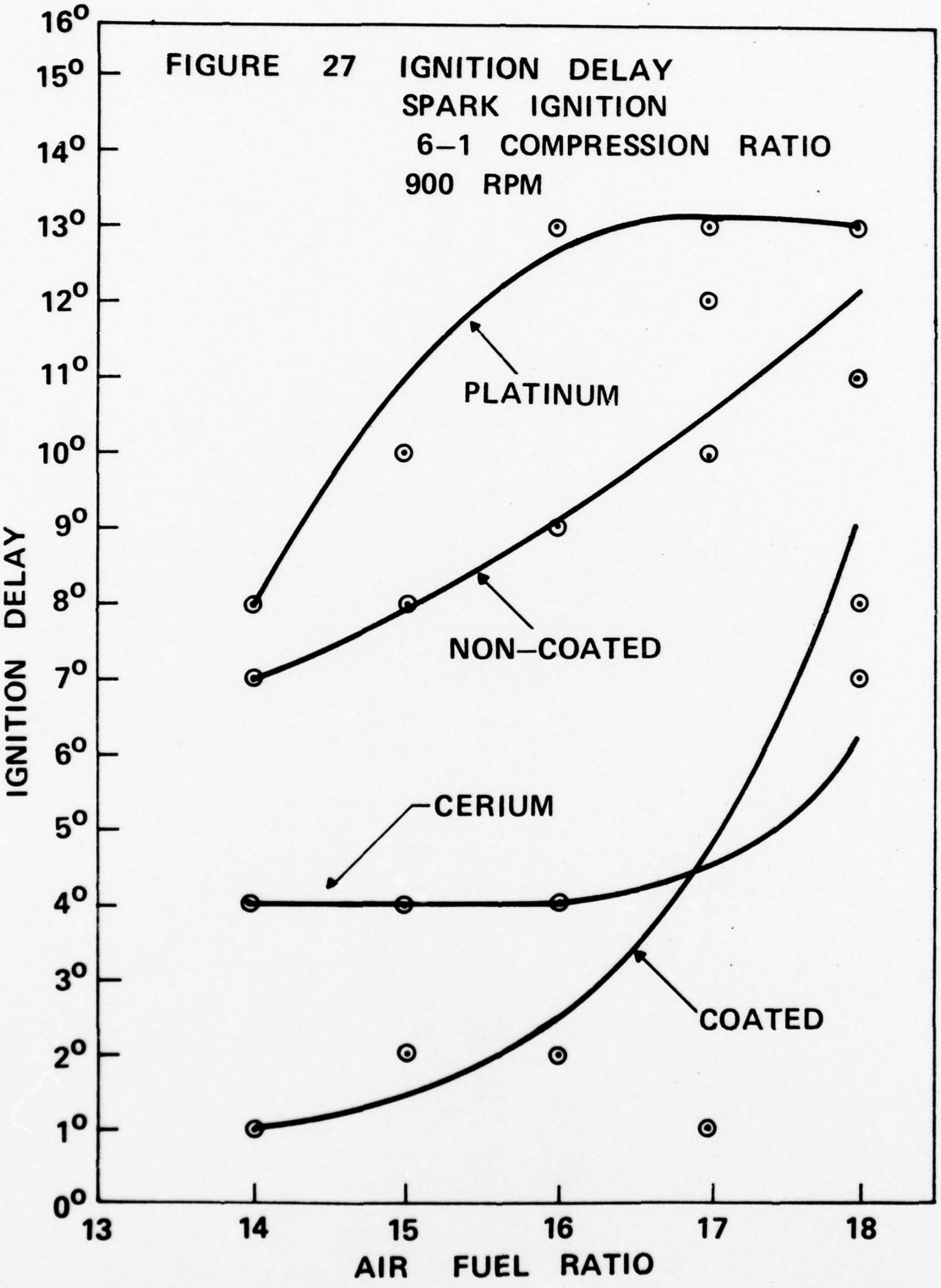

FIGURE 27 IGNITION DELAY
SPARK IGNITION
6–1 COMPRESSION RATIO
900 RPM

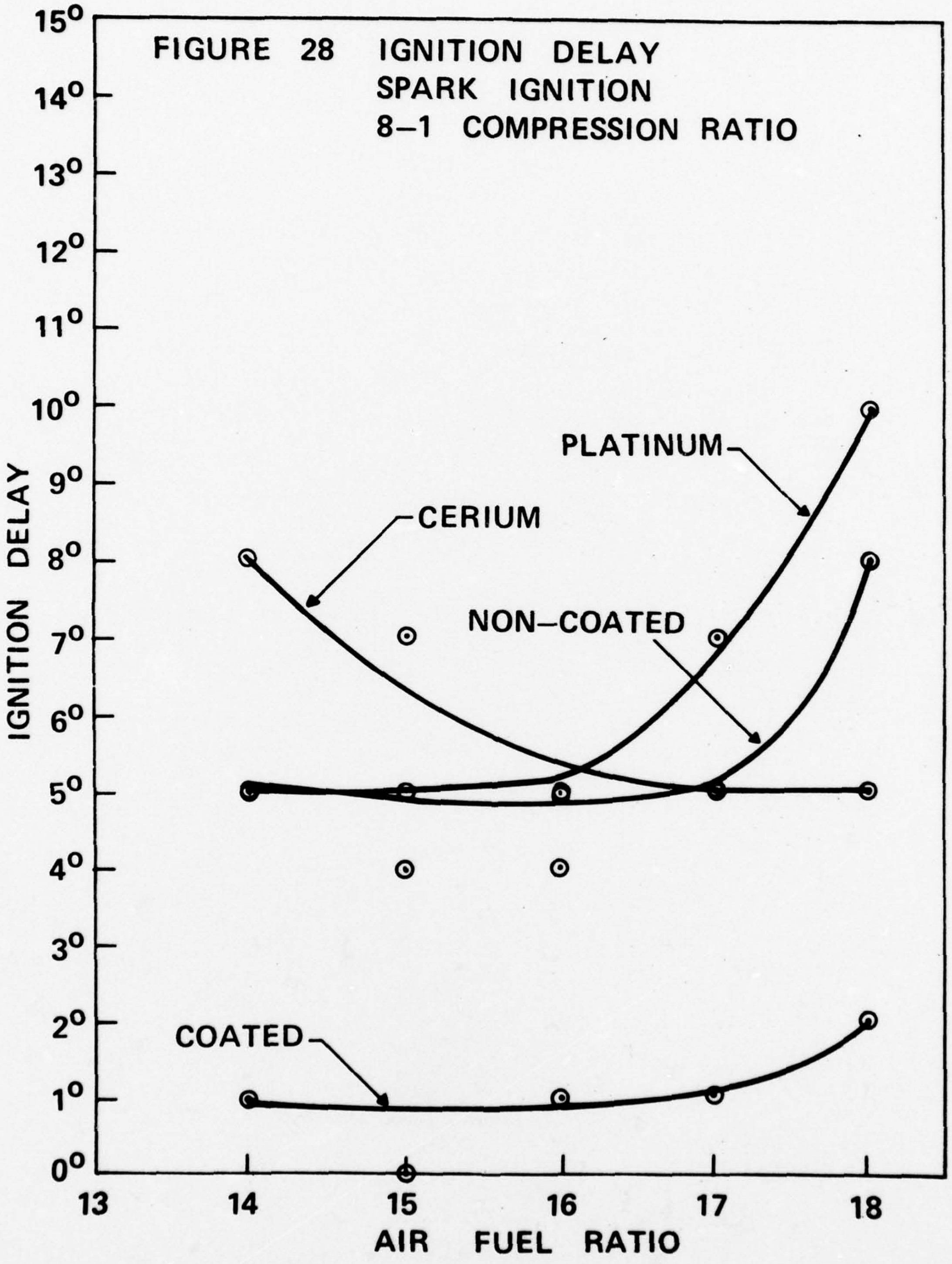

FIGURE 28 IGNITION DELAY
SPARK IGNITION
8–1 COMPRESSION RATIO

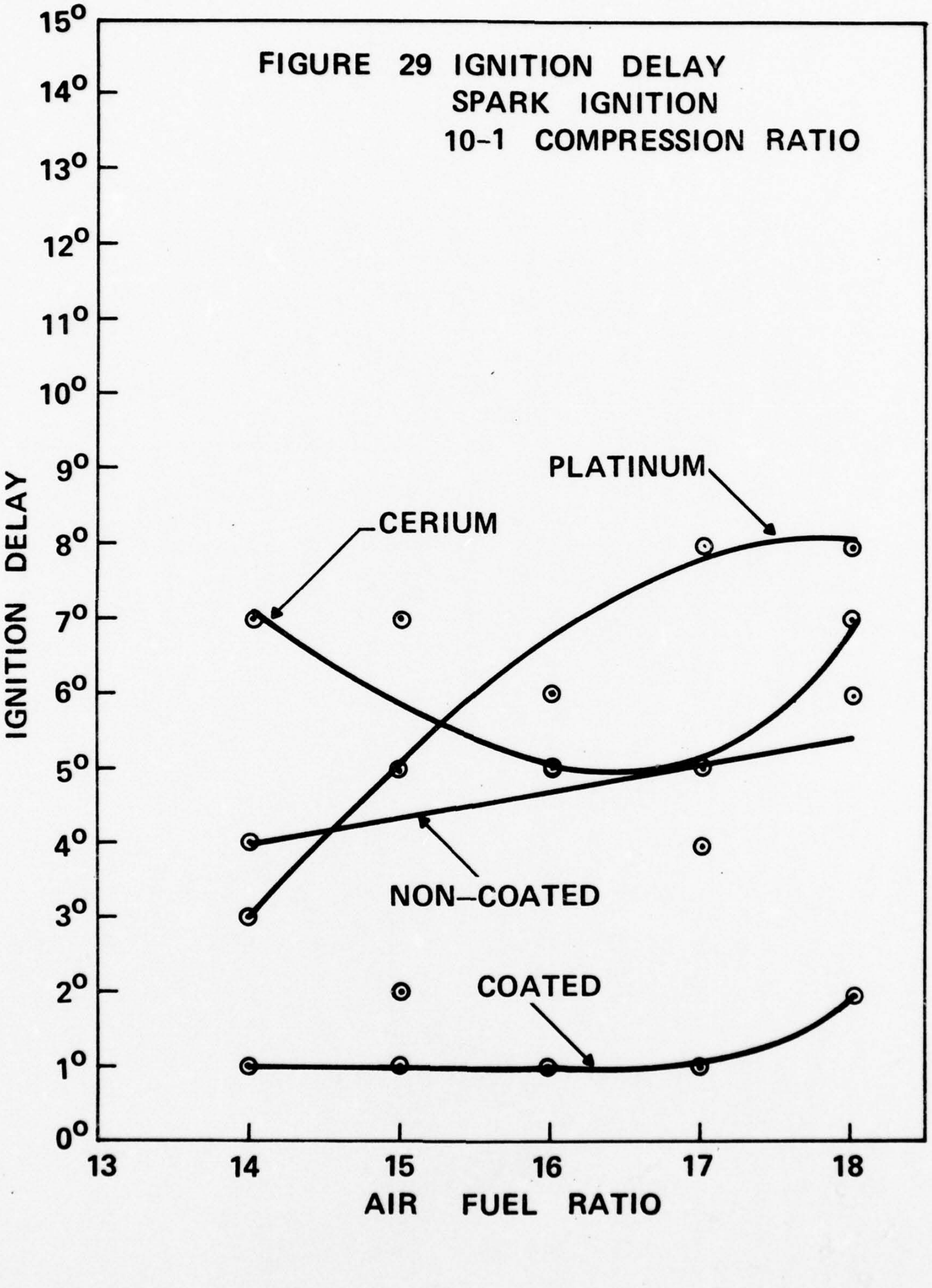

FIGURE 29 IGNITION DELAY
SPARK IGNITION
10-1 COMPRESSION RATIO

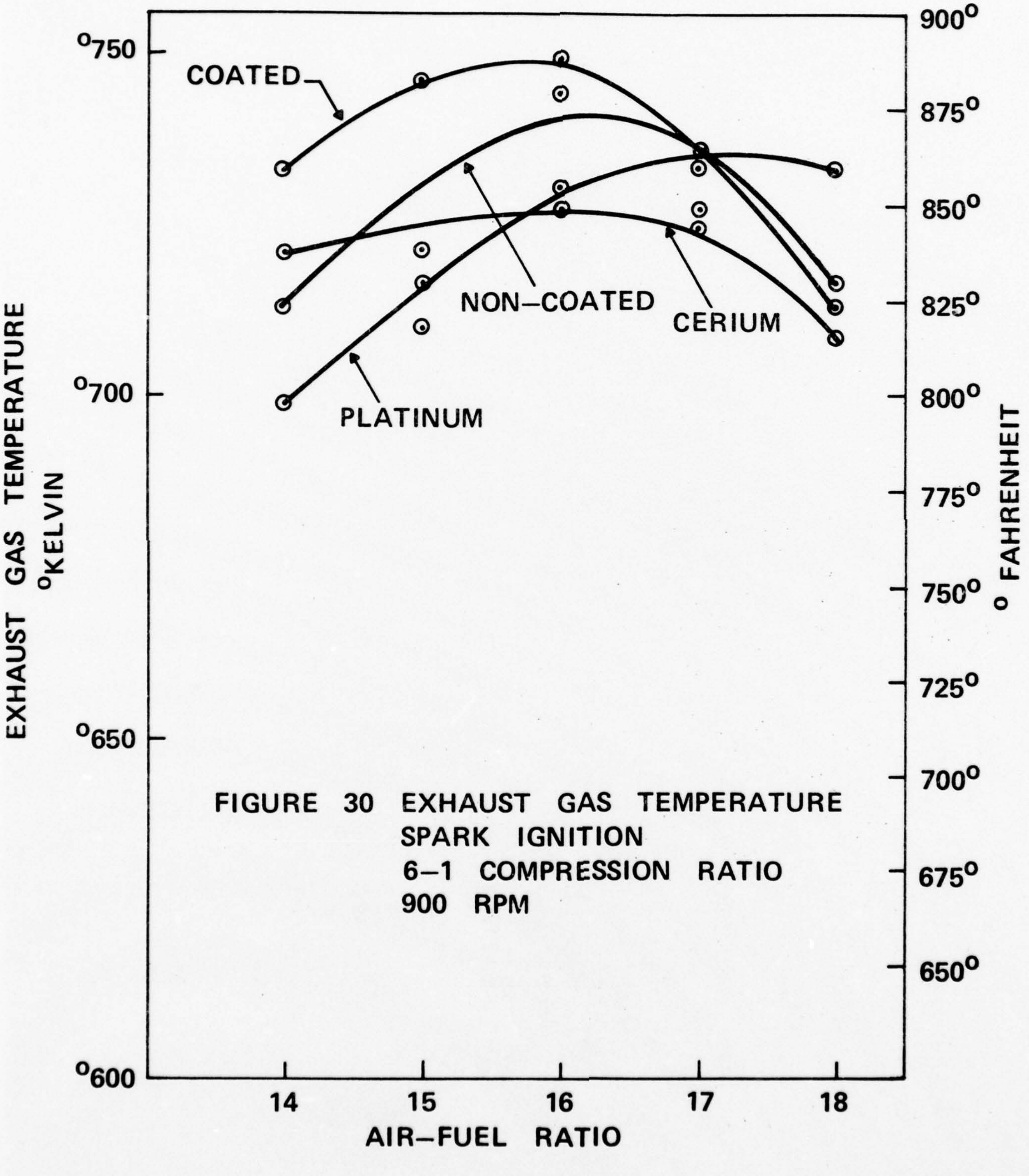

FIGURE 30 EXHAUST GAS TEMPERATURE
SPARK IGNITION
6-1 COMPRESSION RATIO
900 RPM

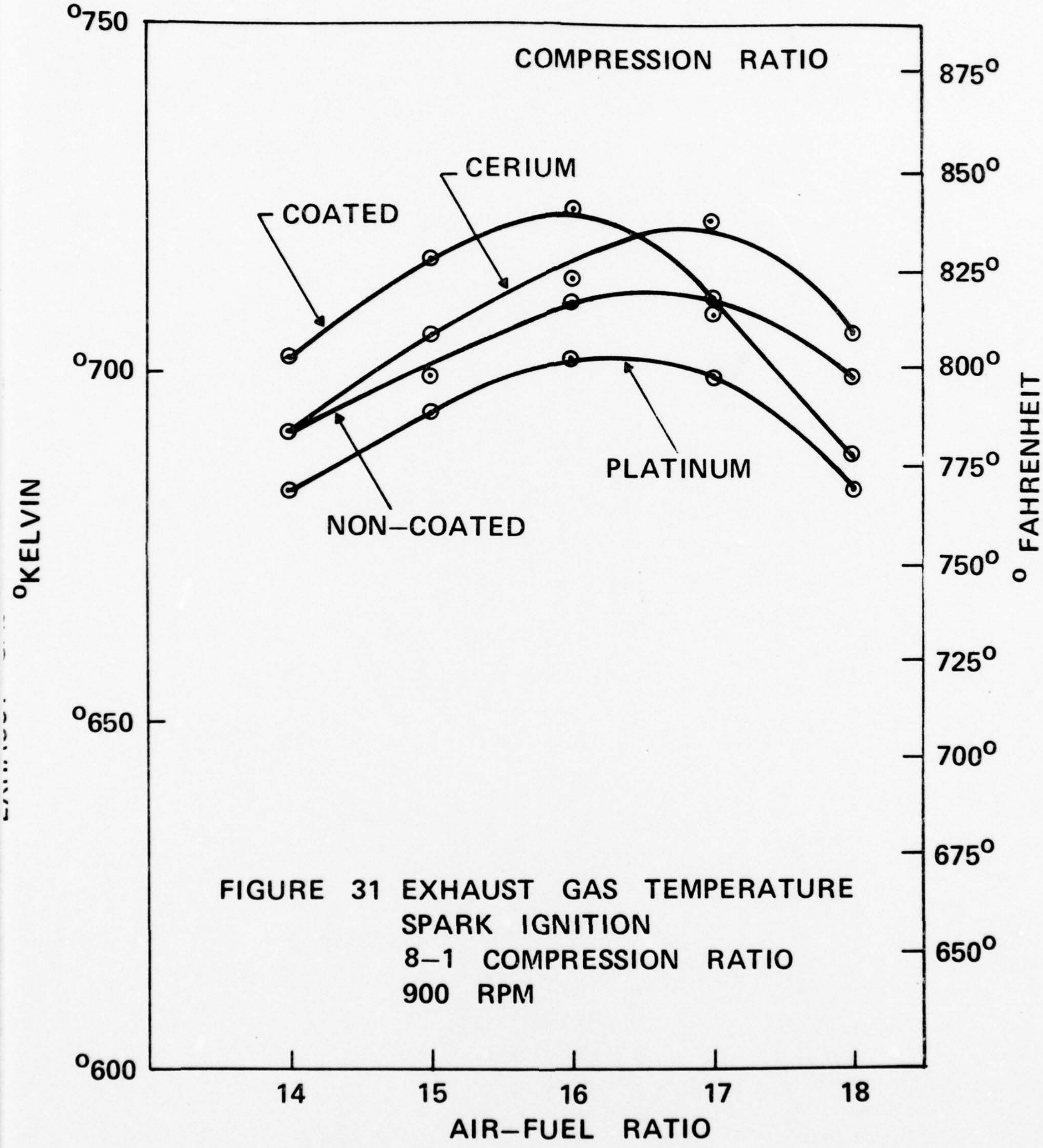

FIGURE 31 EXHAUST GAS TEMPERATURE
SPARK IGNITION
8-1 COMPRESSION RATIO
900 RPM

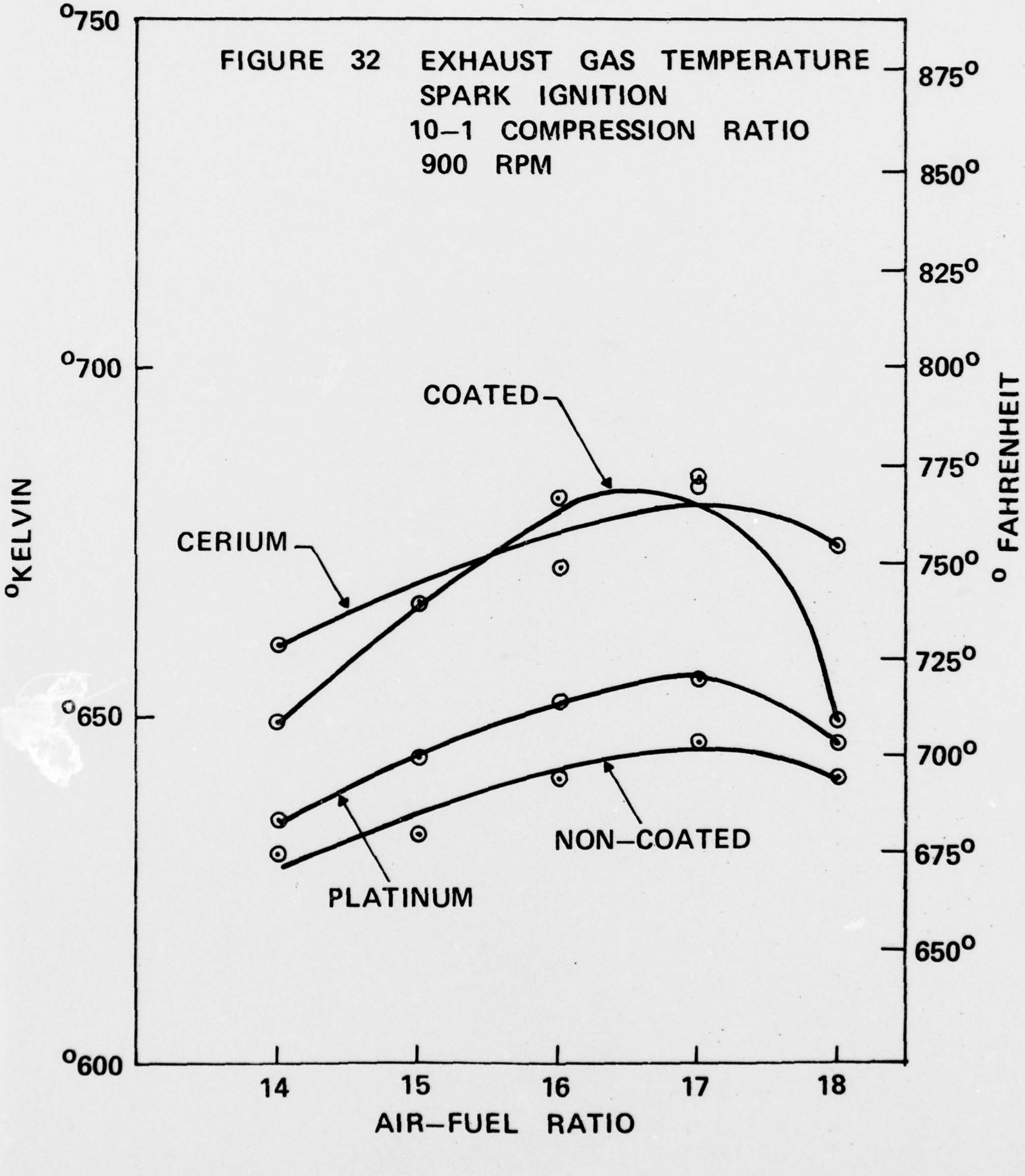

FIGURE 32 EXHAUST GAS TEMPERATURE
SPARK IGNITION
10–1 COMPRESSION RATIO
900 RPM

concentrations as shown in Figures 33 to 38. Again, this trend indicates that the catalytic surfaces acted as a deterrent to preflame reactions and inhibited complete combustion.

Oxides of nitrogen concentration is much the same for non-coated and catalytic performance (see Figures 39 to 41) with a large increase shown for coated operation. The expected peak concentration on the lean side of stoichiometric is found only for coated zirconium performance. The behavior of this data places some doubt on its validity even though it was repeatable and consistent. Additional tests may be justified and may point to an unexpected problem with sample handling.

C-I Data Analysis

Engine power is significantly reduced for C-I operation with zirconium or catalytic coatings as shown in Figures 42 to 46. This unexpected event could be the result of several factors, the most notable being: 1) an increased heating of the new air charge during the intake and compression strokes resulting in an increase in negative compression work, 2) a change in precombustion (catalytic) reactions at the surface that delay and inhibit combustion, and 3) an absorption of impinging fuel into the porous ceramic coating causing late and incomplete combustion.

While all of the above factors probably play a role in the poorer coated and catalytic performance, it is believed that the third is the most influential. Impingement has been a significant problem in C-I operation due to the open chamber design. The small bore cylindrical shaped combustion chamber as well as the side location of the injector produces some degree of impingement even with an improved injector hole arrangement. This impingement is far more critical on a porous ceramic surface where a portion of the fuel can be absorbed than on a smooth metal where it remains in intimate contact with the combustion

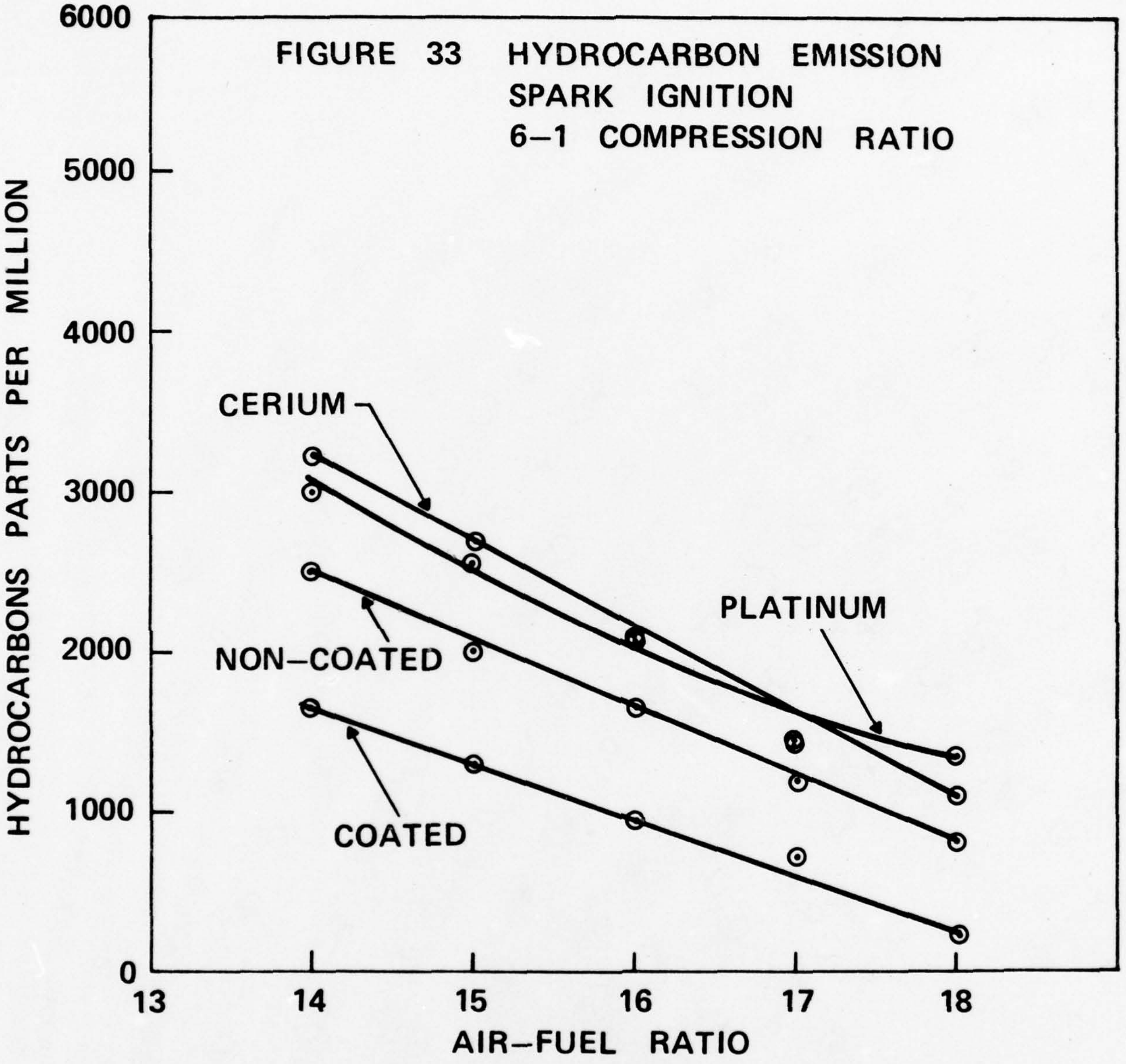
FIGURE 33 HYDROCARBON EMISSION
SPARK IGNITION
6–1 COMPRESSION RATIO

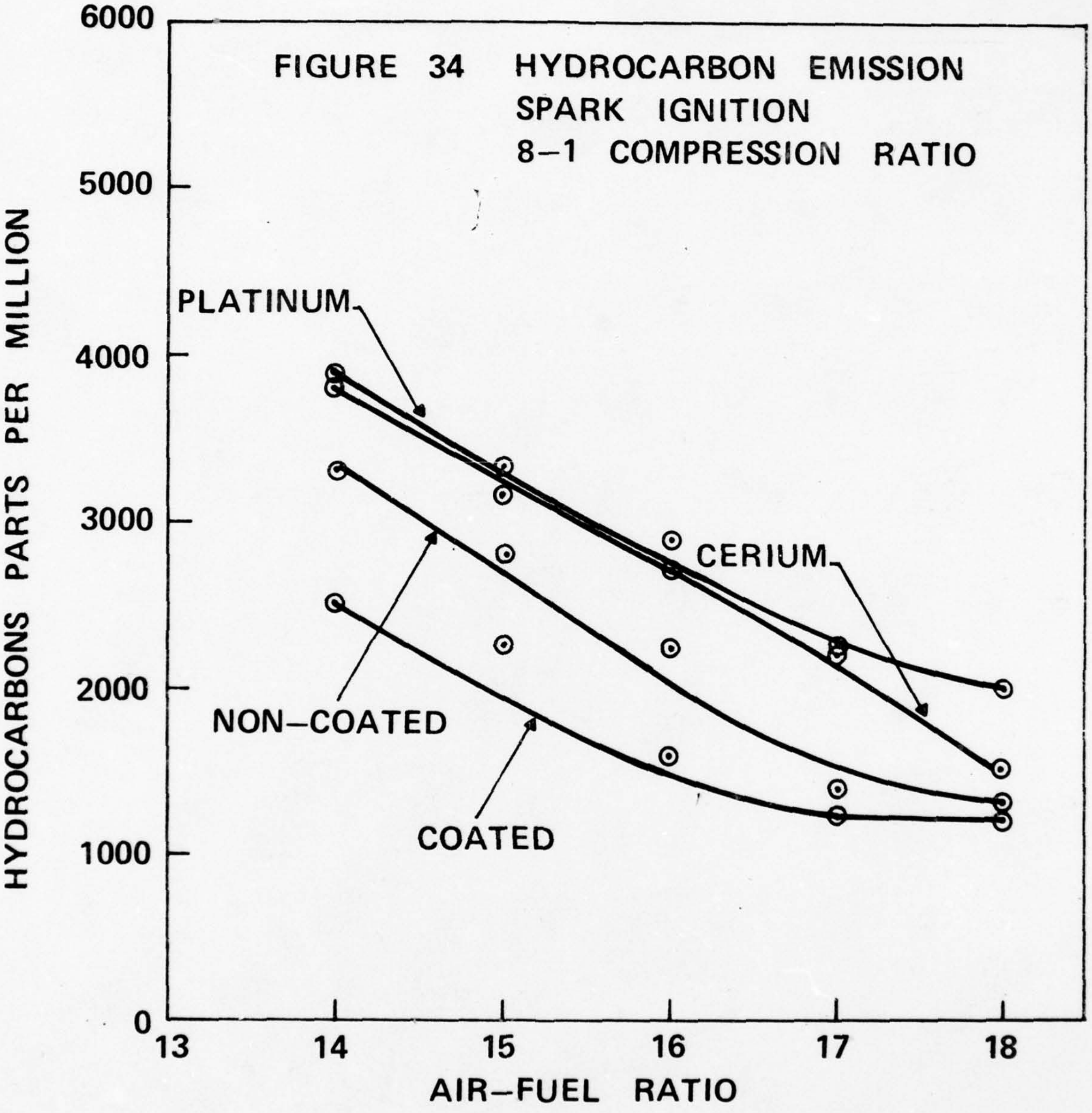

FIGURE 34 HYDROCARBON EMISSION
SPARK IGNITION
8–1 COMPRESSION RATIO

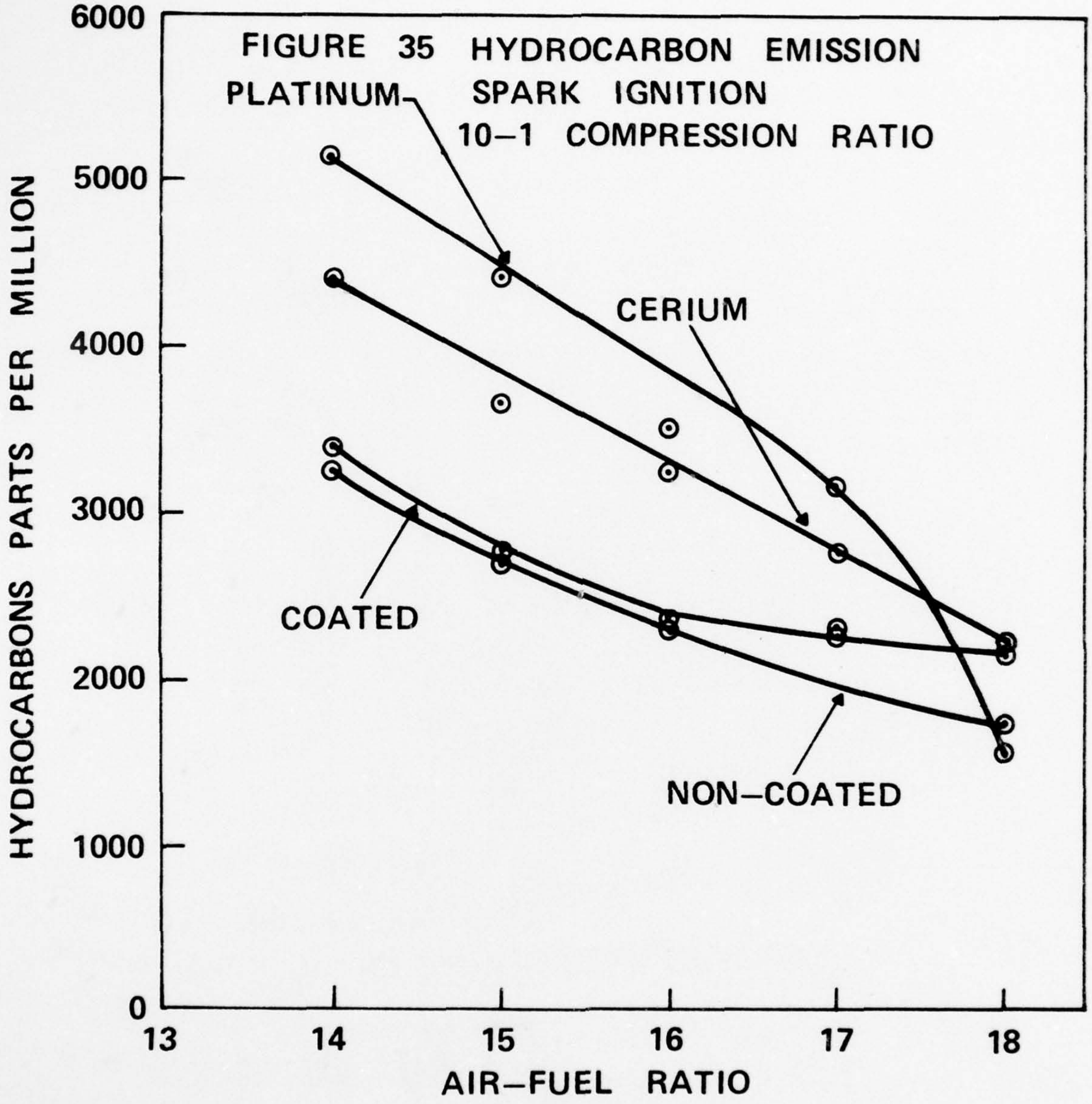
FIGURE 35 HYDROCARBON EMISSION
SPARK IGNITION
10–1 COMPRESSION RATIO
PLATINUM
CERIUM
COATED
NON–COATED
HYDROCARBONS PARTS PER MILLION
6000
5000
4000
3000
2000
1000
0
13
14
15
16
17
18
AIR–FUEL RATIO

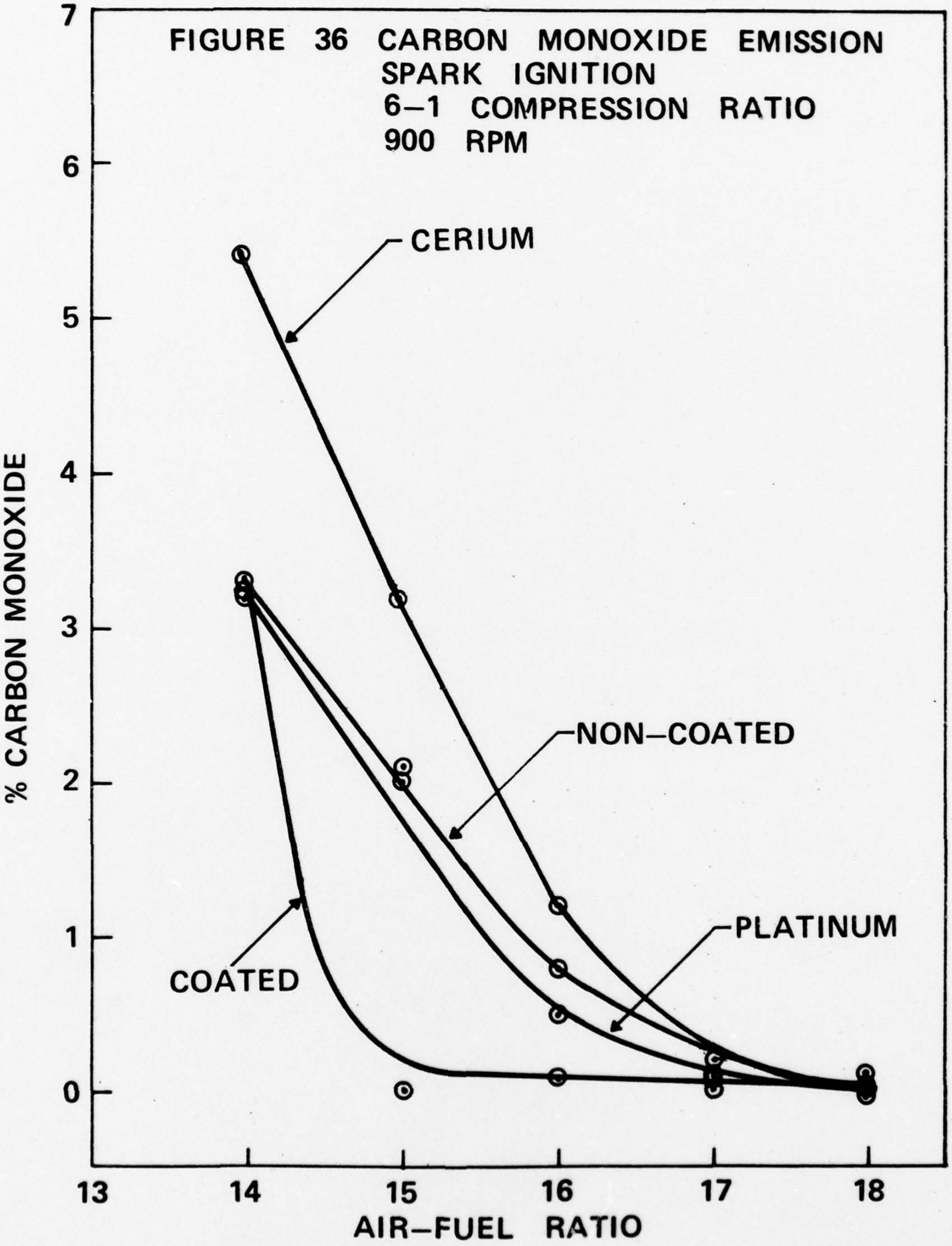

FIGURE 36 CARBON MONOXIDE EMISSION
SPARK IGNITION
6–1 COMPRESSION RATIO
900 RPM

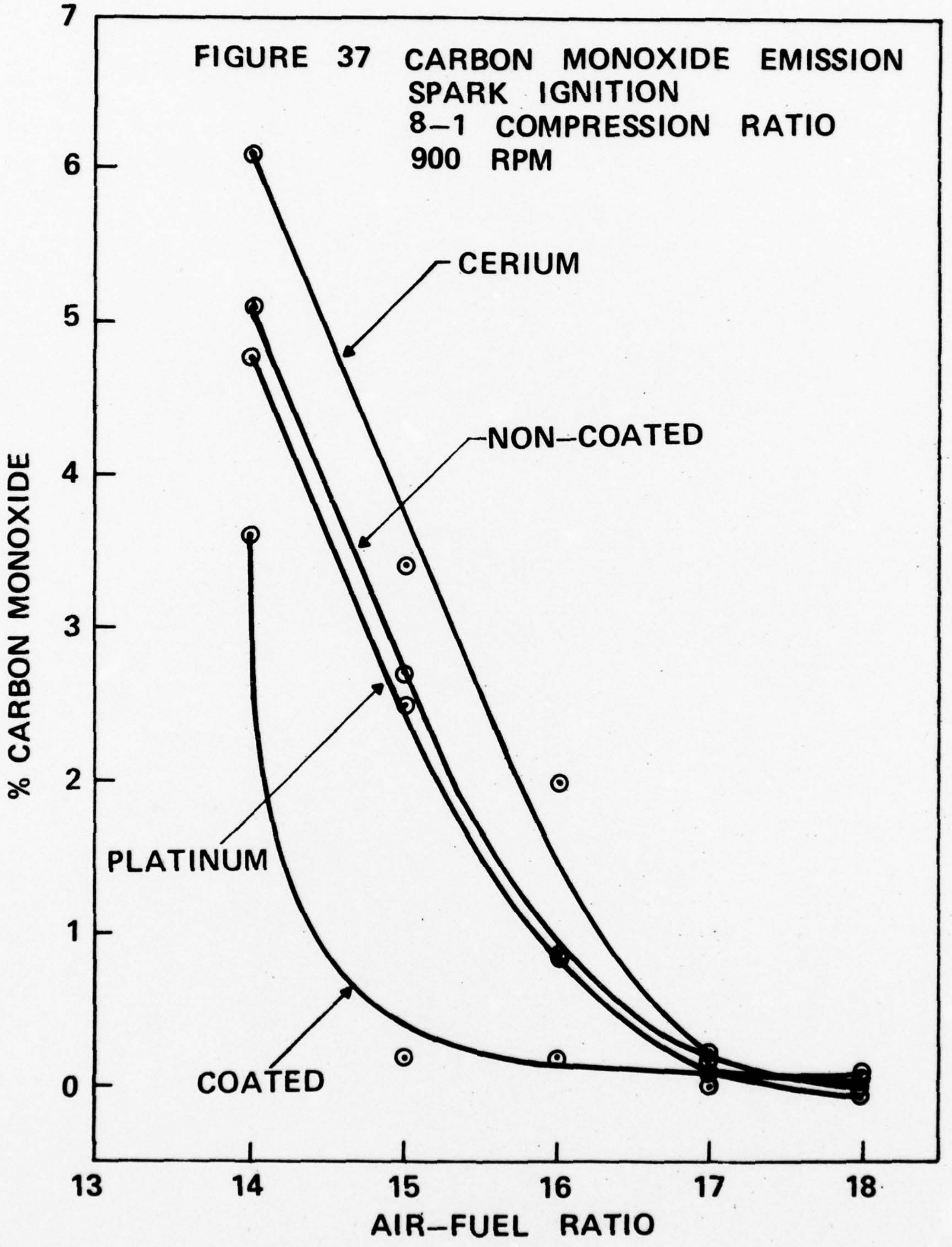

FIGURE 37 CARBON MONOXIDE EMISSION
SPARK IGNITION
8–1 COMPRESSION RATIO
900 RPM

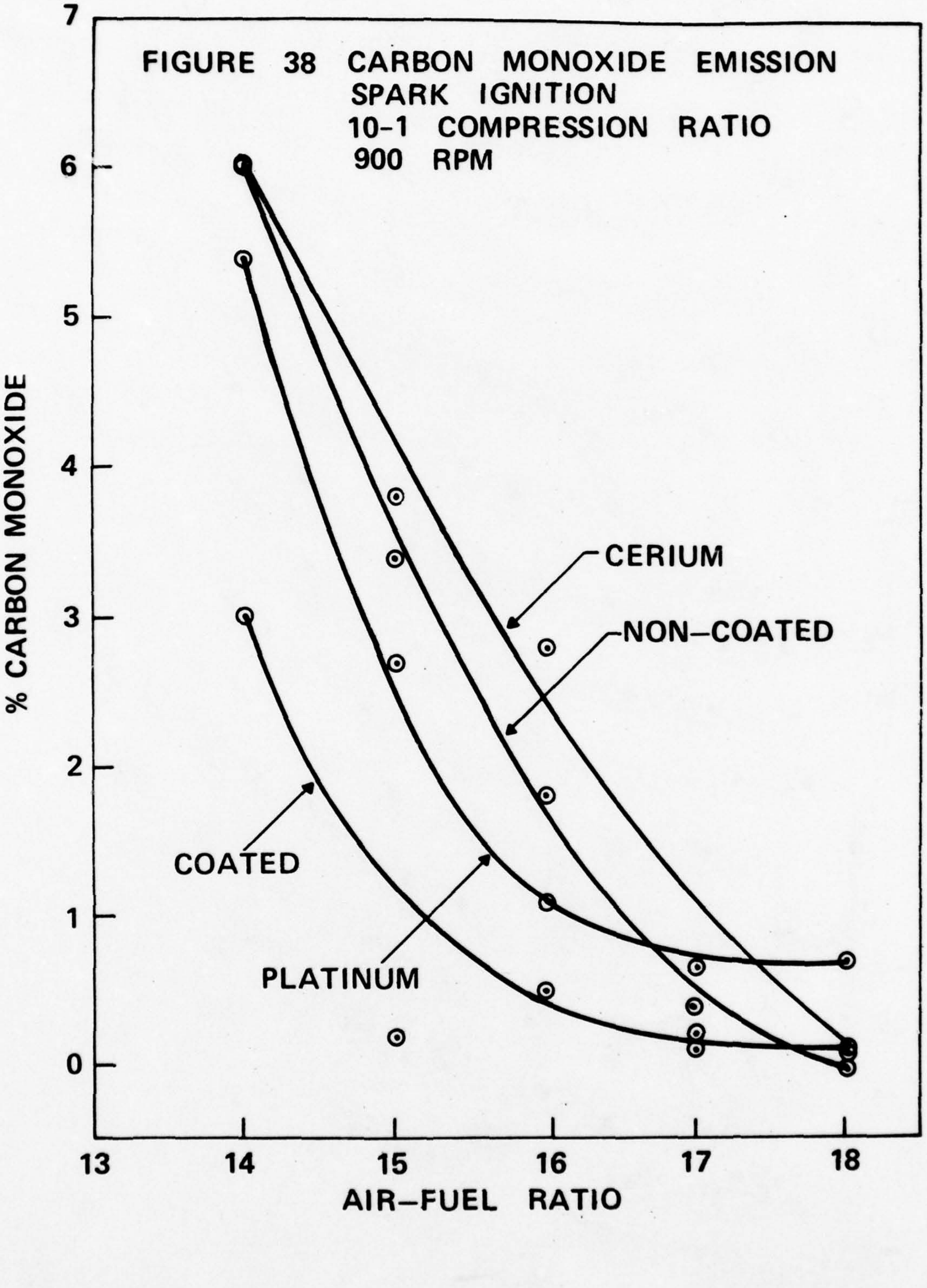

FIGURE 38 CARBON MONOXIDE EMISSION
SPARK IGNITION
10-1 COMPRESSION RATIO
900 RPM

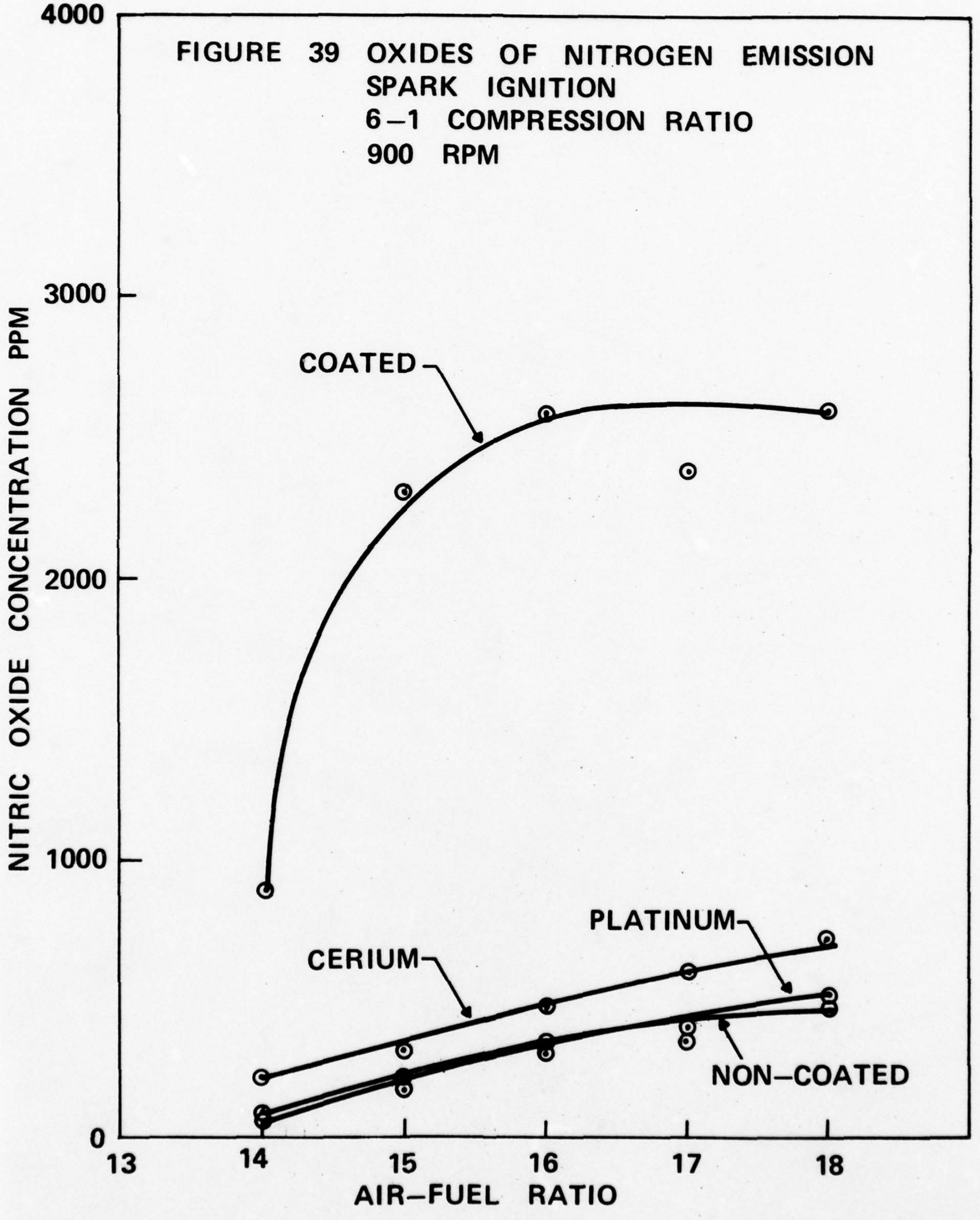

FIGURE 39 OXIDES OF NITROGEN EMISSION
SPARK IGNITION
6–1 COMPRESSION RATIO
900 RPM

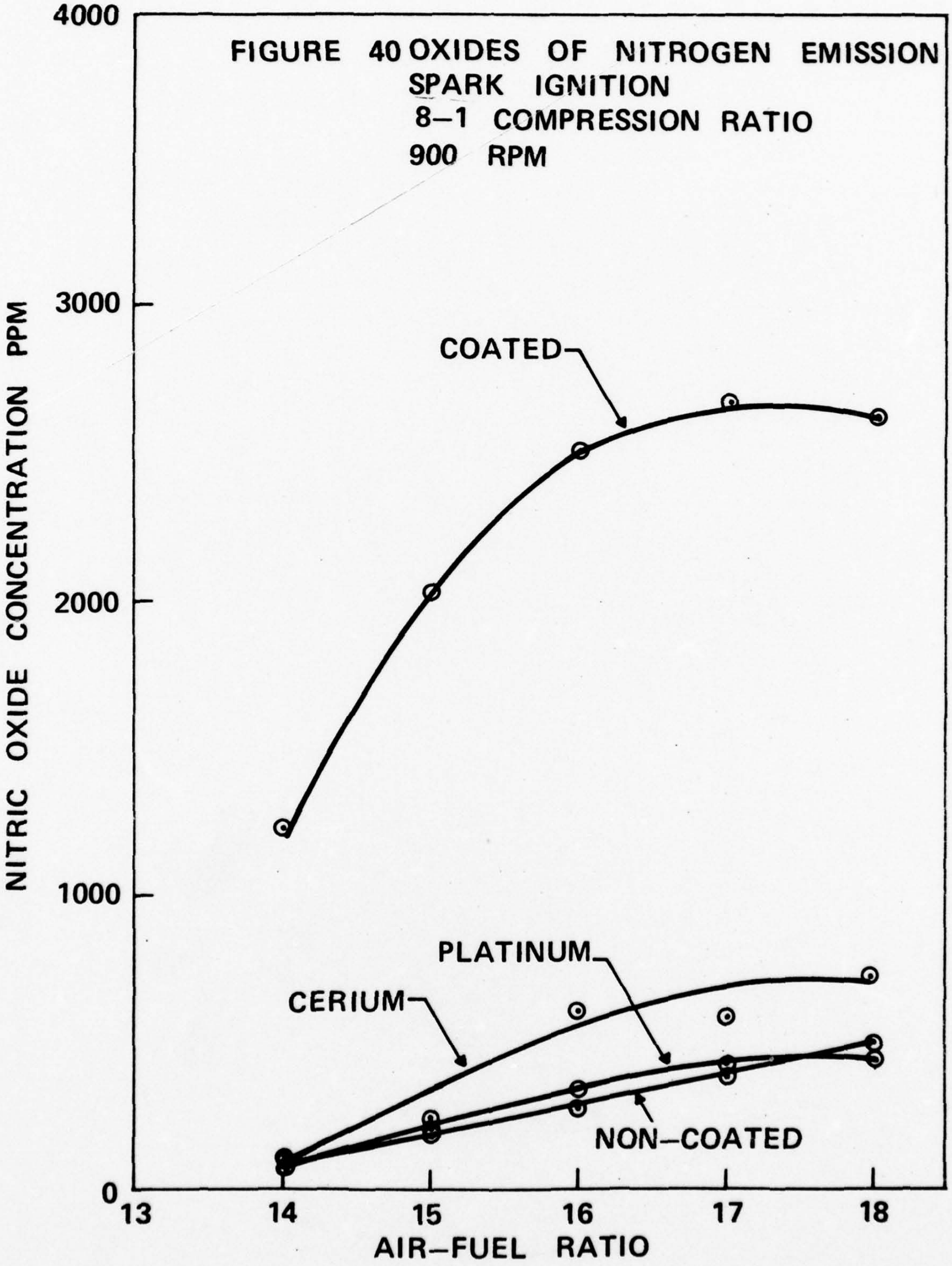

FIGURE 40 OXIDES OF NITROGEN EMISSION
SPARK IGNITION
8–1 COMPRESSION RATIO
900 RPM

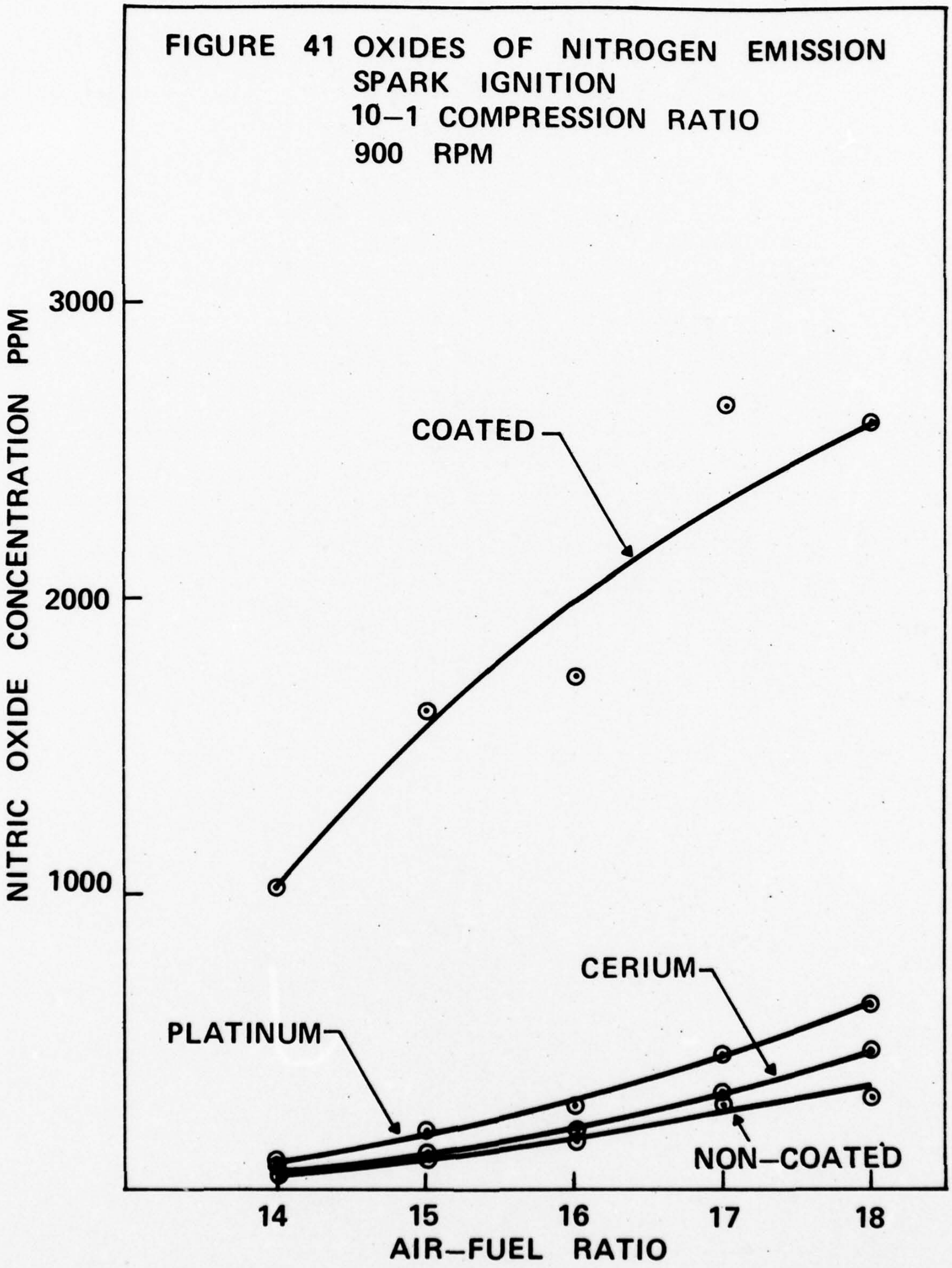

FIGURE 41 OXIDES OF NITROGEN EMISSION
SPARK IGNITION
10–1 COMPRESSION RATIO
900 RPM

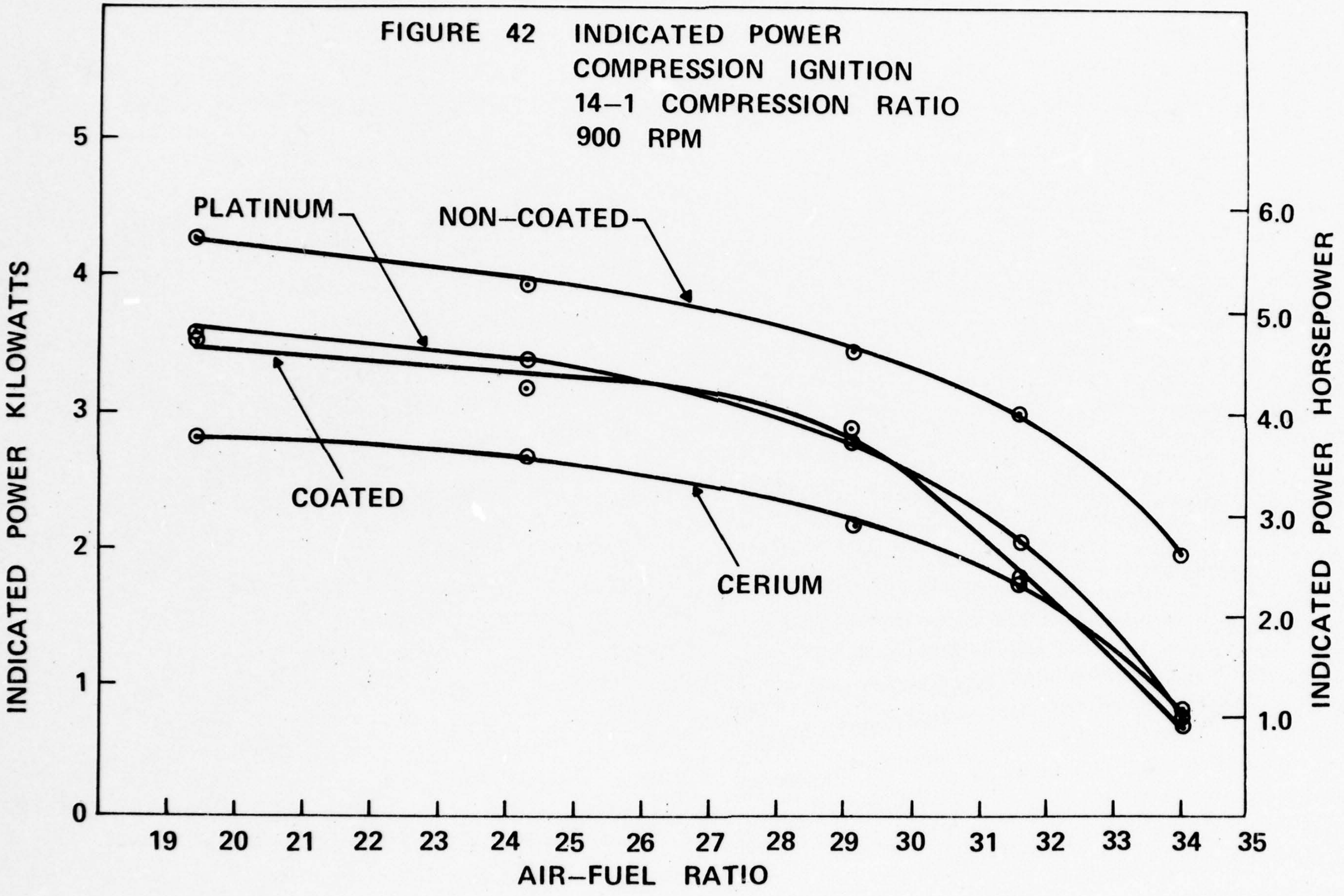
FIGURE 42 INDICATED POWER
COMPRESSION IGNITION
14–1 COMPRESSION RATIO
900 RPM

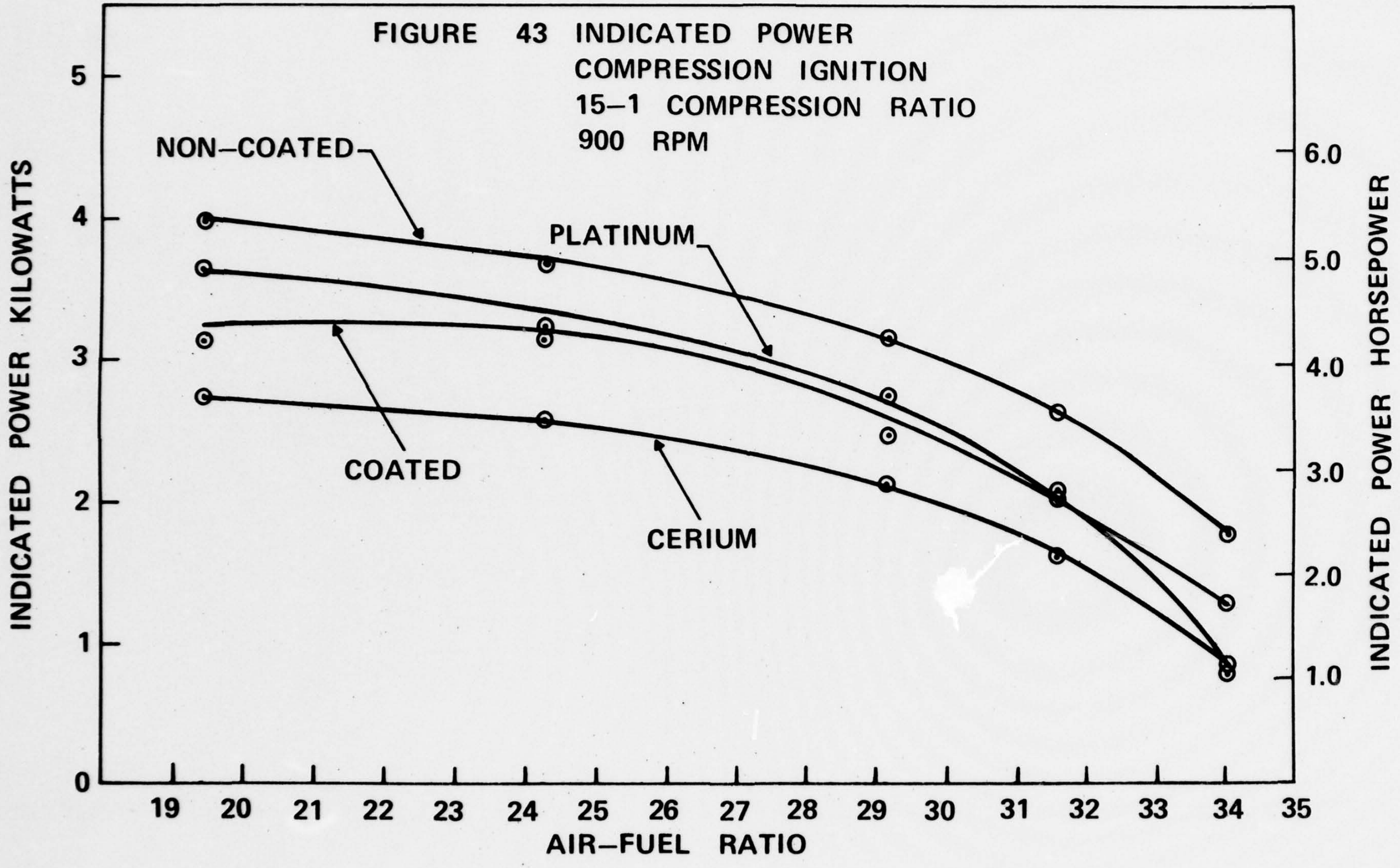

FIGURE 43 INDICATED POWER
COMPRESSION IGNITION
15–1 COMPRESSION RATIO
900 RPM

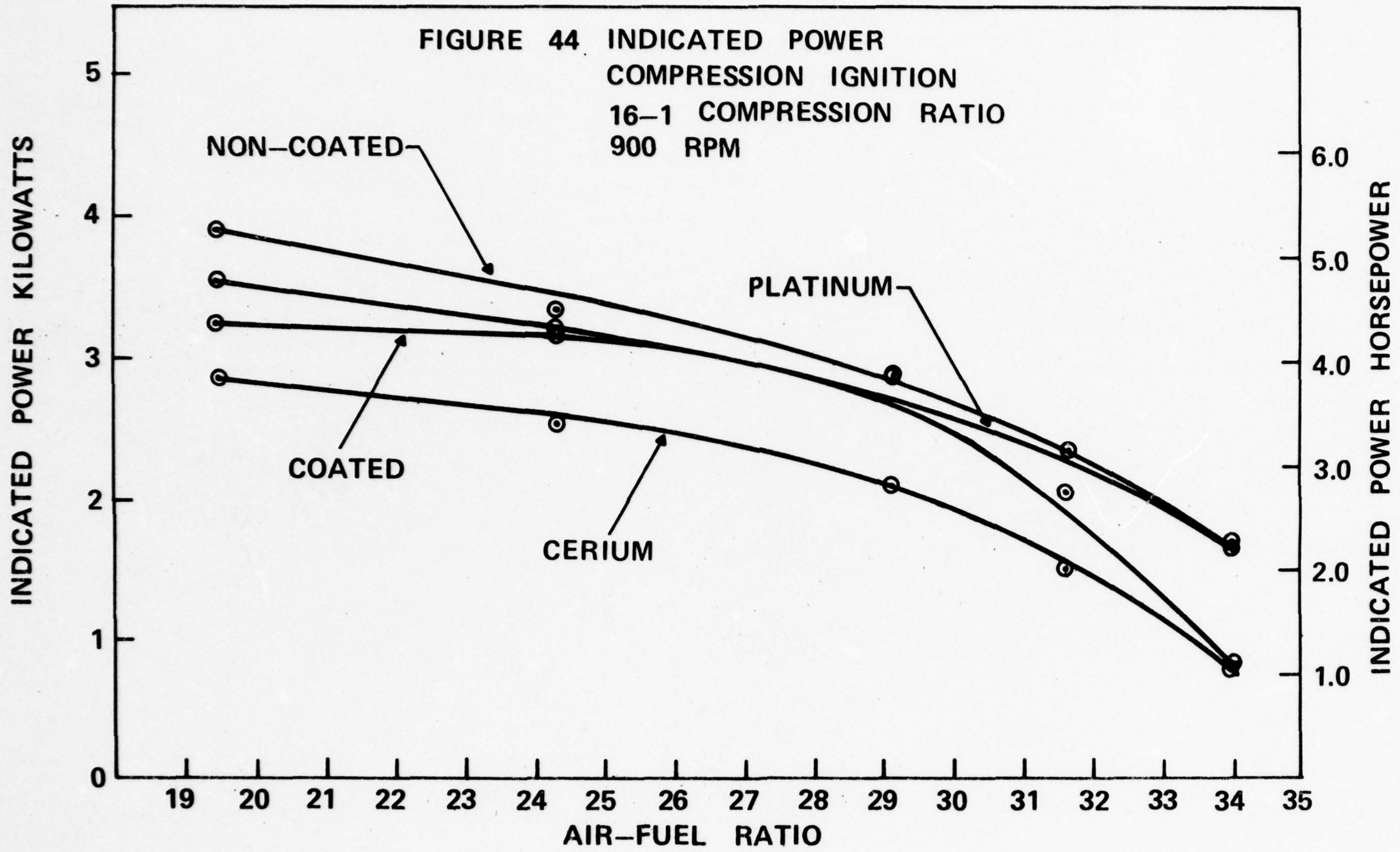

FIGURE 44 INDICATED POWER
COMPRESSION IGNITION
16–1 COMPRESSION RATIO
900 RPM

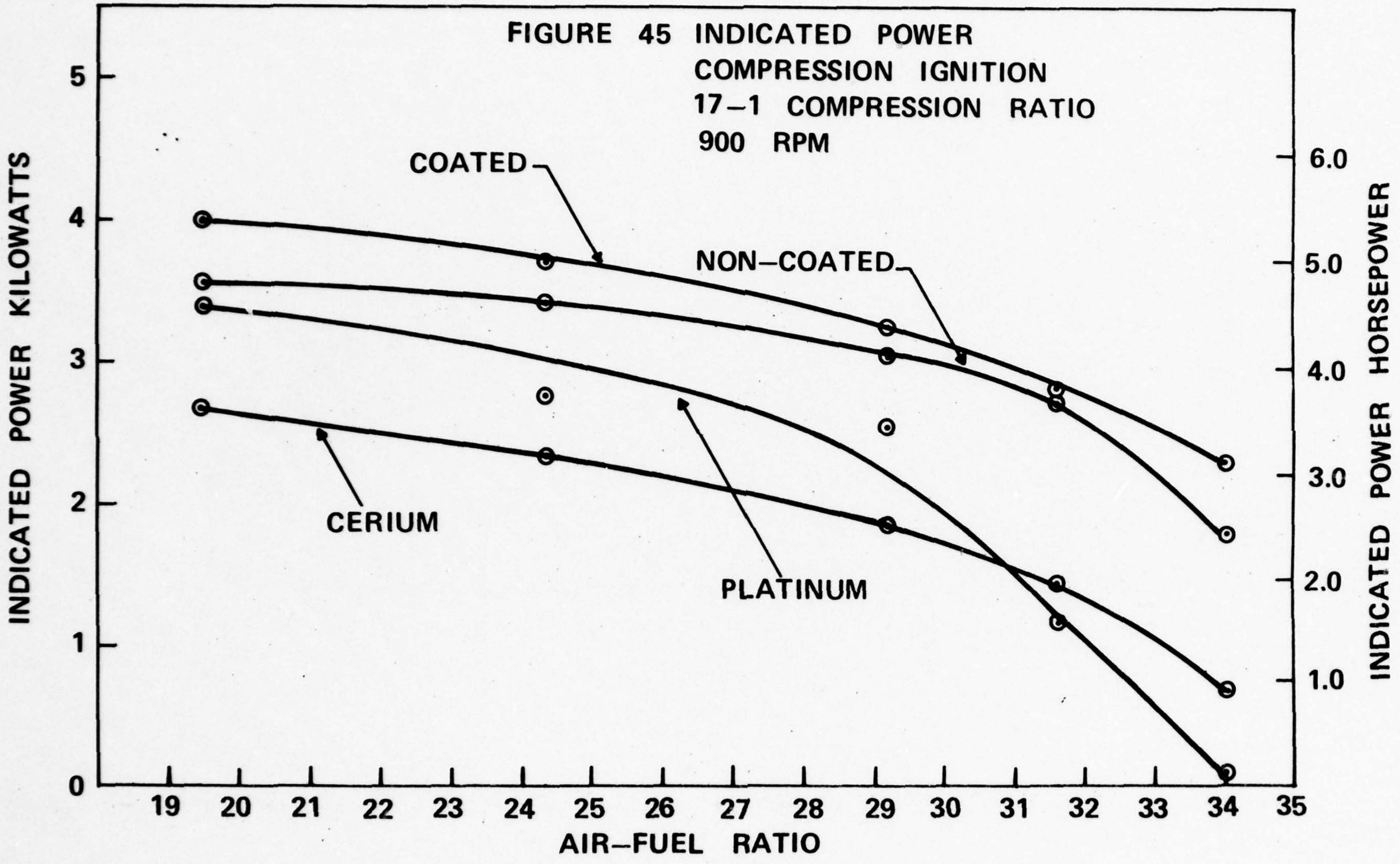

FIGURE 45 INDICATED POWER
COMPRESSION IGNITION
17–1 COMPRESSION RATIO
900 RPM

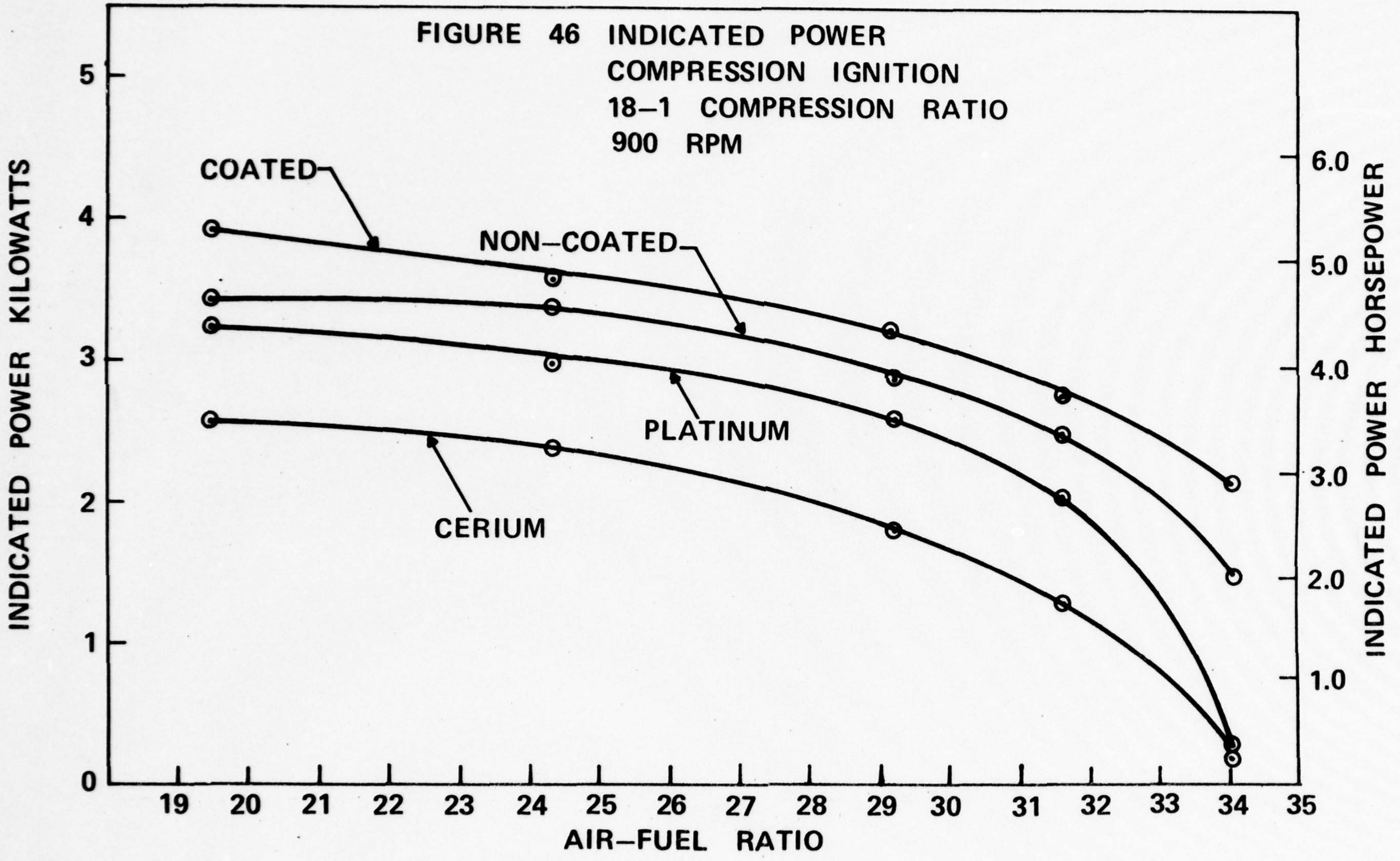

FIGURE 46 INDICATED POWER
COMPRESSION IGNITION
18–1 COMPRESSION RATIO
900 RPM

air.

It seems likely that modifications in combustion chamber and injection design can promote better combustion and produce increased power. An open chamber with a central injector location or a pre-combustion chamber design should prevent impingement and combustion problems and produce the performance improvements seen in S-I operation and predicted by theory.

Figures 47 to 51 portray fuel consumption characteristics for C-I operation. The greater power output of non-coated operation produces the lowest fuel consumption that in turn correlates with the above discussion on engine output.

Compression ignition exhaust gas temperature characteristics (see Figures 57 to 61) for coated, non-coated, and catalytic performance follow expected and predictable trends with non-coated operation generally at the lowest value. This behavior would agree with and compliment the above discussion relating to delayed combustion caused by impingement and catalysts. Note, that as the A-F becomes quite lean the EGT suddenly increases dramatically. This phenomenon is explained by a weak combustion process that propagates a delayed inflammation that, in turn, exists into the exhaust valve opening interval.

Hydrocarbon emissions generally indicate that the catalytic surfaces are effective in reducing exhaust contaminants as shown in Figures 62 to 66.

This trend in conjunction with the CO emissions of Figures 67 to 71 and the EGT data indicates that the zirconium and catalytic surfaces do not prevent complete combustion they only slow down the rate, producing generally higher EGT with lower contaminant concentrations downstream at the exhaust gas sampling station.

Nitric oxide emissions (see Figures 72 to 76) are much less in C-I than in S-I operation, with catalytic exhaust still producing dramatically lower

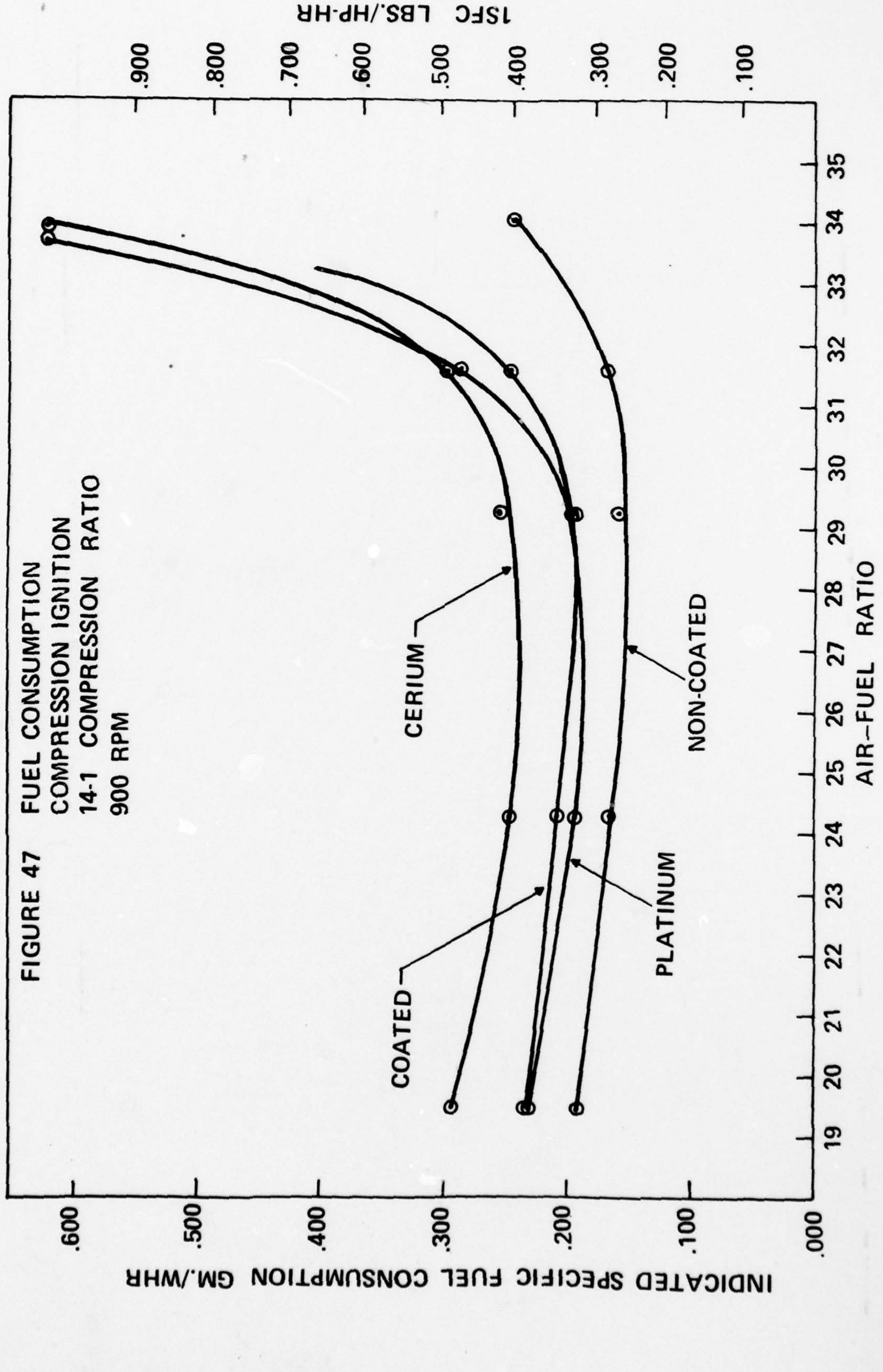

FIGURE 47 FUEL CONSUMPTION COMPRESSION IGNITION 14-1 COMPRESSION RATIO 900 RPM

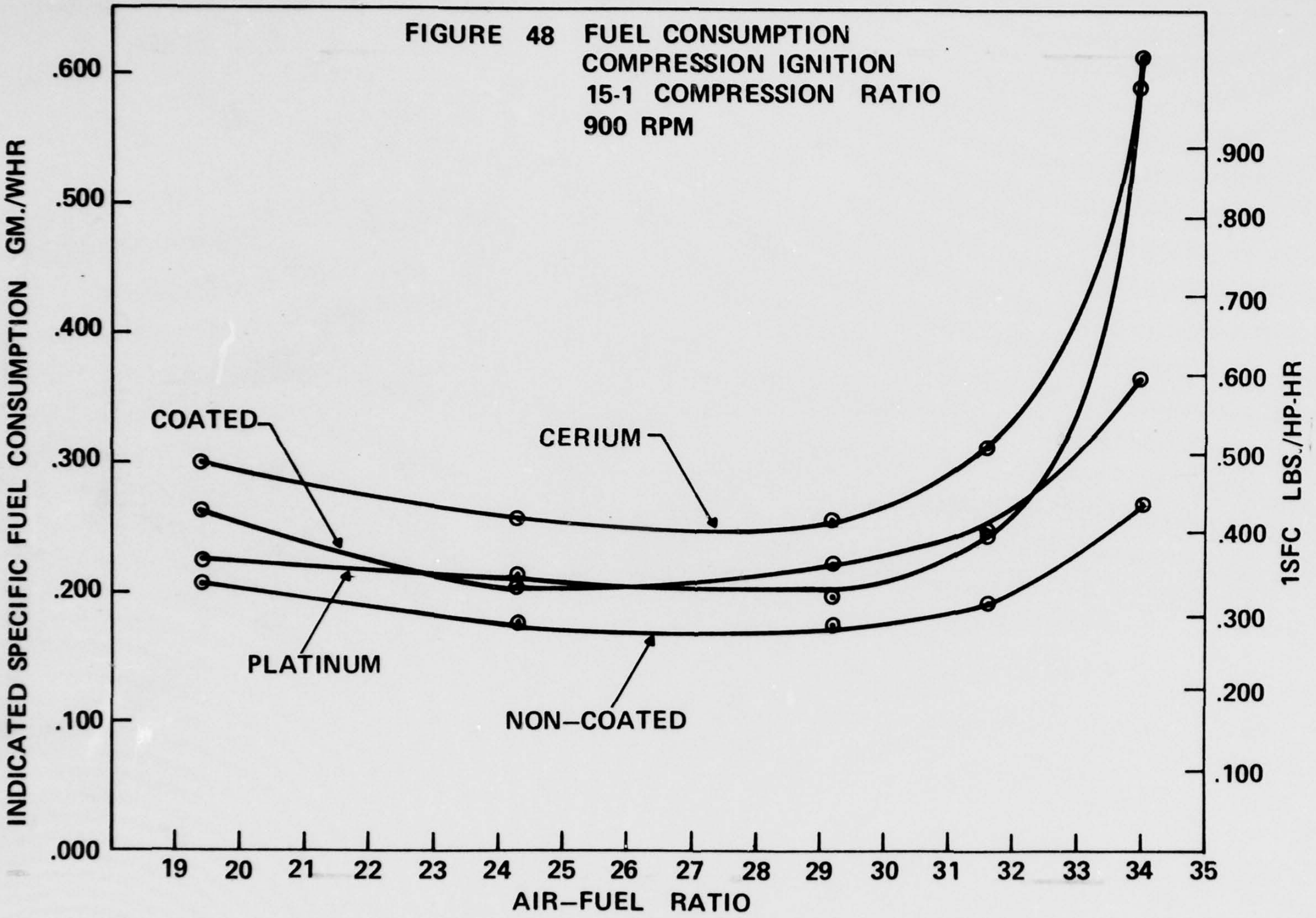

FIGURE 48 FUEL CONSUMPTION
COMPRESSION IGNITION
15-1 COMPRESSION RATIO
900 RPM

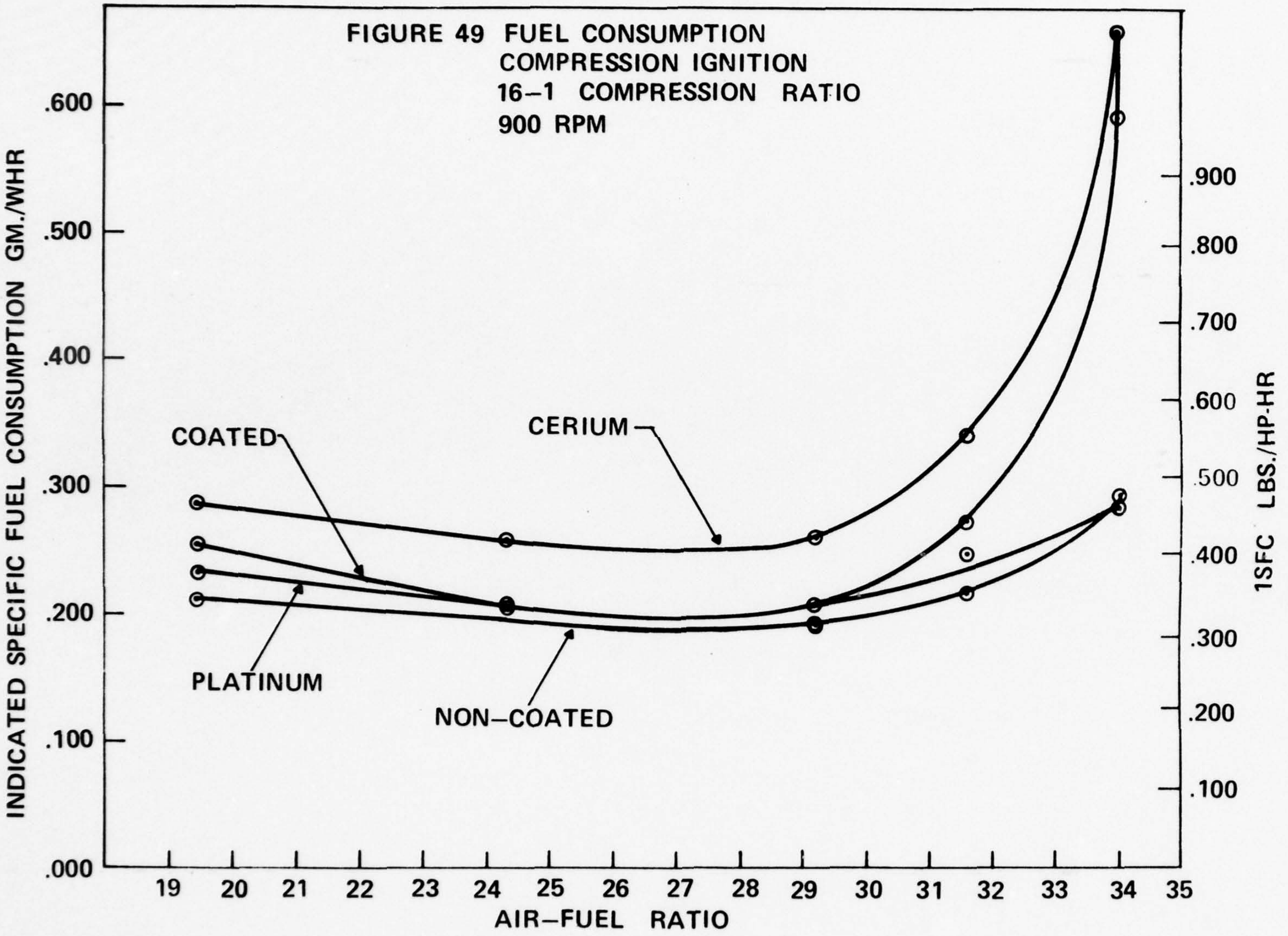

FIGURE 49 FUEL CONSUMPTION
COMPRESSION IGNITION
16–1 COMPRESSION RATIO
900 RPM

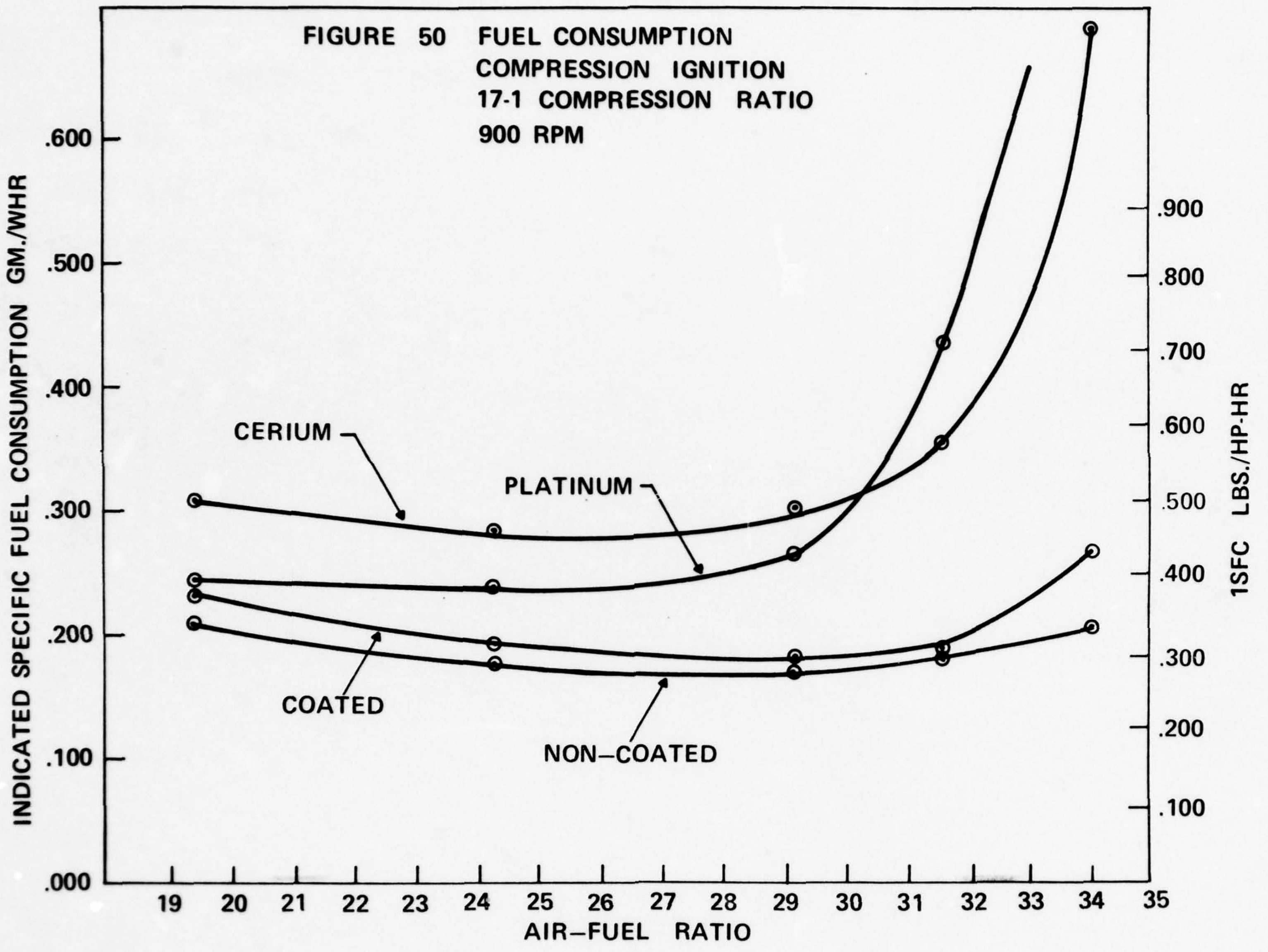

FIGURE 50 FUEL CONSUMPTION
COMPRESSION IGNITION
17-1 COMPRESSION RATIO
900 RPM

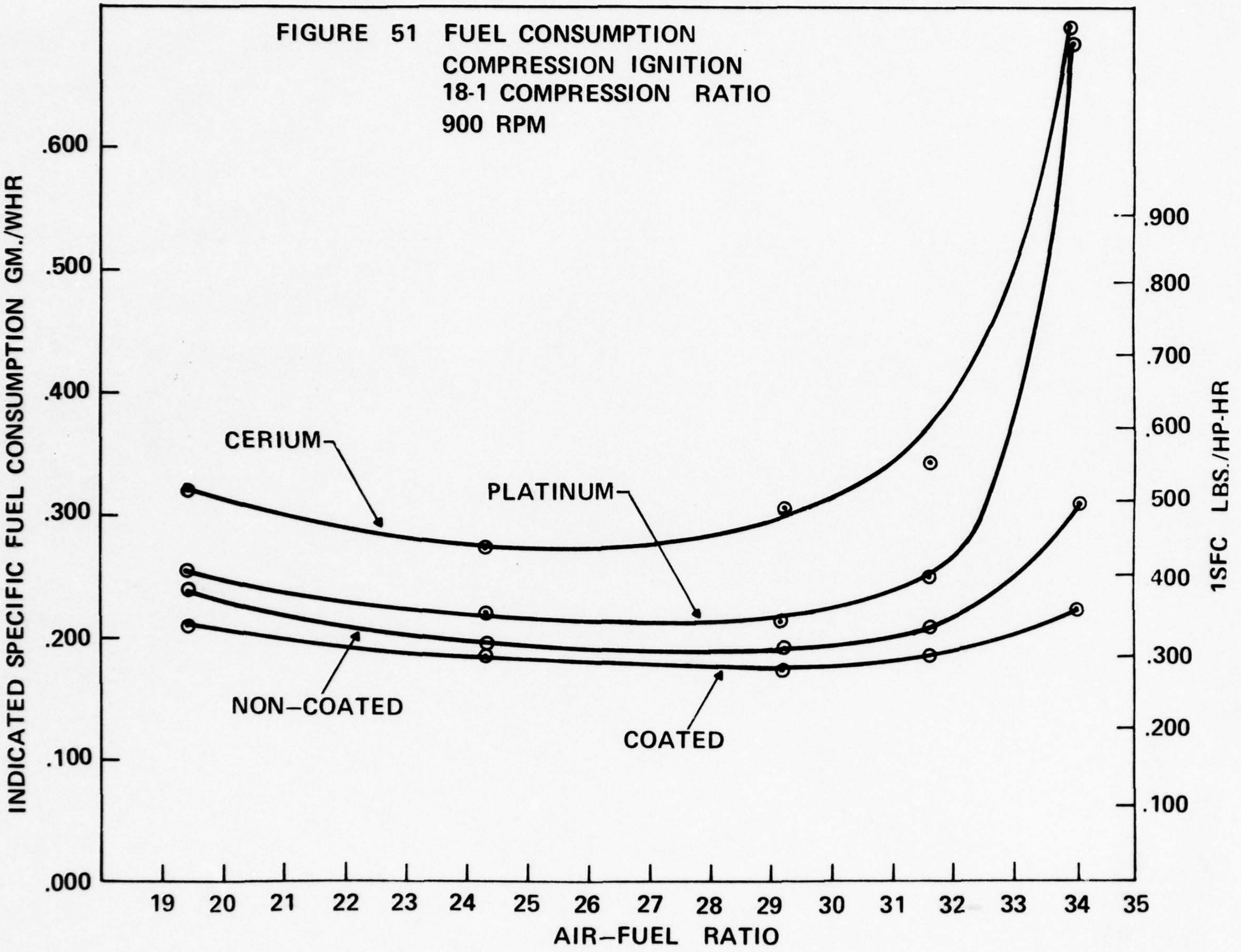
FIGURE 51 FUEL CONSUMPTION
COMPRESSION IGNITION
18-1 COMPRESSION RATIO
900 RPM

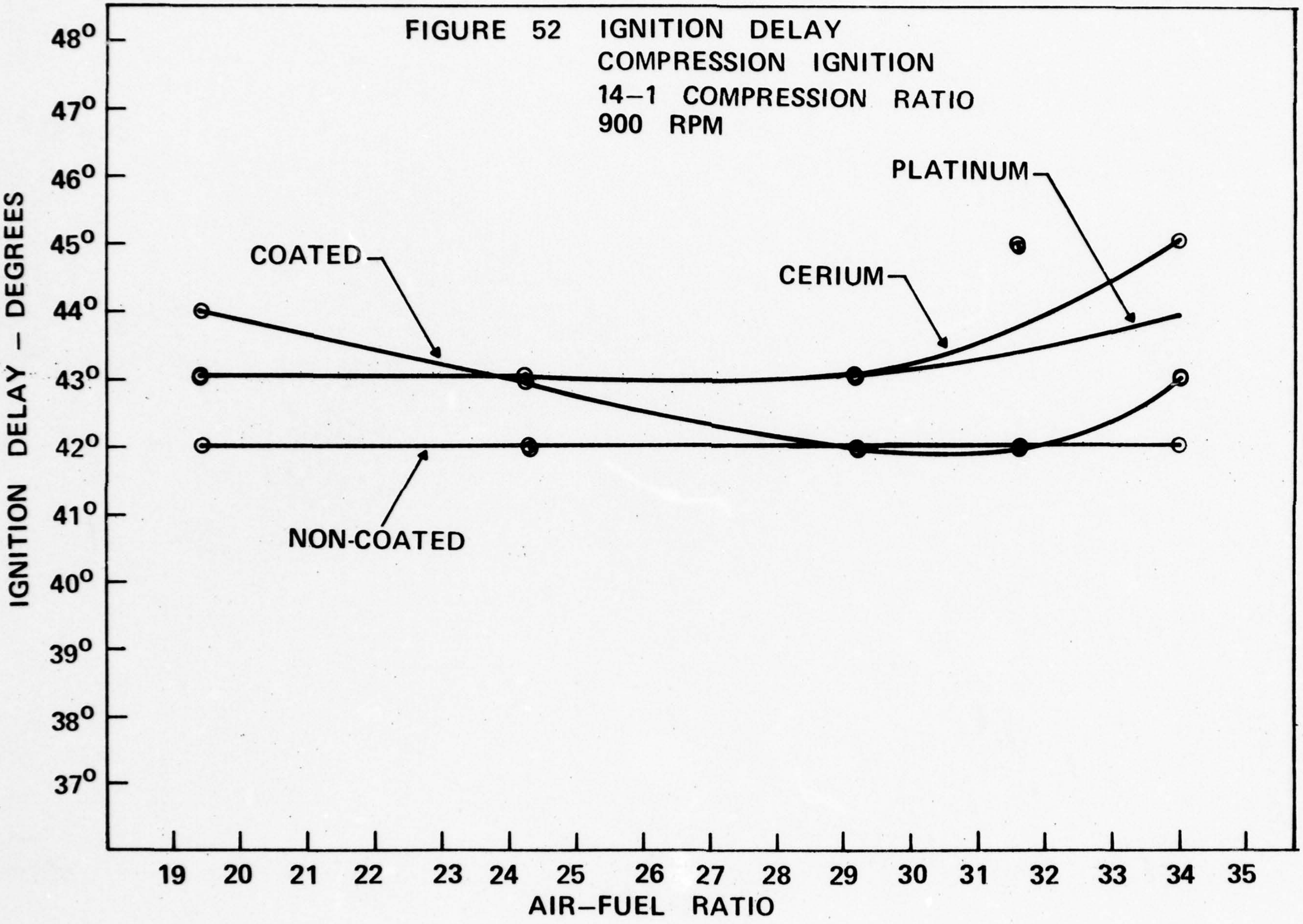

FIGURE 52 IGNITION DELAY
COMPRESSION IGNITION
14–1 COMPRESSION RATIO
900 RPM

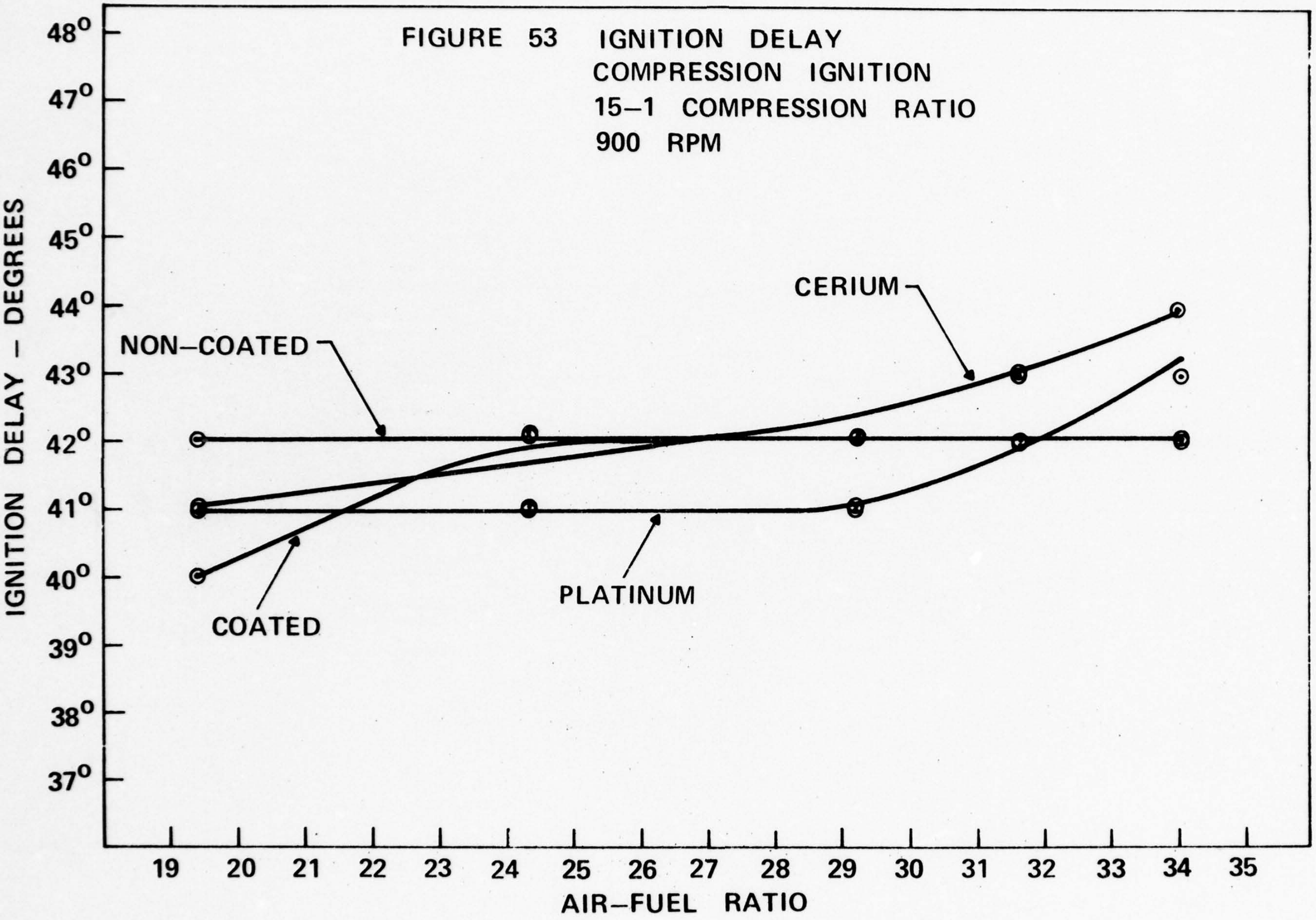

FIGURE 53 IGNITION DELAY
COMPRESSION IGNITION
15–1 COMPRESSION RATIO
900 RPM

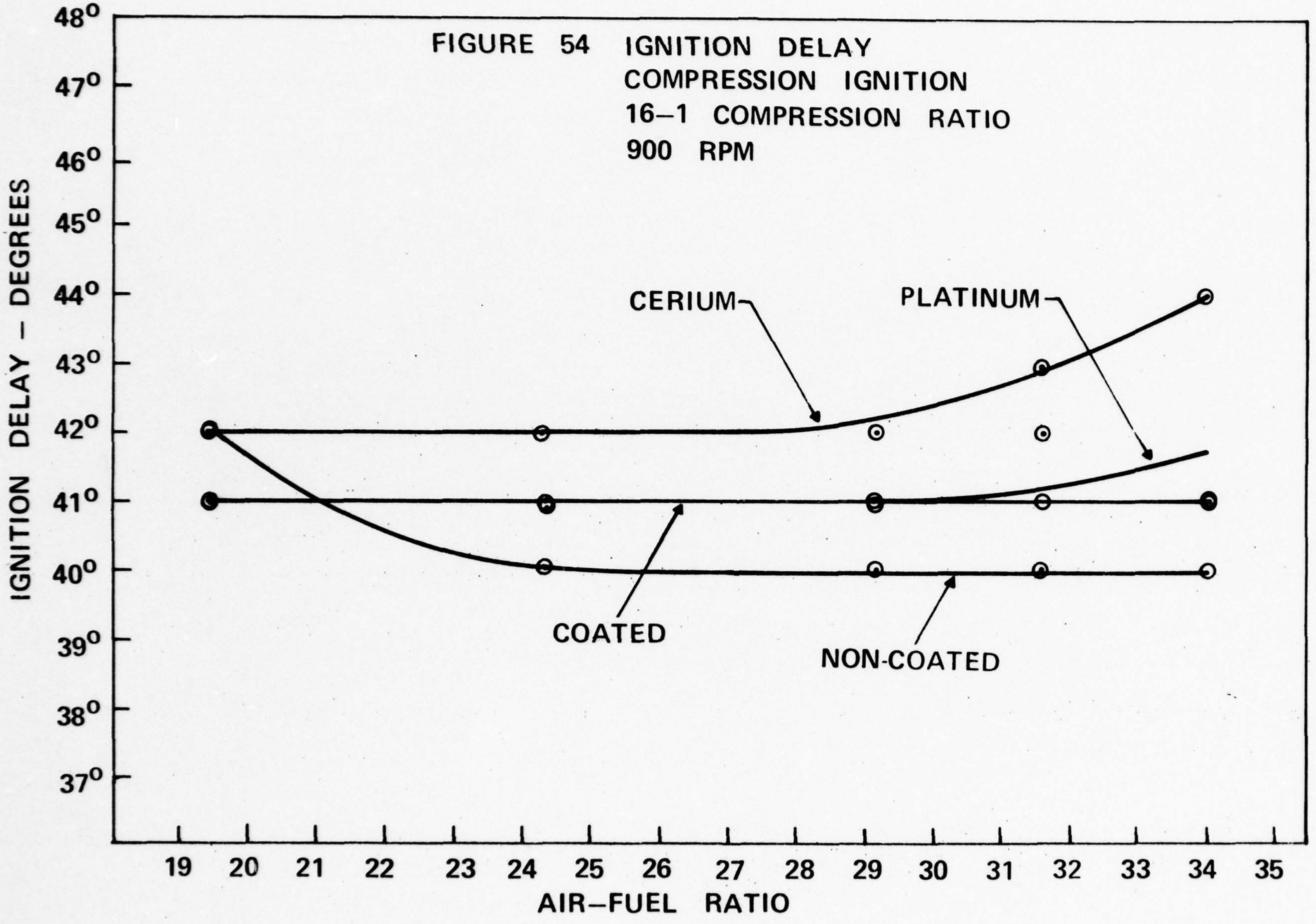

FIGURE 54 IGNITION DELAY
COMPRESSION IGNITION
16–1 COMPRESSION RATIO
900 RPM

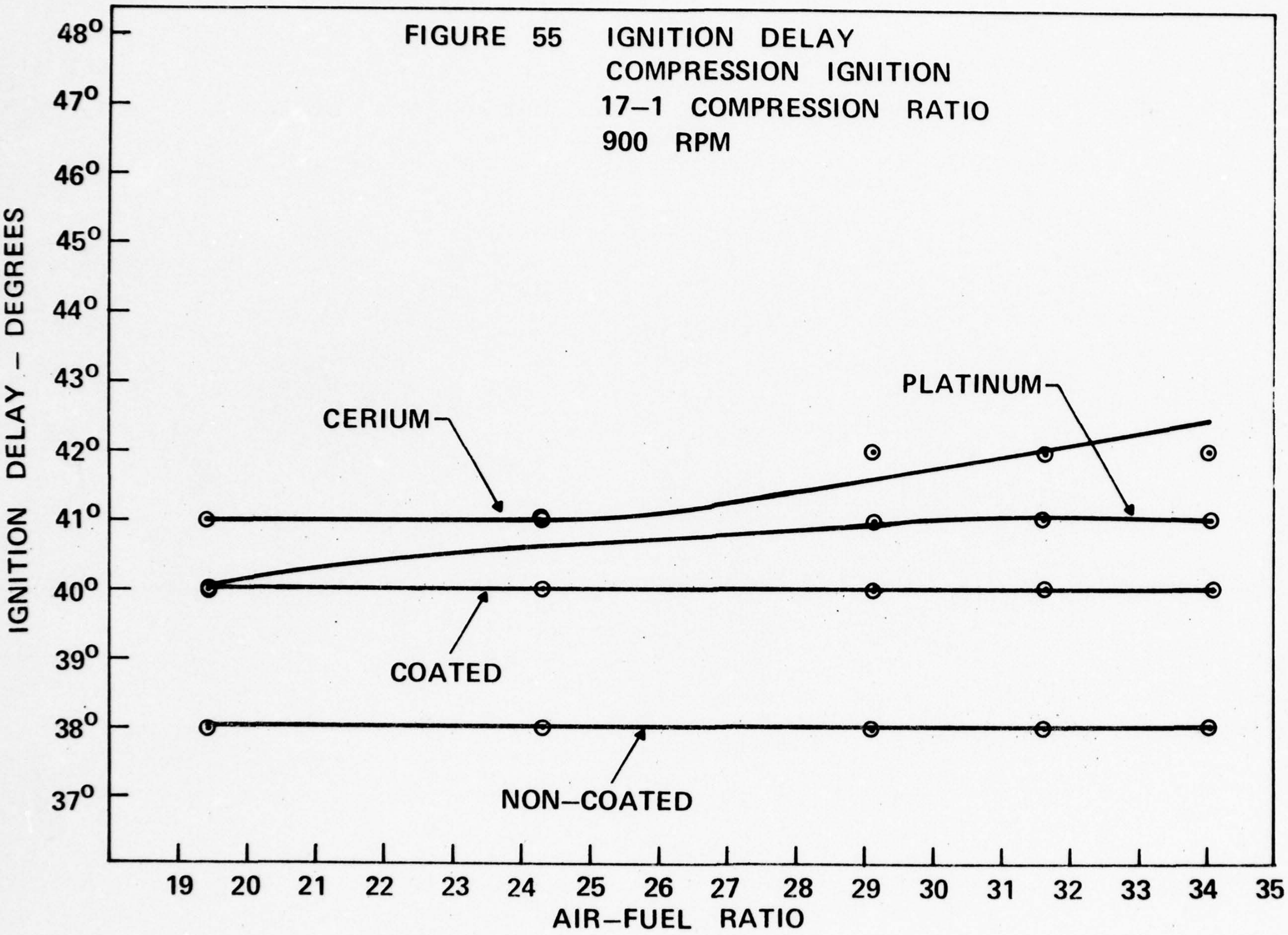

FIGURE 55 IGNITION DELAY
COMPRESSION IGNITION
17–1 COMPRESSION RATIO
900 RPM

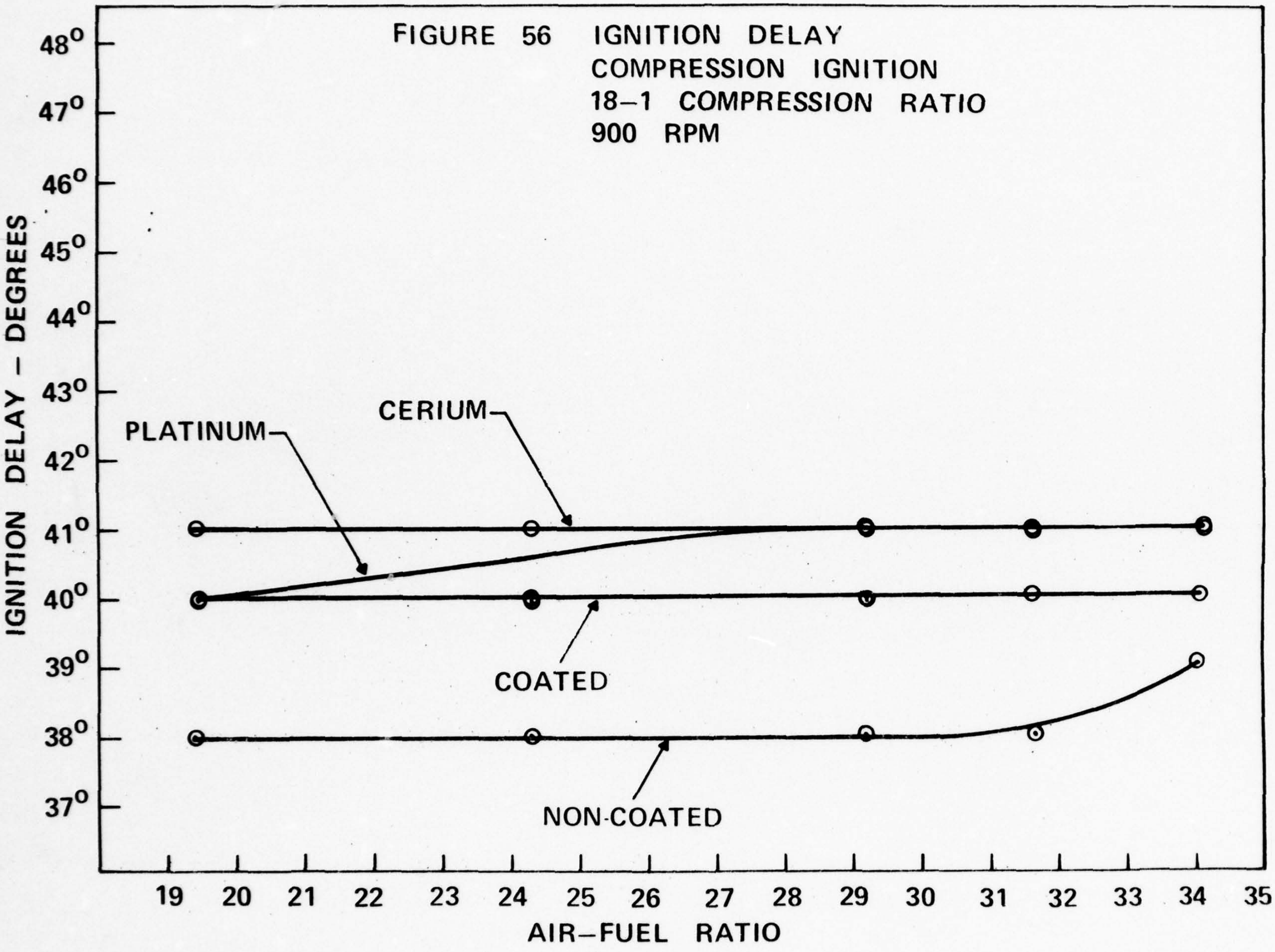

FIGURE 56 IGNITION DELAY
COMPRESSION IGNITION
18–1 COMPRESSION RATIO
900 RPM

FIGURE 57 EXHAUST GAS TEMPERATURE
COMPRESSION IGNITION
14–1 COMPRESSION RATIO
900 RPM

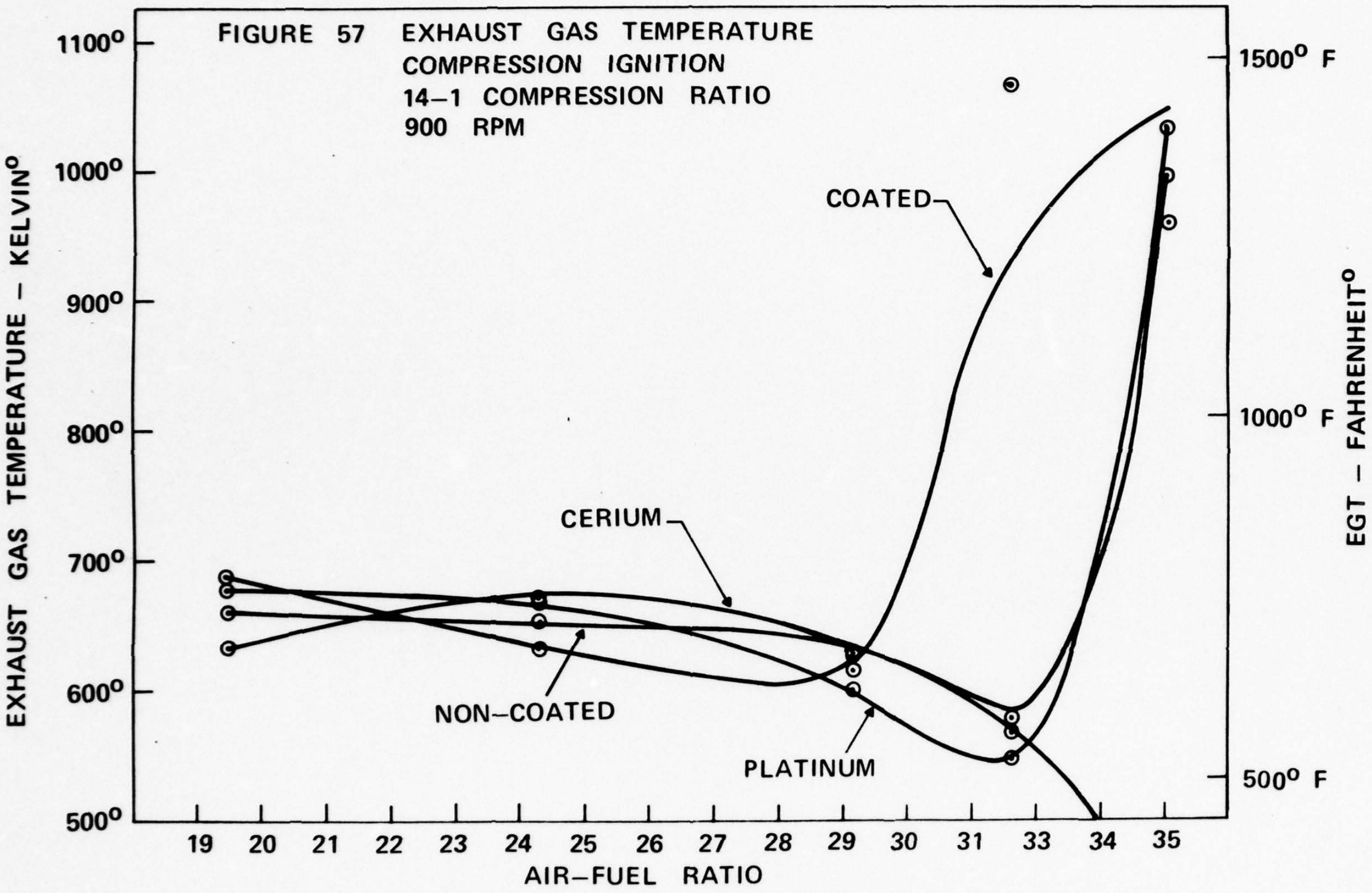

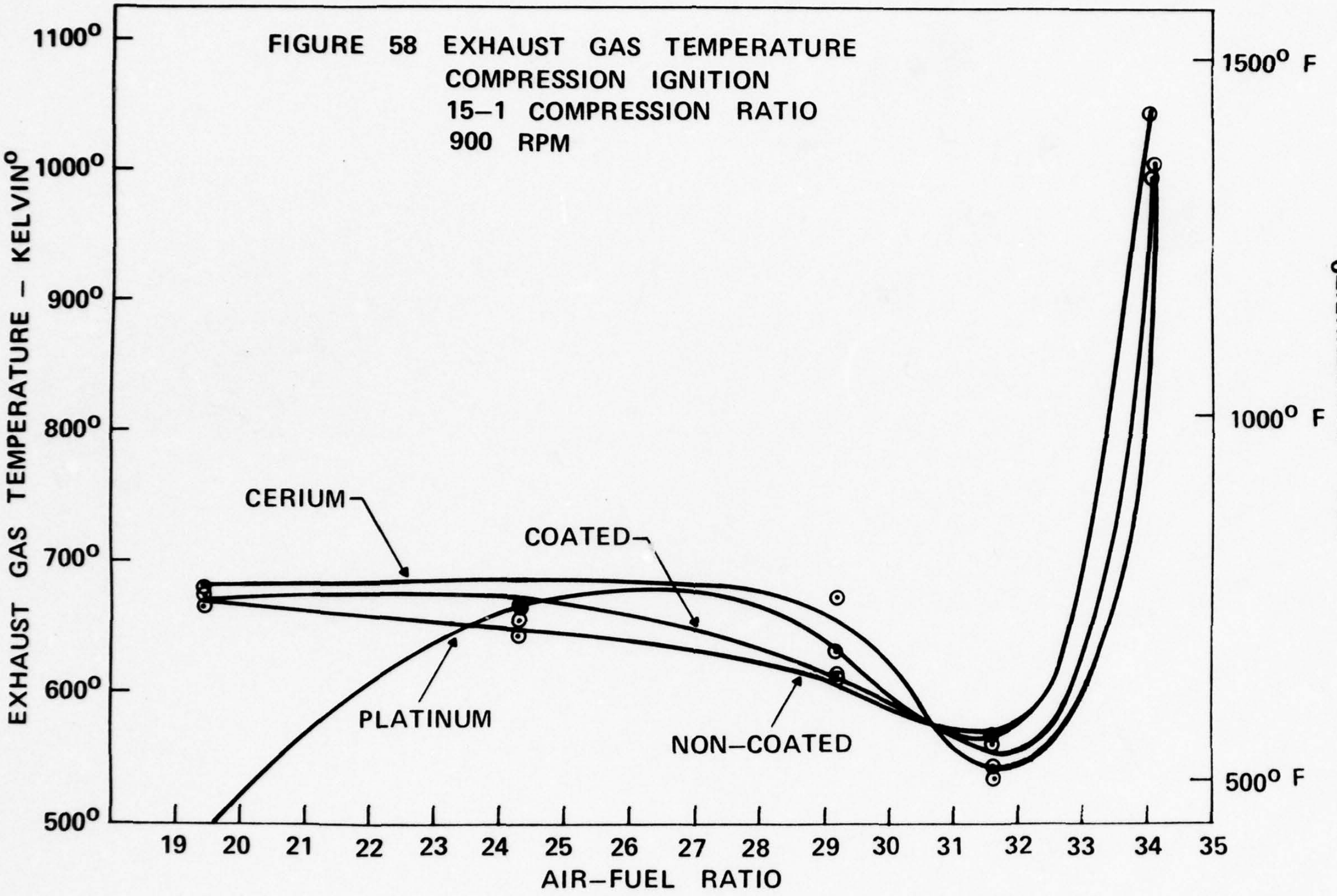

FIGURE 58 EXHAUST GAS TEMPERATURE
COMPRESSION IGNITION
15–1 COMPRESSION RATIO
900 RPM

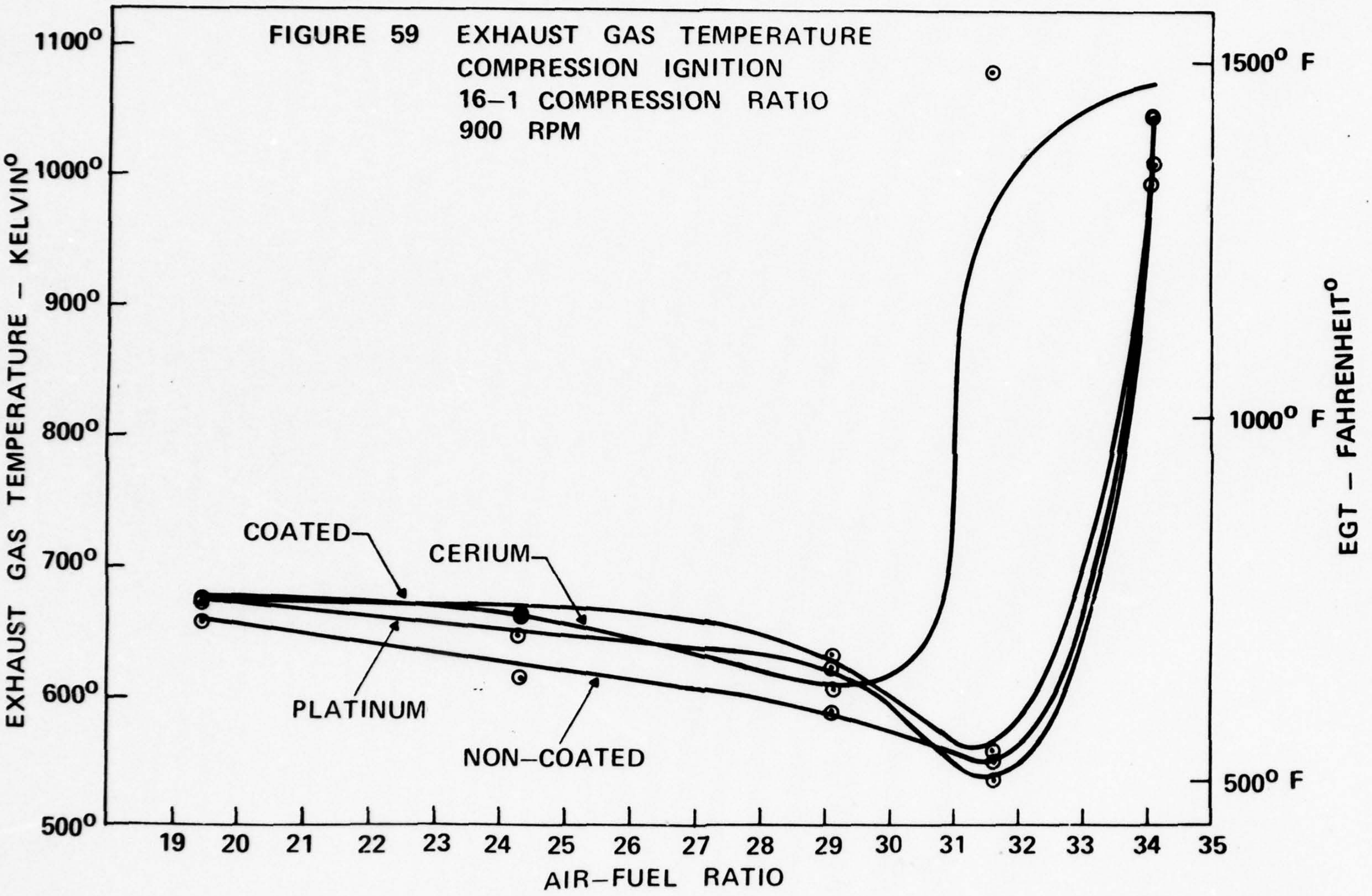

FIGURE 59 EXHAUST GAS TEMPERATURE
COMPRESSION IGNITION
16–1 COMPRESSION RATIO
900 RPM

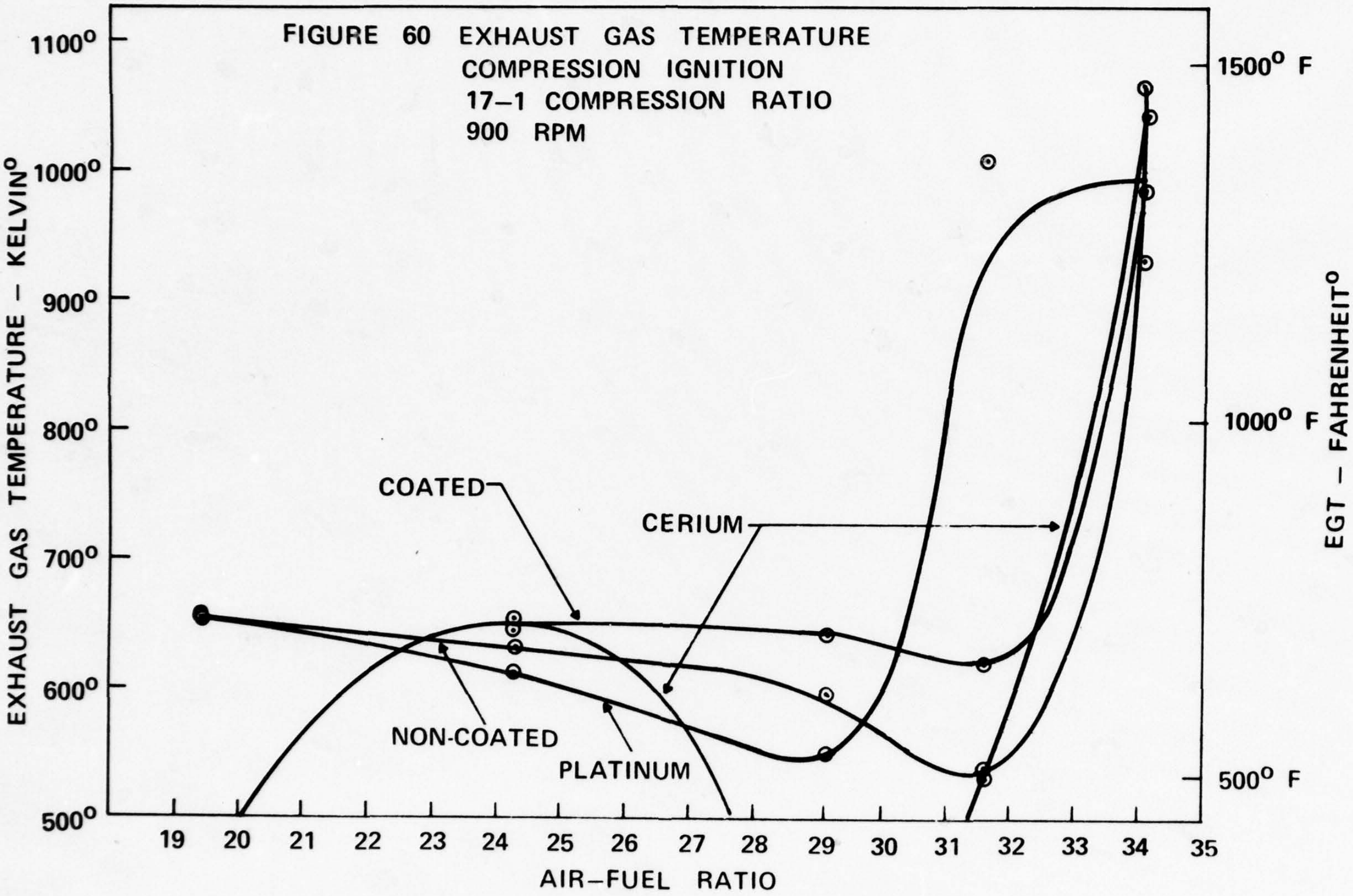

FIGURE 60 EXHAUST GAS TEMPERATURE
COMPRESSION IGNITION
17–1 COMPRESSION RATIO
900 RPM

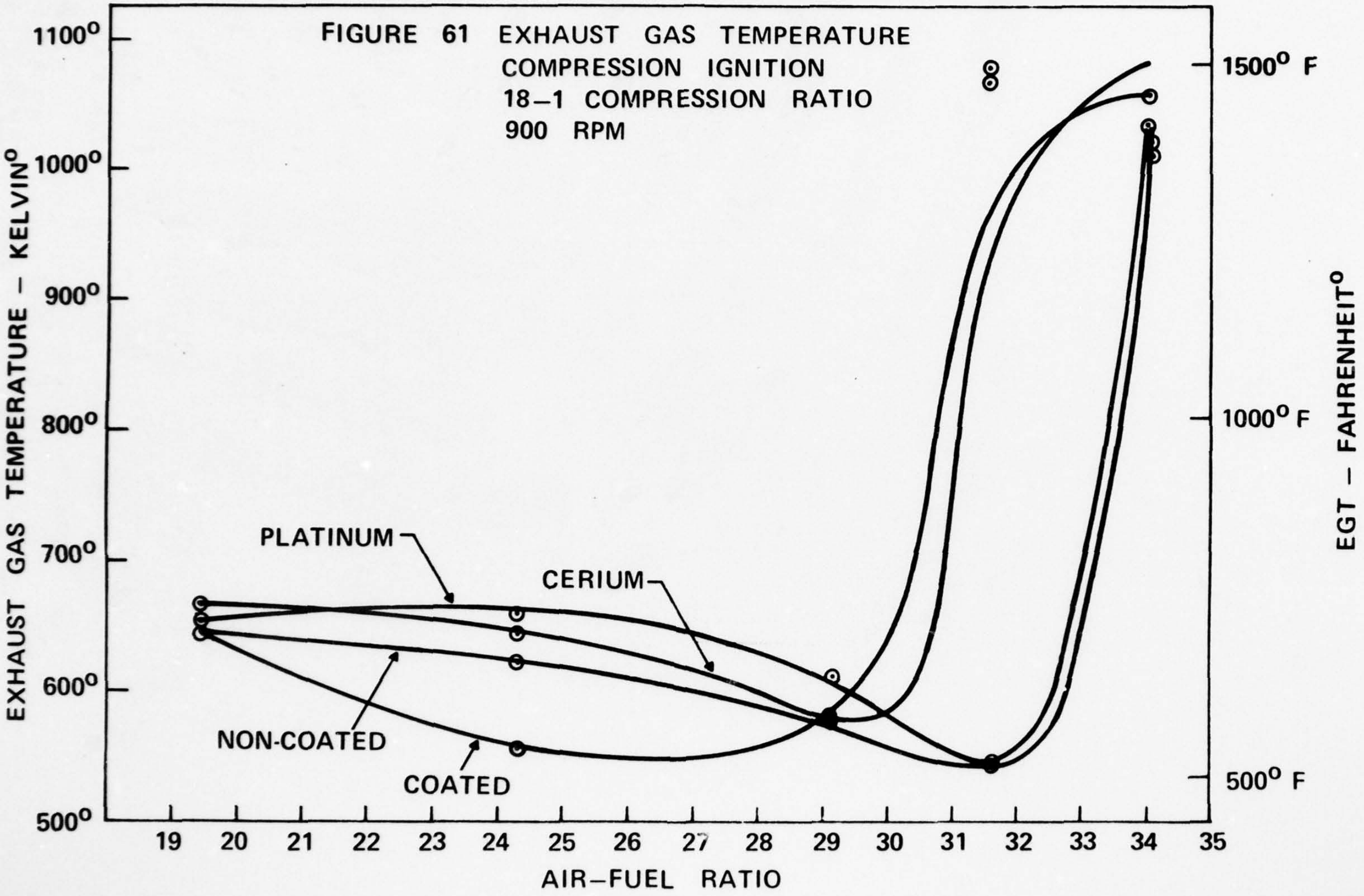

FIGURE 61 EXHAUST GAS TEMPERATURE
COMPRESSION IGNITION
18–1 COMPRESSION RATIO
900 RPM

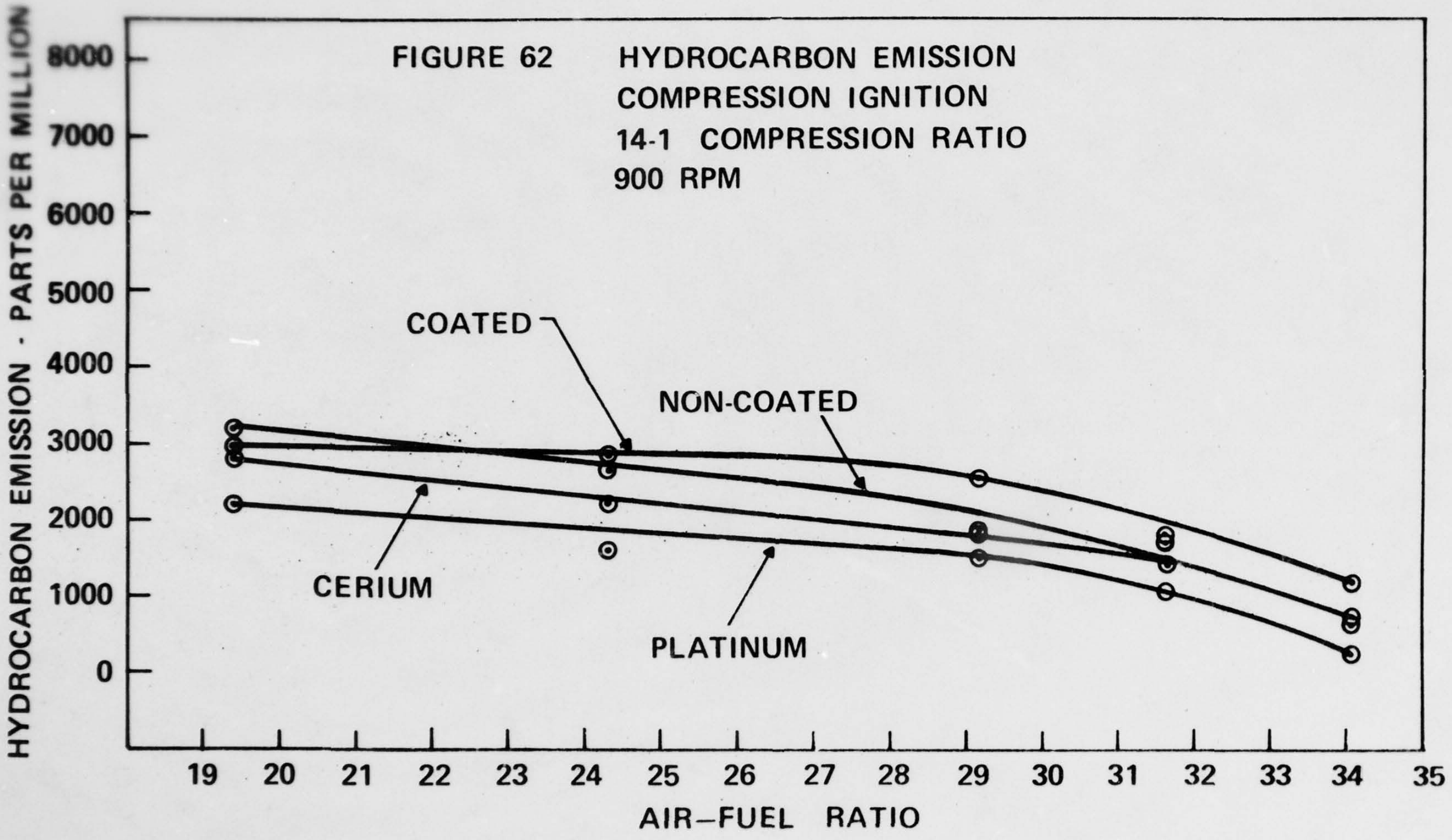

FIGURE 62 HYDROCARBON EMISSION
COMPRESSION IGNITION
14-1 COMPRESSION RATIO
900 RPM

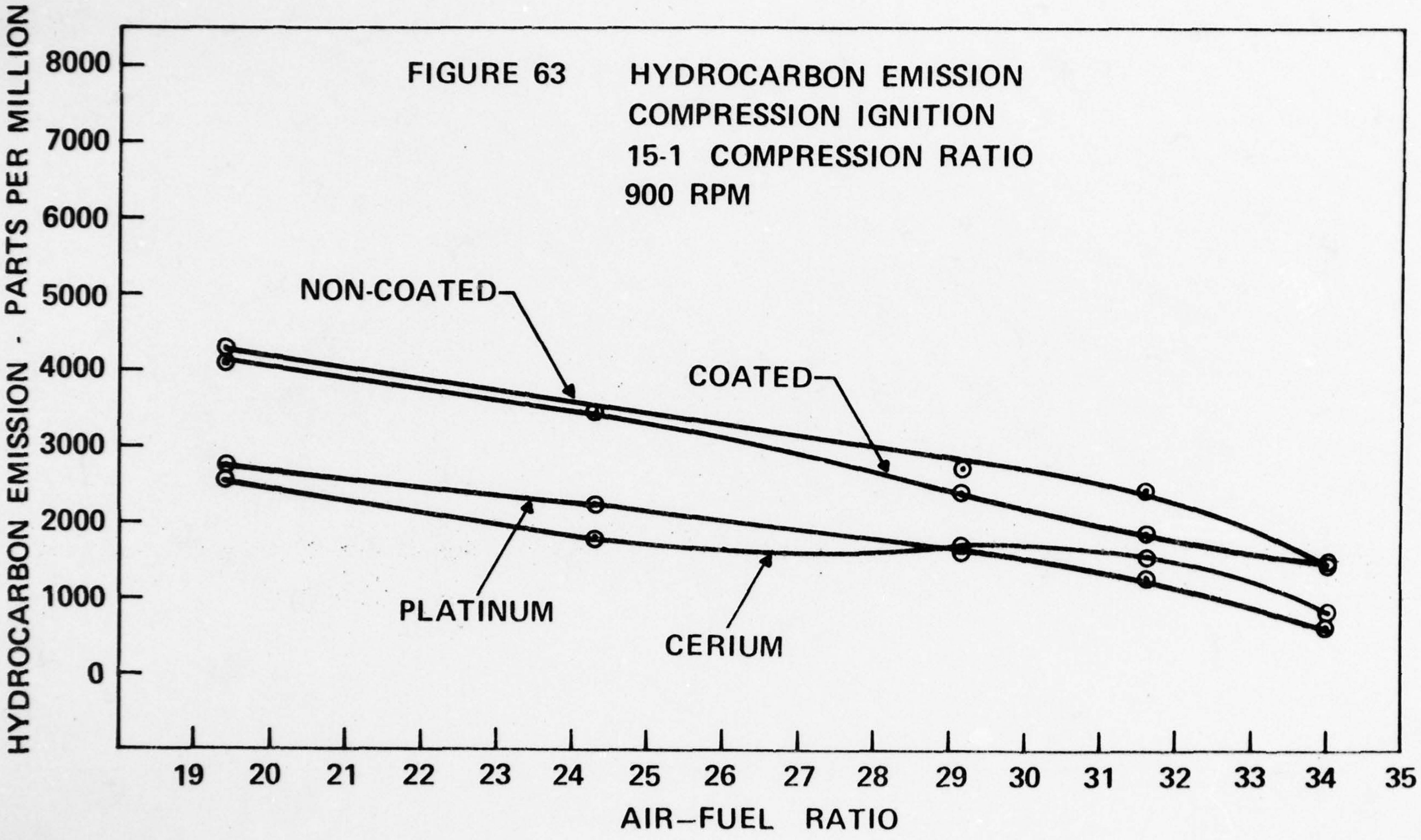

FIGURE 63 HYDROCARBON EMISSION
COMPRESSION IGNITION
15-1 COMPRESSION RATIO
900 RPM

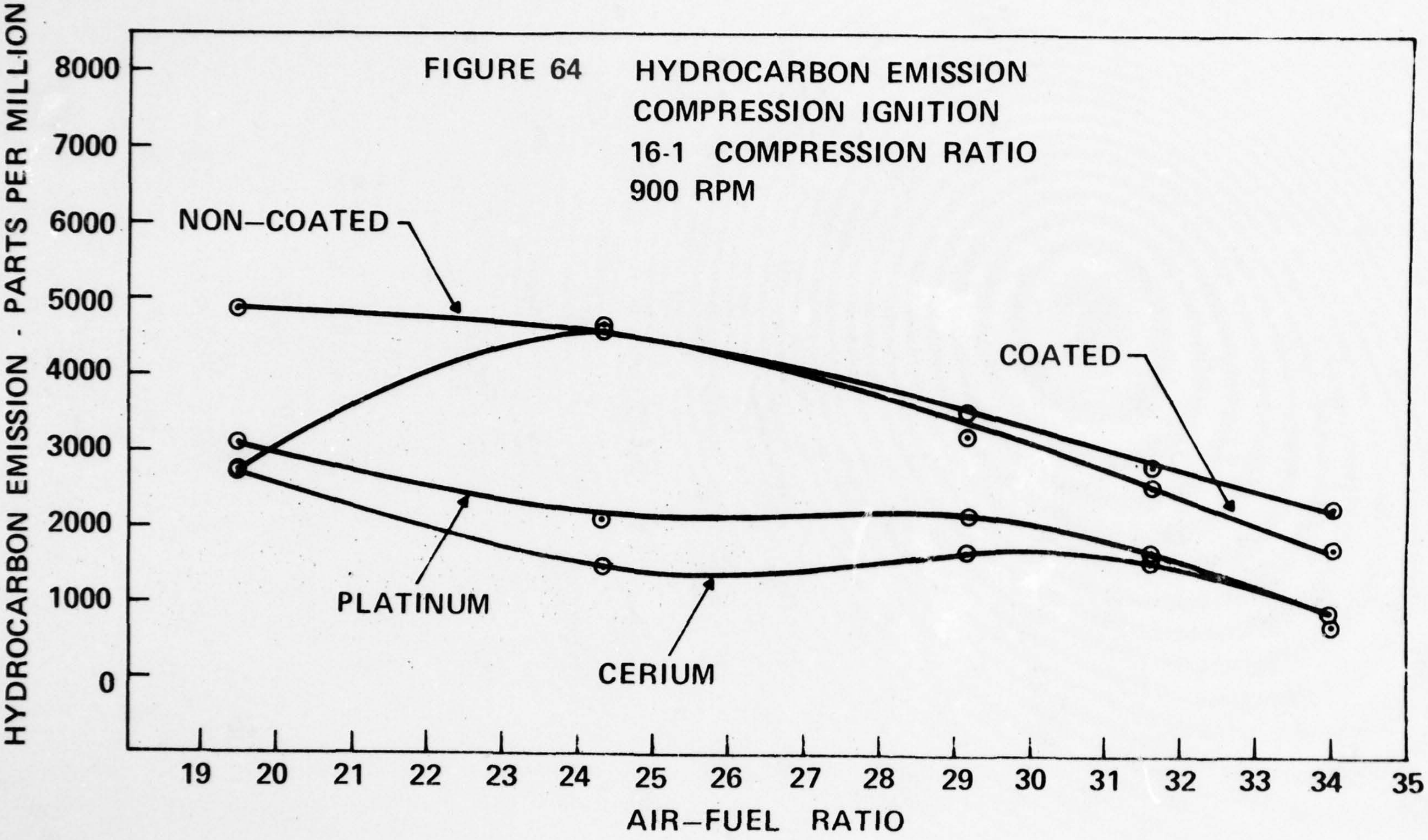

FIGURE 64 HYDROCARBON EMISSION
COMPRESSION IGNITION
16-1 COMPRESSION RATIO
900 RPM

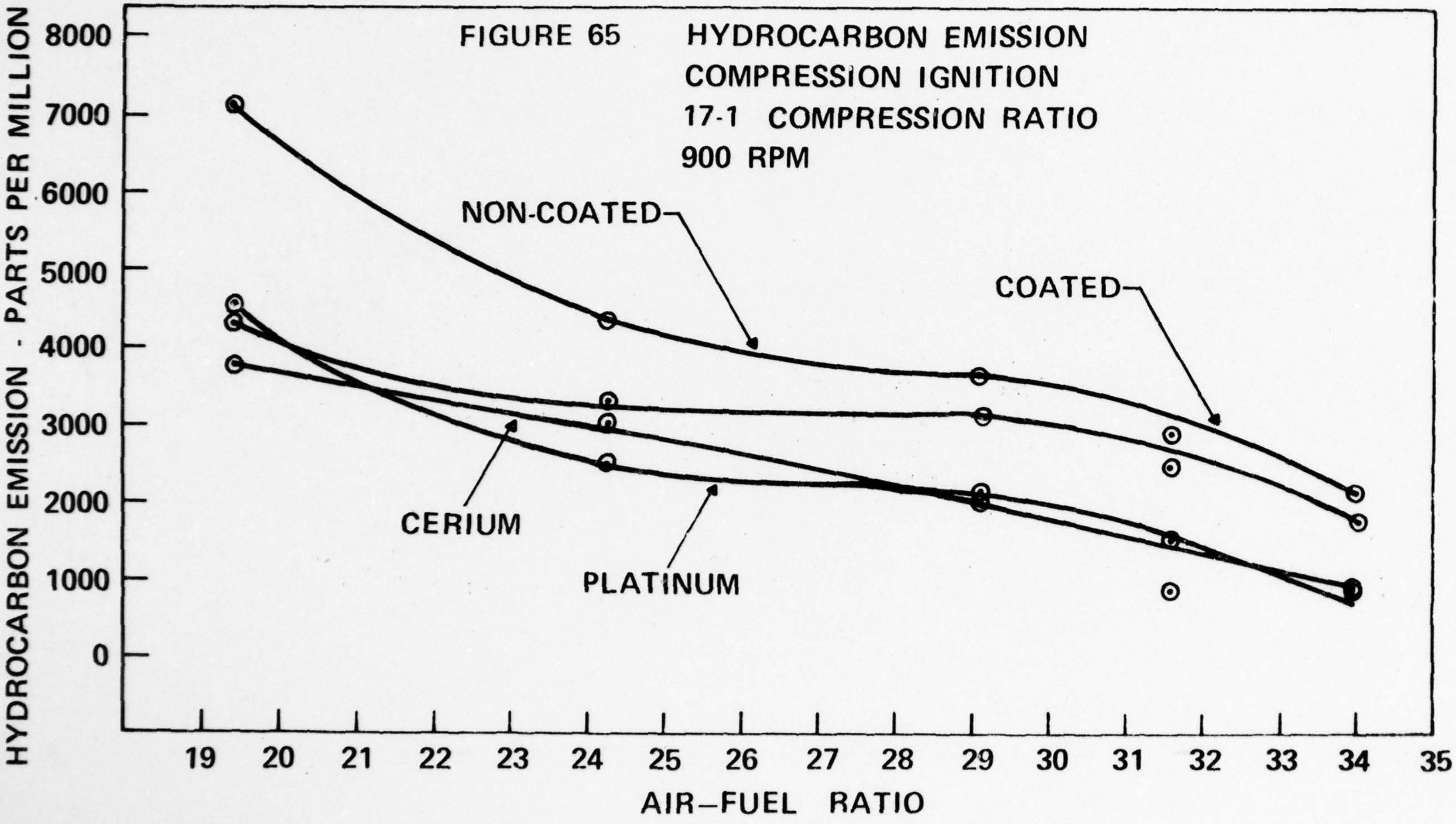

FIGURE 65 HYDROCARBON EMISSION
COMPRESSION IGNITION
17-1 COMPRESSION RATIO
900 RPM

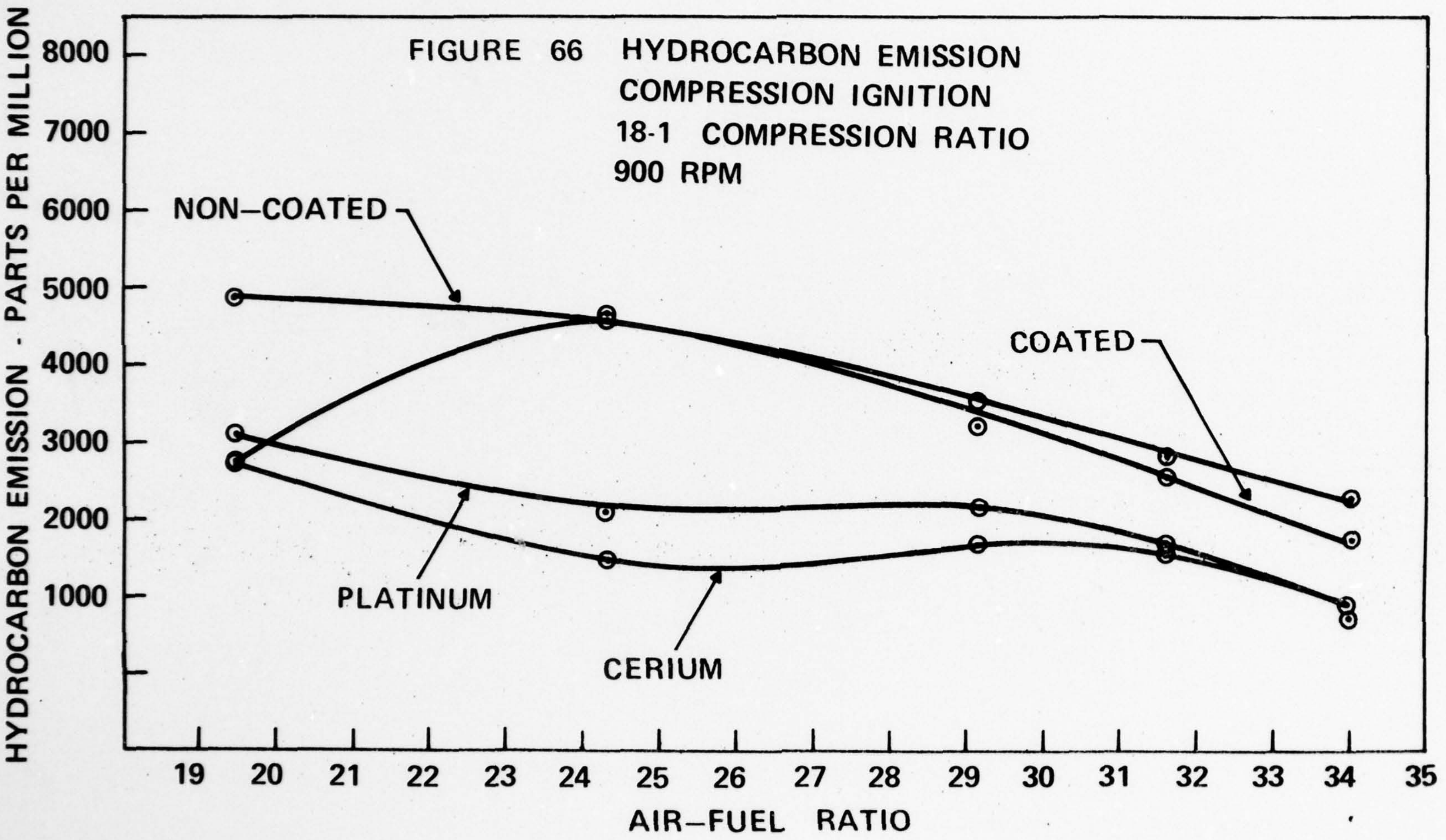

FIGURE 66 HYDROCARBON EMISSION
COMPRESSION IGNITION
18-1 COMPRESSION RATIO
900 RPM

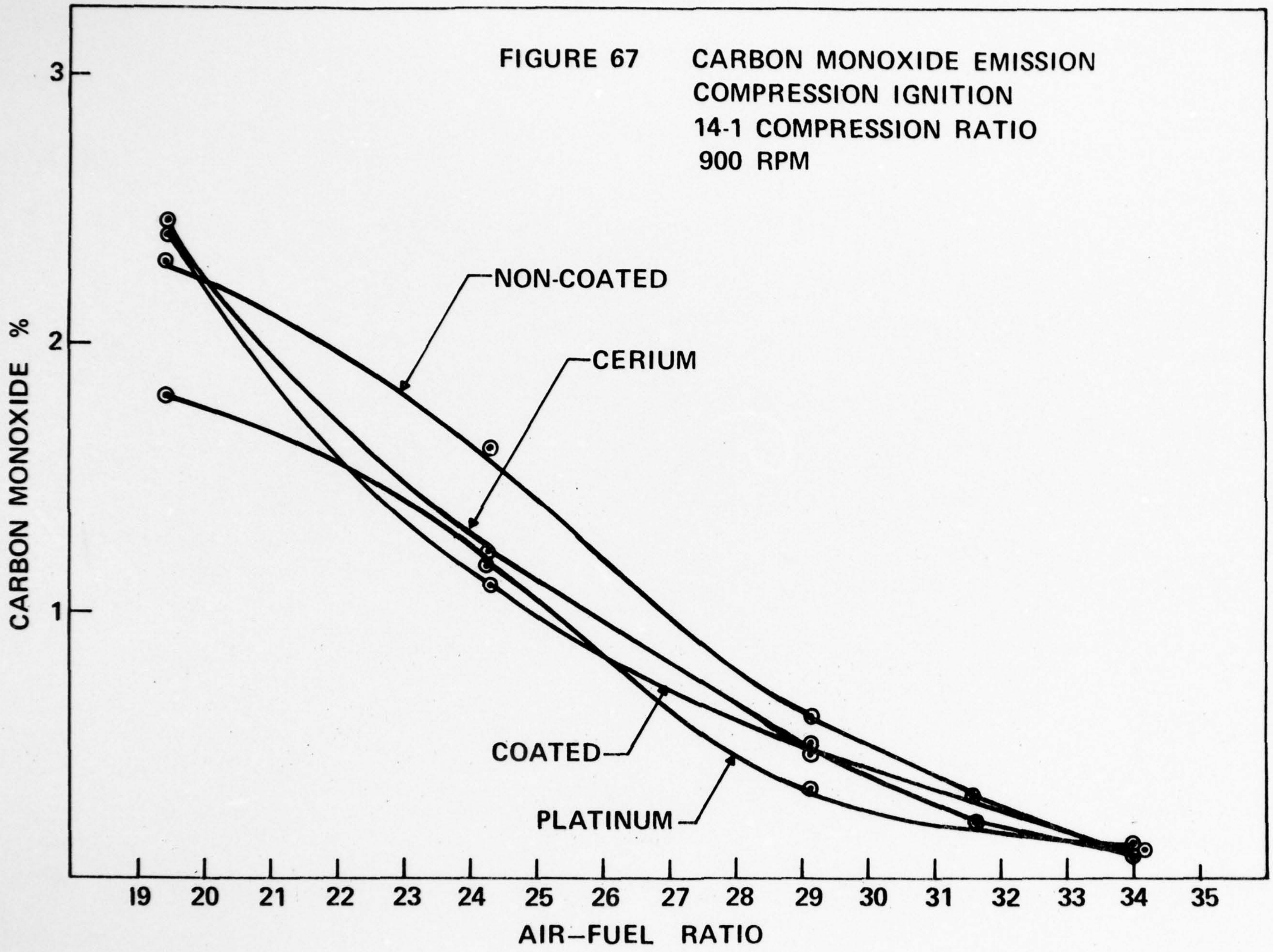

FIGURE 67 CARBON MONOXIDE EMISSION
COMPRESSION IGNITION
14-1 COMPRESSION RATIO
900 RPM

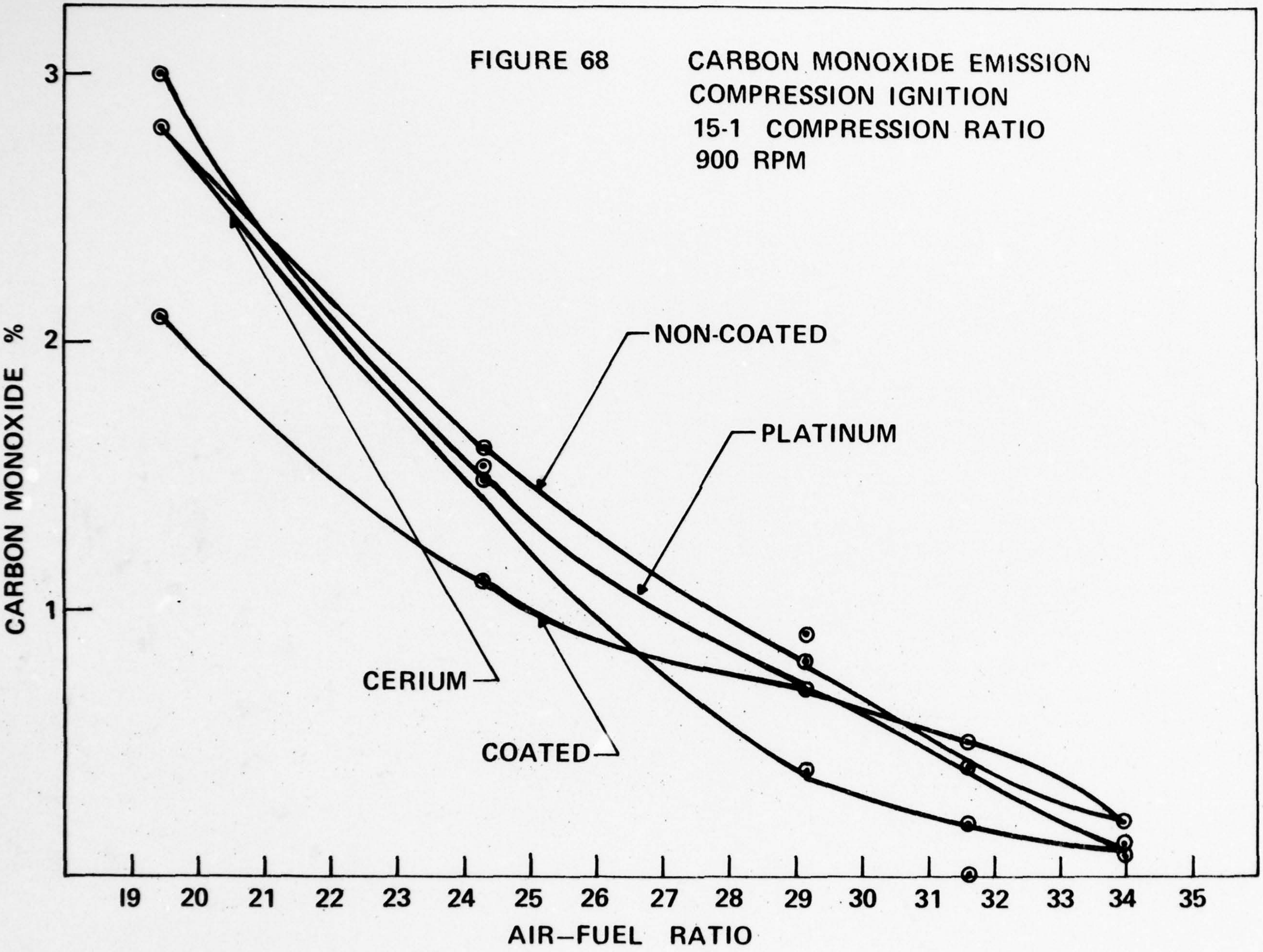

FIGURE 68 CARBON MONOXIDE EMISSION
COMPRESSION IGNITION
15-1 COMPRESSION RATIO
900 RPM

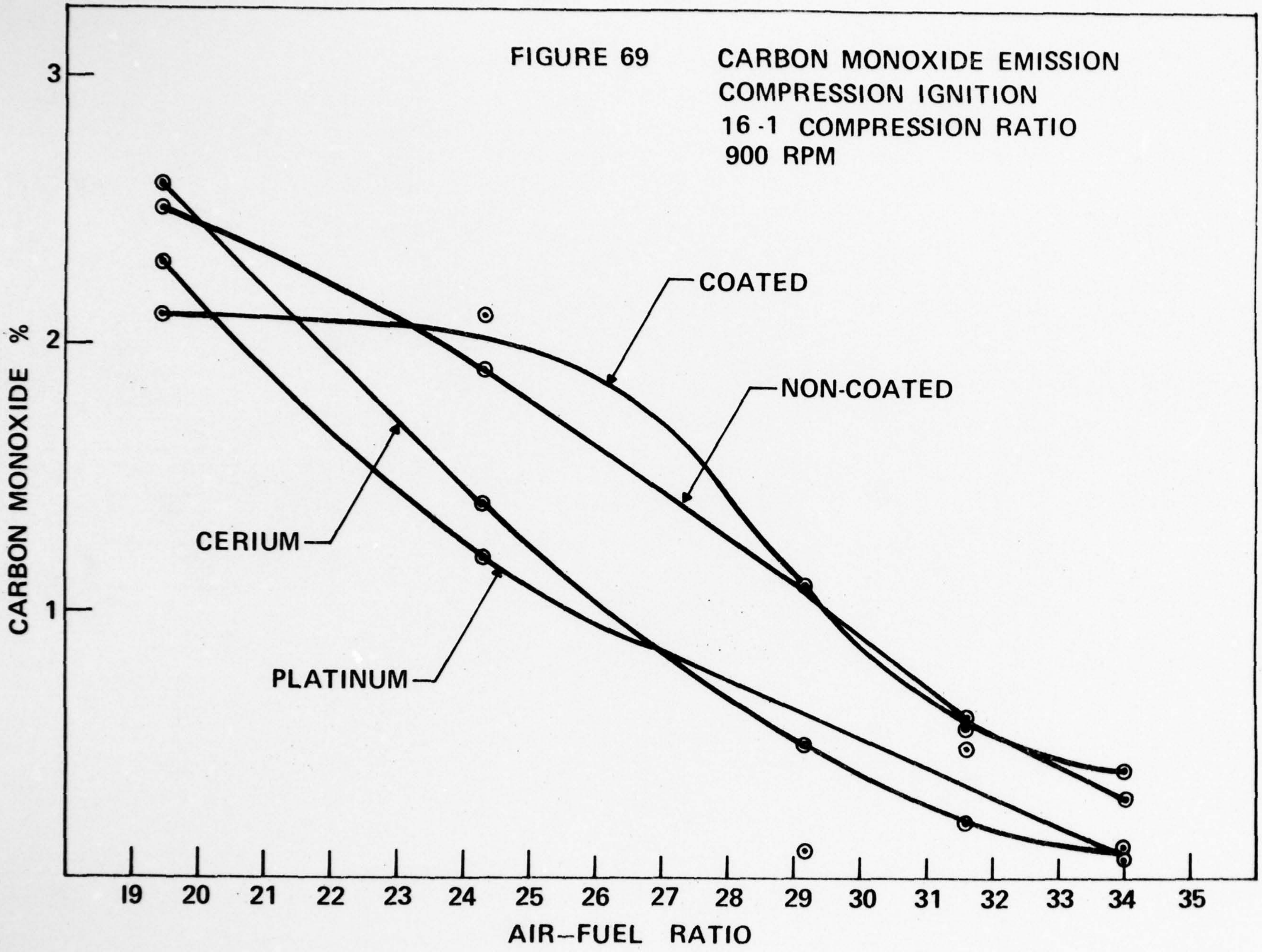

FIGURE 69 CARBON MONOXIDE EMISSION
COMPRESSION IGNITION
16-1 COMPRESSION RATIO
900 RPM

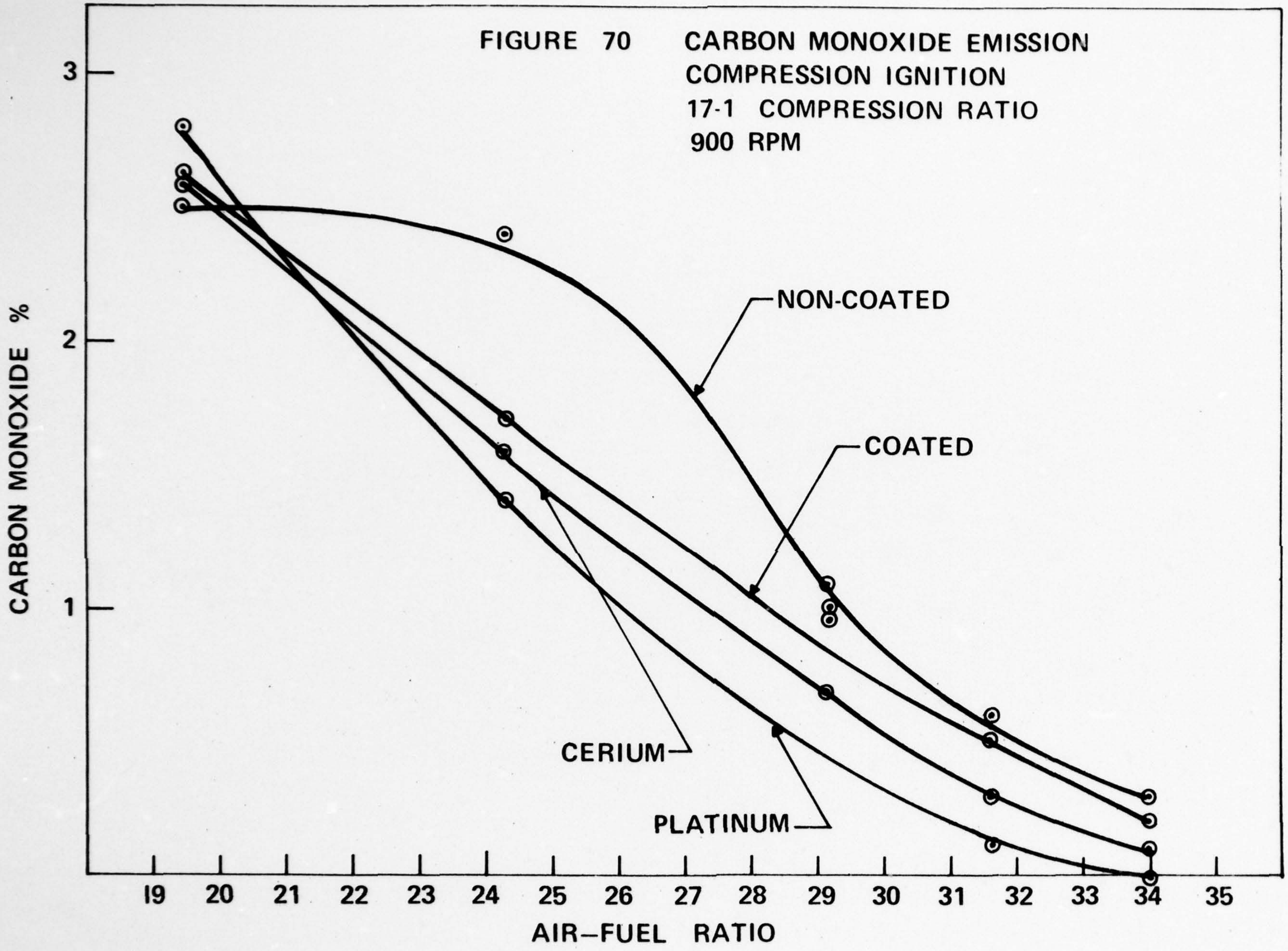

FIGURE 70 CARBON MONOXIDE EMISSION
COMPRESSION IGNITION
17-1 COMPRESSION RATIO
900 RPM

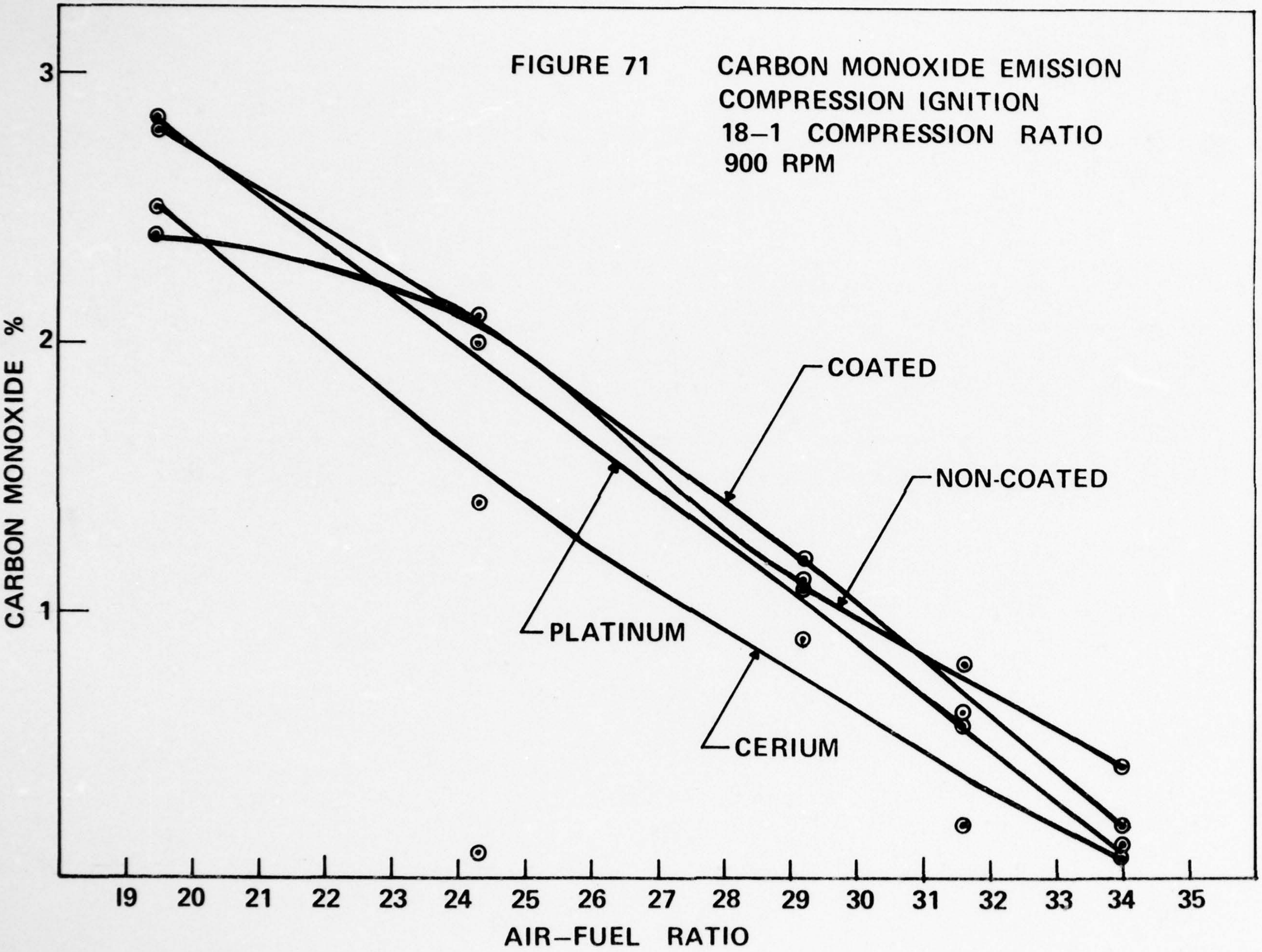

FIGURE 71 CARBON MONOXIDE EMISSION
COMPRESSION IGNITION
18–1 COMPRESSION RATIO
900 RPM

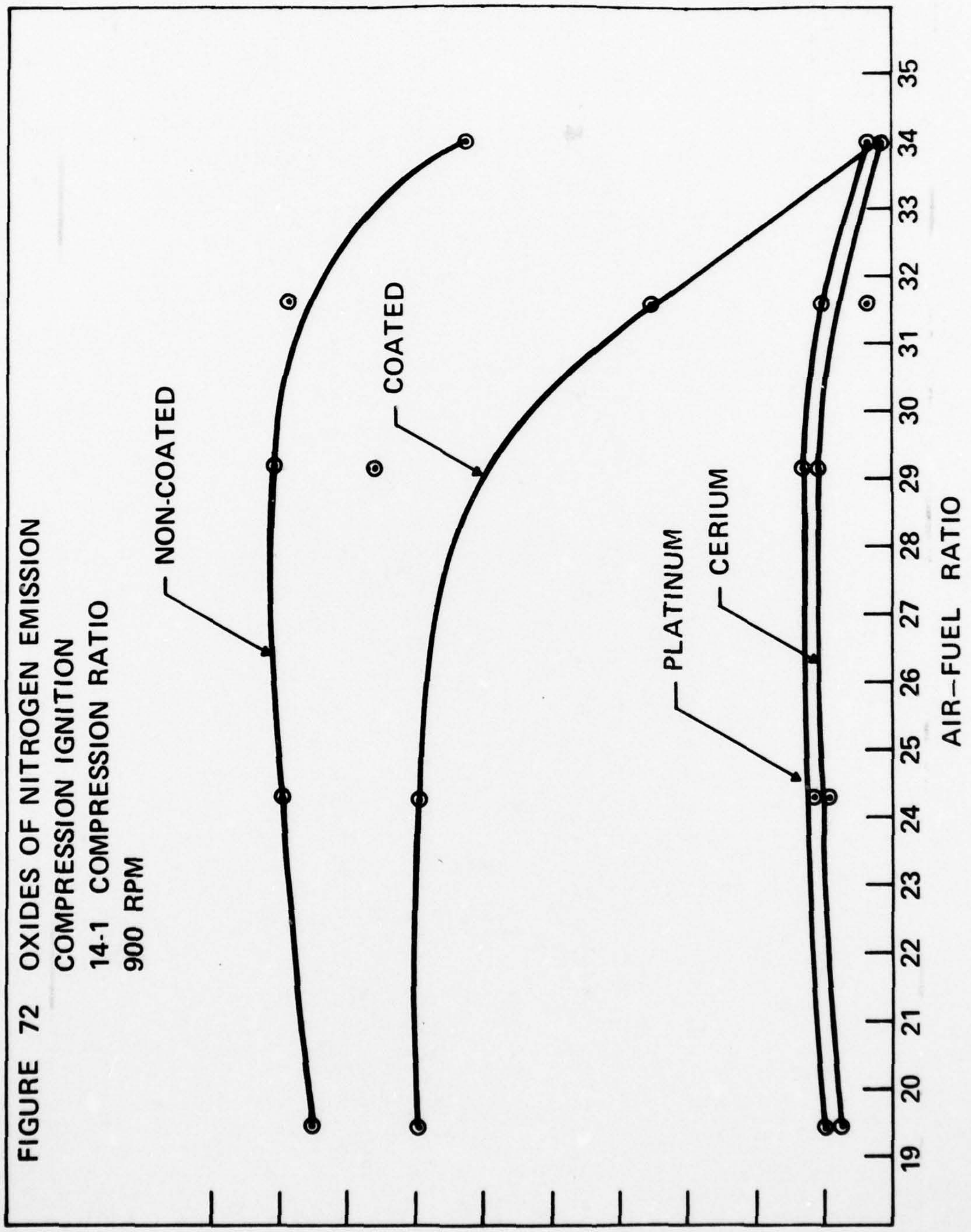

FIGURE 72 OXIDES OF NITROGEN EMISSION
COMPRESSION IGNITION
14-1 COMPRESSION RATIO
900 RPM

FIGURE 73 OXIDES OF NITROGEN EMISSION
COMPRESSION IGNITION
15-1 COMPRESSION RATIO
900 RPM

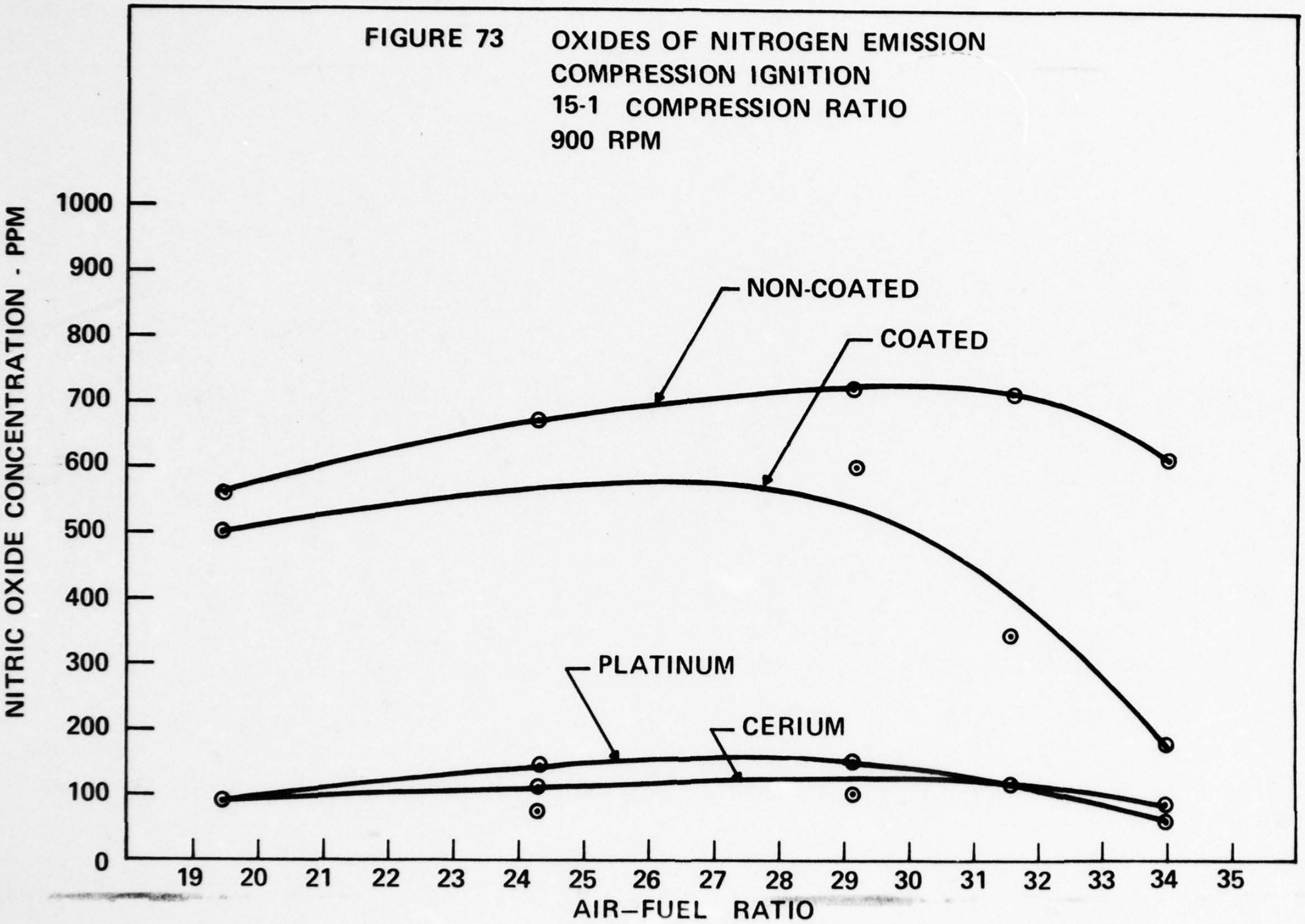

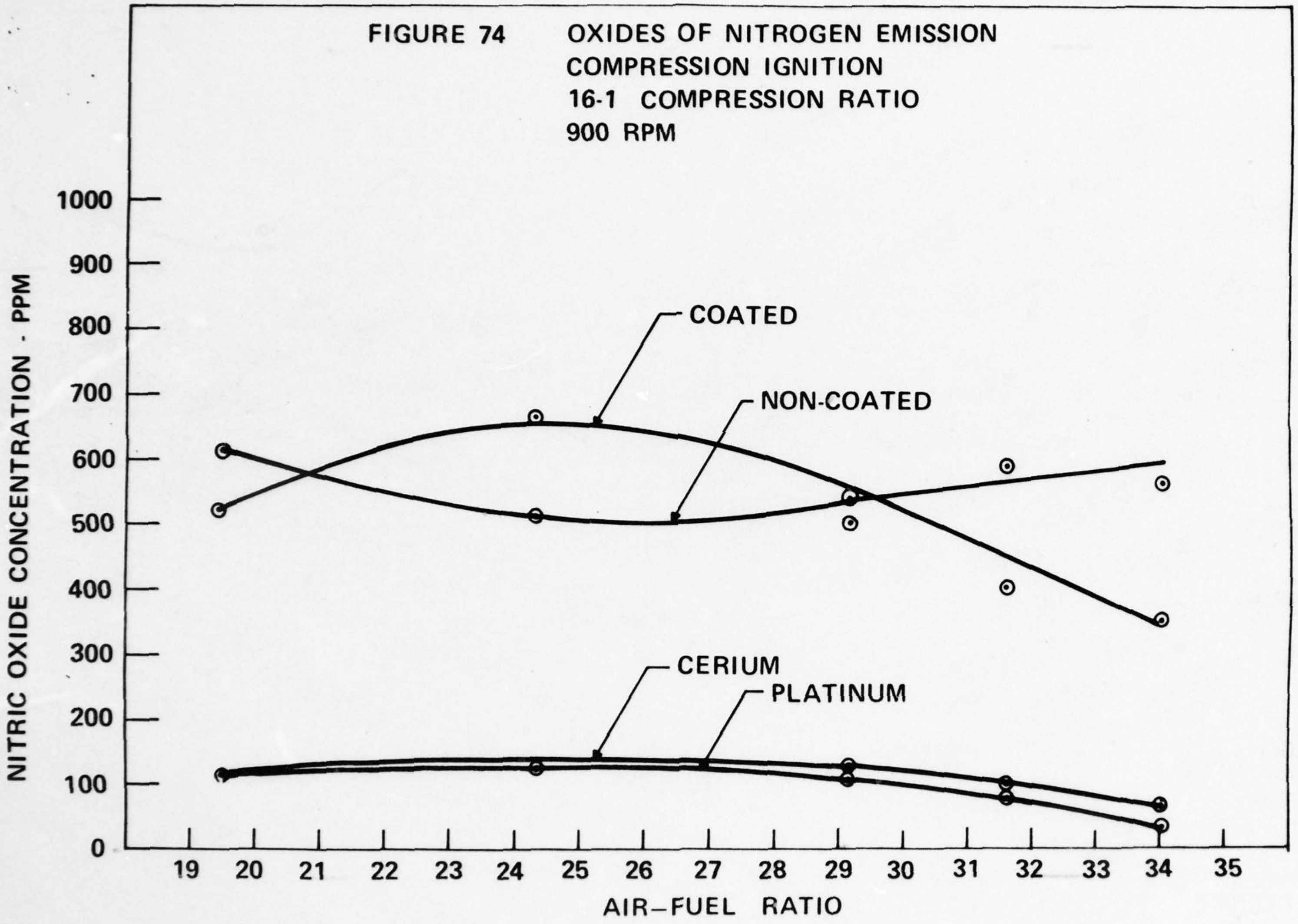

FIGURE 74 OXIDES OF NITROGEN EMISSION
COMPRESSION IGNITION
16-1 COMPRESSION RATIO
900 RPM

FIGURE 75 OXIDES OF NITROGEN EMISSION
COMPRESSION IGNITION
17-1 COMPRESSION RATIO
900 RPM

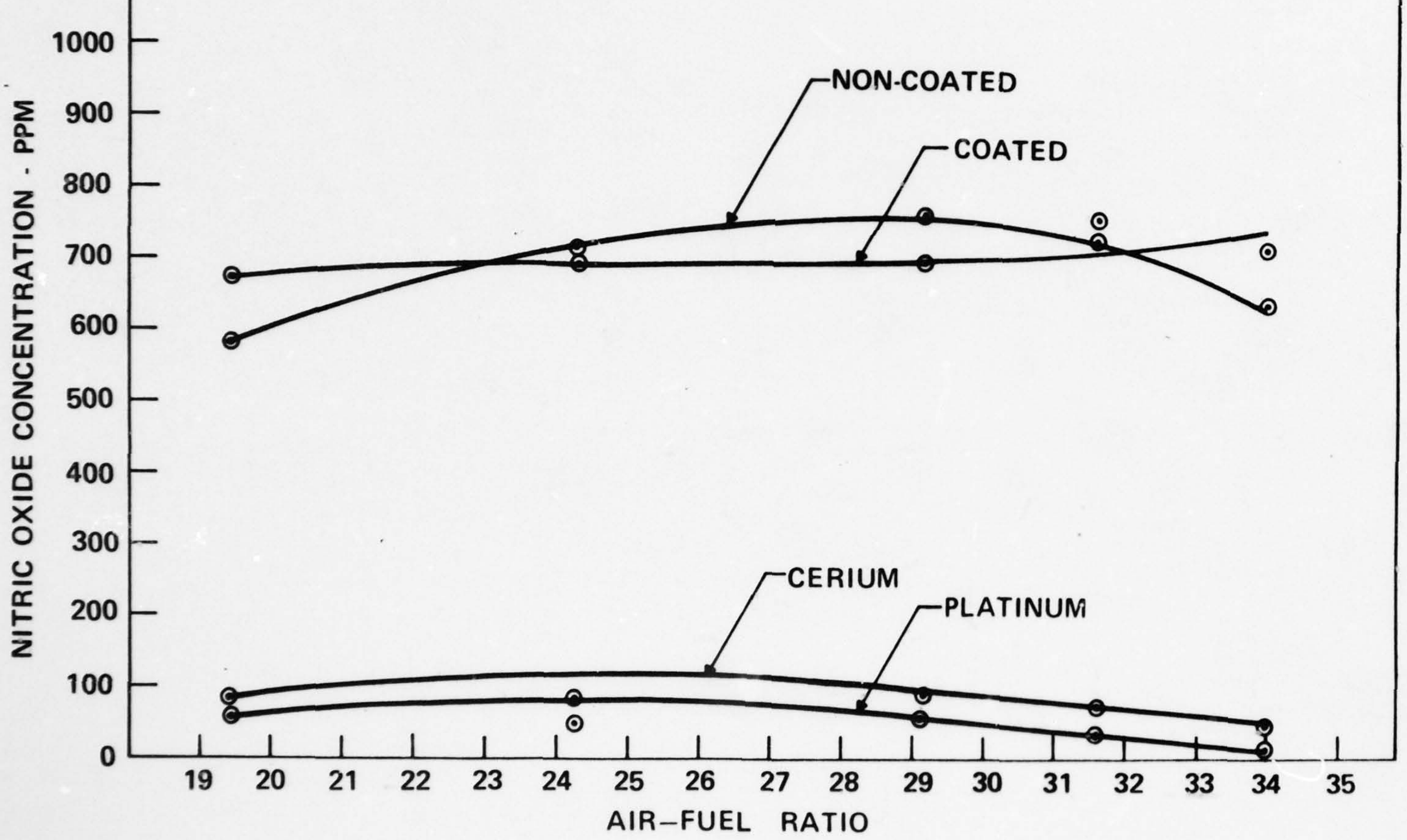

AD-A058 637 OKLAHOMA STATE UNIV STILLWATER COLL OF ENGINEERING F/G 21/7
IMPROVED ENGINE PERFORMANCE THROUGH HEAT TRANSFER CONTROL.(U)
JUL 78 R G MURRAY DAAG29-76-G-0263

UNCLASSIFIED ARO-14099.2-EX NL

2 OF 2
AD
A058637

END
DATE
FILMED
11-78
DDC

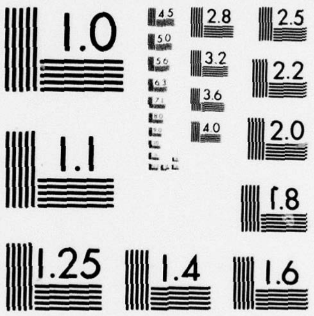

MICROCOPY RESOLUTION TEST CHART
NATIONAL BUREAU OF STANDARDS-1963-A

FIGURE 76 OXIDES OF NITROGEN EMISSION
COMPRESSION IGNITION
18-1 COMPRESSION RATIO
900 RPM

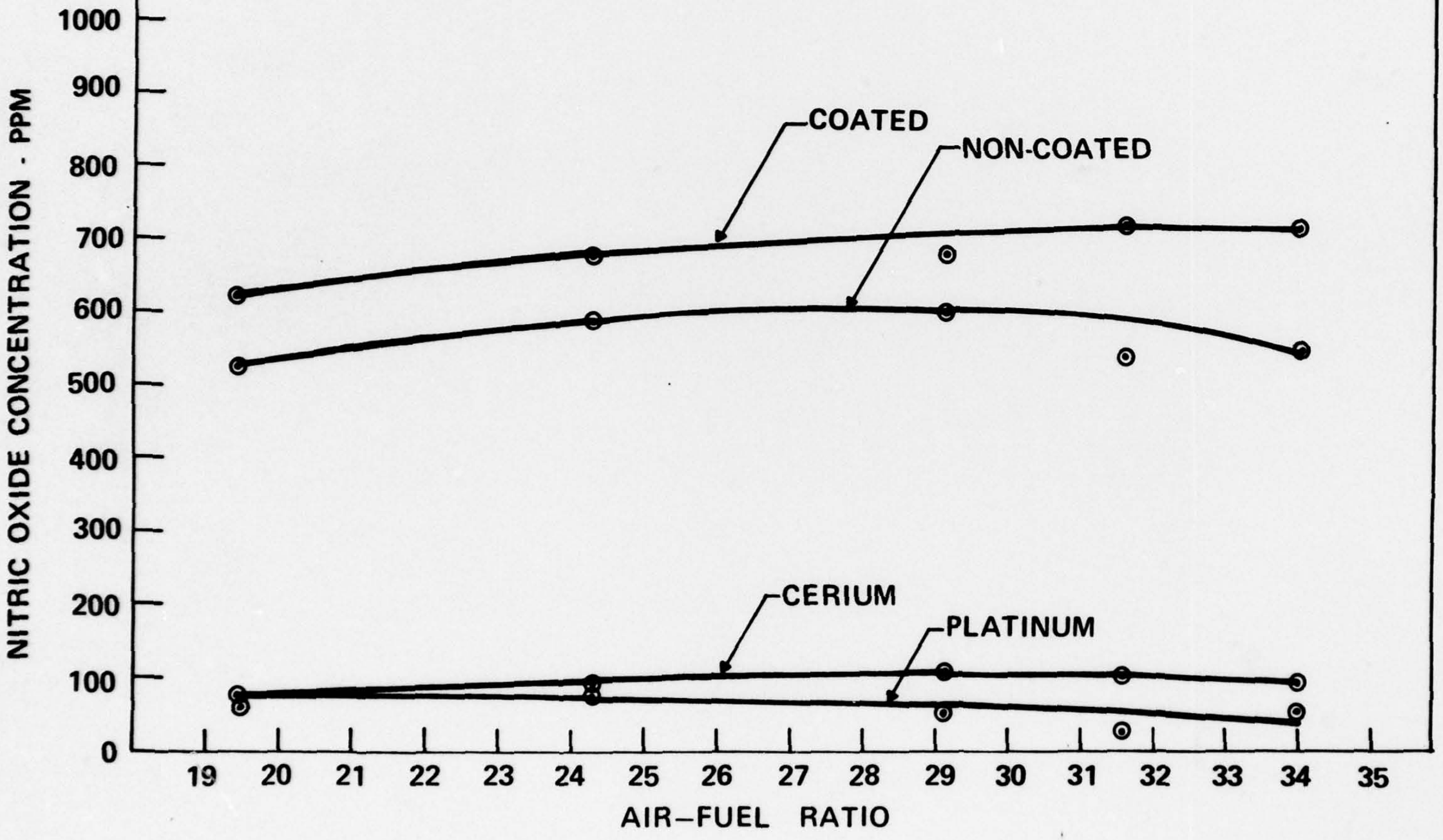

emissions. Again, this data should be viewed with some question as with the S-I data. The data was reproducible and consistent, however, the large differences between different operational modes remains largely unexplained. Further examination into this phenomenon is warranted.

PROJECT PERSONNEL

Dr. Richard G. Murray served as Director for this project.

One Mechanical Engineering Master's candidate, Mr. Breene Kerr and the following undergraduate students participated in this effort.

Mark Dronberger
Barney G. Russell
Arthur Voss
John Stoeckl
Phillip May
Glen May
Steve Gardner
Jack Carter
Shane Dixon
Leon Griffin
Guy Dutton
Scott Miller

The author wishes to express his gratitude to these individuals for their exceptional efforts and their dedicated work that overcame many very difficult obstacles.

While no technical papers were written by the above students the author has submitted a draft to AUTOMOTIVE ENGINEERING magazine for possible publication. Copies of this draft have been submitted to the U.S. Army Research Office.

SUMMARY AND CONCLUSIONS

A study into thermodynamics, heat transfer and engine operational theory, indicates that thermal insulation on combustion chamber surfaces should: 1) increase engine efficiency, 2) decrease component metallic temperature thereby promoting lighter, stronger engines, and 3) increase engine tolerance to low grade fuel. The engine test program described in the preceding sections verified some of the above expectations in certain modes of operation and disproved them in others.

Additional areas of importance were: 1) the affect of catalytic surfaces within the combustion chamber, and 2) the endurance characteristics of zirconium oxide plasma sprayed coatings within an engine.

Little doubt exists as to the endurance of the zirconium oxide coatings; they can survive under severe engine conditions for extended time intervals with little or no deterioration. Figure 77 illustrates one such piston surface that survived over 100 hours of S-I and C-I operation with intermittent violent knock. The only deterioration to this surface is a slight feathering or rounding of the coating on the perimeter. No coating separations or failures occured during this entire U.S. Army funded project. Coatings were applied to both cast iron and steel.

In general, it was determined that the placement of platinum and cerium catalytic surfaces into an engine combustion chamber inhibited or delayed combustion. While the chemical reaction tended towards completion, the rate of combustion was slowed producing poorer performance and efficiency.

Non-knocking S-I engine power and efficiency showed a significant improvement with the addition of a yttria stabilizing zirconium oxide coating to all combustion chamber surfaces.

Figure 77

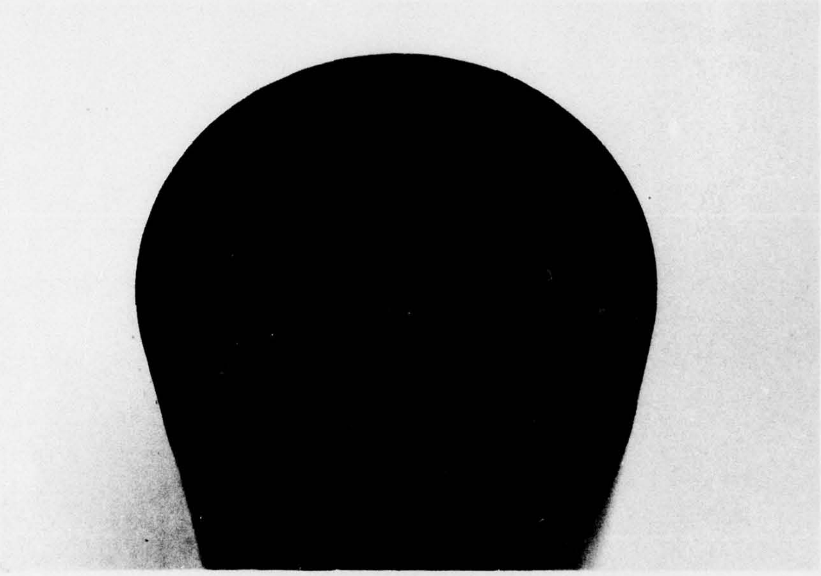

Cerium Coated Piston

Zirconium coated engines encountered knock at a lower compression ratio and knocked more severely than did non-coated engines.

Compression ignition engines encountered a performance degradation with a zirconium coating; both power and efficiency were reduced significantly. This unexpected result did not agree with theory and is believed to be primarily a result of combustion chamber design rather than an outcome of the coating itself.

It is apparent from this study that ceramic surfaces offer promise in future engine technology but much research and testing is necessary before they can be fully understood and utilized.

REFERENCES

1. Woschni, G., "A Universally Applicable Equation For The Instantaneous Heat Transfer Coefficient In The Internal Combustion Engine," SAE Paper No. 670931, 1967.

2. Annand, J. D., "Heat Transfer In The Cylinders Of Reciprocating Internal Combustion Engines," Proc. Inst. Mech. Eng., Vol. 177, No. 36 (1963).

3. Myers, P. S. and Oyehara, O. A., "Radiation Heat Transfer In Internal Combustion Engines," JSME 1967, International Symposium Tokyo (1967).

4. U.S. Patent 3,625,054.

5. Anderson, J. R., Structure Of Metalic Catalysts, Academic Press, New York, 1975.

6. Ingalls, Albert G., "A Review Of The Newest Developments In Science and Engineering," Scientific American, January 1926.

```
      REAL IMEP,IHP,ITQ,IEFF,MEP
      INTEGER TP,DAY,YR,HC,EXT,DEL
    1 CONTINUE
      FV=0.050
      I=1
      PRINT 4
      PRINT 101
      PRINT 102
    2 READ(5,3,END=554)N,TP,CR,IG,DEL,T,INT,EXT,DP,MEP,HC,CO,NOX,MON,DAY
     C,YR
      I=I+1
      IMEP=MEP*(1.0/.00333)
      XHP=(3.25*3.25*3.1416*4.5*900.)/(4.*2.*33000.*12.)
      IF(TP.GT.4)GOTO6
C     DIFFERENT HEAT CONTENT AND DENSITY VALUES EXIST FOR DIESEL AND SPARK
C     IGNITION FUELS
      HV=19100.
      WF=FV*1.6051
      GOTO7
    6 CONTINUE
      HV=18966.
      WF=FV*1.8890
    7 CONTINUE
      IF(EXT.EQ.0) GO TO 8
      IF(EXT.LT.500)EXT=1000+EXT
    8 WA=DP*(11.5/4.0)*.08160*(T/60.)
      AF=WA/WF
      IHP=IMEP*XHP
      HP=IHP
      ITQ=IMEP*(3.25*3.25*3.1416*4.5)/(150.8*4.)
      EFF=(IHP*2545.)/(HV*WF*3600/T)
      IEFF=EFF*100.
      BSFC=WF*3600./(IHP*T)
C CONVERT TO METRIC UNITS
      BSFC=0.6088*BSFC
      IHP=0.7457*IHP
      ITQ=1.3558*ITQ
      IMEP=6.89476*IMEP
      EXT=(5*(EXT-32)/9)+273
      IF(TP.EQ.1)GO TO 115
      IF(TP.EQ.2)GO TO 120
      IF(TP.EQ.3)GO TO 121
      IF(TP.EQ.4)GO TO 122
      IF(TP.EQ.5)GO TO 106
      IF(TP.EQ.6)GO TO 116
      IF(TP.EQ.7)GO TO 123
      IF(TP.EQ.8)GO TO 124
      IF(TP.EQ.9)GO TO 125
      WRITE(6,108)N,CR,AF,IHP,BSFC,IMEP,ITQ,IEFF,IG,DEL,EXT,HC,CO,NOX
      GOTO107
  106 CONTINUE
      WRITE(6,109)N,CR,AF,IHP,BSFC,IMEP,ITQ,IEFF,IG,DEL,EXT,HC,CO,NOX
      GOTO107
  115 WRITE(6,117)N,CR,AF,IHP,BSFC,IMEP,ITQ,IEFF,IG,DEL,EXT,HC,CO,NOX
      GO TO 107
  116 WRITE(6,118)N,CR,AF,IHP,BSFC,IMEP,ITQ,IEFF,IG,DEL,EXT,HC,CO,NOX
      GO TO 107
  120 WRITE(6,130)N,CR,AF,IHP,BSFC,IMEP,ITQ,IEFF,IG,DEL,EXT,HC,CO,NOX
      GO TO 107
```

```
      GO TO 107
  122 WRITE(6,132)N,CR,AF,IHP,BSFC,IMEP,ITQ,IEFF,IG,DEL,EXT,HC,CO,NOX
      GO TO 107
  123 WRITE(6,133)N,CR,AF,IHP,BSFC,IMEP,ITQ,IEFF,IG,DEL,EXT,HC,CO,NOX
      GO TO 107
  124 WRITE(6,134)N,CR,AF,IHP,BSFC,IMEP,ITQ,IEFF,IG,DEL,EXT,HC,CO,NOX
      GO TO 107
  125 WRITE(6,135)N,CR,AF,IHP,BSFC,IMEP,ITQ,IEFF,IG,DEL,EXT,HC,CO,NOX
  101 FORMAT(1X,'TEST    COMP    AIR      I-PWR  ISFC       IMEP    ITQ      I
     CEFF     IGN    EGT     HC       CO       NOX      TYPE              CATALYST'
     C)
  102 FORMAT(1X,'NO.        RATIO  FUEL     KW      GM/WHR     KPA     NM
     C%      AN   DE <       PPM     %        PPM',/)
    3 FORMAT(I4,1X,I1,1X,F4.1,2(1X,I2),1X,F5.1,1X,I3,1X,I4,1X,F4.2,1X,F4
     C.3,1X,I4,1X,F4.1,1X,I4,3(1X,I2))
    4 FORMAT(1H1,' SEMI-ADIABATIC ENGINE STUDY'//)
  108 FORMAT(1X,I4,3X,F4.1,2X,F5.2,4X,F4.2,3X,F5.3,4X,F5.0,3X,F5.2,3X,F5
     C.2,2X,I2,1X,I2,2X,I4,3X,I4,3X,F4.1,3X,I4,3X,'S-I NON COATED'/)
  109 FORMAT(1X,I4,3X,F4.1,2X,F5.2,4X,F4.2,3X,F5.3,4X,F5.0,3X,F5.2,3X,F5
     C.2,2X,I2,1X,I2,2X,I4,3X,I4,3X,F4.1,3X,I4,3X,'C-I NON COATED'/)
  117 FORMAT(1X,I4,3X,F4.1,2X,F5.2,4X,F4.2,3X,F5.3,4X,F5.0,3X,F5.2,3X,F5
     C.2,2X,I2,1X,I2,2X,I4,3X,I4,3X,F4.1,3X,I4,3X,'S-I COATED'/)
  118 FORMAT(1X,I4,3X,F4.1,2X,F5.2,4X,F4.2,3X,F5.3,4X,F5.0,3X,F5.2,3X,F5
     C.2,2X,I2,1X,I2,2X,I4,3X,I4,3X,F4.1,3X,I4,3X,'C-I COATED'/)
  130 FORMAT(1X,I4,3X,F4.1,2X,F5.2,4X,F4.2,3X,F5.3,4X,F5.0,3X,F5.2,3X,F5
     C.2,2X,I2,1X,I2,2X,I4,3X,I4,3X,F4.1,3X,I4,3X,'S-I COATED      PLATIN
     CUM'/)
  131 FORMAT(1X,I4,3X,F4.1,2X,F5.2,4X,F4.2,3X,F5.3,4X,F5.0,3X,F5.2,3X,F5
     C.2,2X,I2,1X,I2,2X,I4,3X,I4,3X,F4.1,3X,I4,3X,'S-I COATED      CERIUM
     C'/)
  132 FORMAT(1X,I4,3X,F4.1,2X,F5.2,4X,F4.2,3X,F5.3,4X,F5.0,3X,F5.2,3X,F5
     C.2,2X,I2,1X,I2,2X,I4,3X,I4,3X,F4.1,3X,I4,3X,'S-I COATED      NICKEL
     C'/)
  133 FORMAT(1X,I4,3X,F4.1,2X,F5.2,4X,F4.2,3X,F5.3,4X,F5.0,3X,F5.2,3X,F5
     C.2,2X,I2,1X,I2,2X,I4,3X,I4,3X,F4.1,3X,I4,3X,'C-I COATED      PLATIN
     CUM'/)
  134 FORMAT(1X,I4,3X,F4.1,2X,F5.2,4X,F4.2,3X,F5.3,4X,F5.0,3X,F5.2,3X,F5
     C.2,2X,I2,1X,I2,2X,I4,3X,I4,3X,F4.1,3X,I4,3X,'C-I COATED      CERIUM
     C'/)
  135 FORMAT(1X,I4,3X,F4.1,2X,F5.2,4X,F4.2,3X,F5.3,4X,F5.0,3X,F5.2,3X,F5
     C.2,2X,I2,1X,I2,2X,I4,3X,I4,3X,F4.1,3X,I4,3X,'C-I COATED      NICKEL
     C'/)
  107 CONTINUE
      IF(I.EQ.27) GO TO 1
      GO TO 2
  554 PRINT 140
  140 FORMAT(1H1)
      STOP
      END

$ENTRY
```

THIS PAGE IS BEST QUALITY PRACTICABLE
FROM COPY FURNISHED TO DDC

TEST NO.	COMP RATIO	AIR FUEL	I-PWR KW	ISFC GM/WHR	IMEP KPA	ITQ NM	IEFF %	IGN AN	IGN DE	EGT K	HC PPM	CO %	NOX PPM	TYPE	CATALYST
2101	6.0	18.04	3.67	0.242	799.	38.91	33.59	24	8	713	223	0.0	2580	S-I	COATED
2102	6.0	17.04	3.80	0.247	828.	40.32	32.88	26	10	727	725	0.0	2380	S-I	COATED
2103	6.0	16.03	3.96	0.252	863.	42.03	32.24	22	2	749	930	0.1	2580	S-I	COATED
2104	6.0	15.03	4.08	0.261	888.	43.24	31.10	21	2	746	1300	0.0	2320	S-I	COATED
2105	6.0	14.03	4.16	0.274	907.	44.15	29.64	20	1	733	1650	3.2	884	S-I	COATED
2106	8.0	18.04	4.16	0.213	907.	44.15	38.11	20	2	688	1200	0.0	2640	S-I	COATED
2107	8.0	17.04	4.35	0.215	948.	46.16	37.64	20	1	708	1255	0.1	2680	S-I	COATED
2108	8.0	16.03	4.49	0.222	979.	47.67	36.57	19	1	723	1600	0.2	2520	S-I	COATED
2109	8.0	15.03	4.56	0.233	994.	48.38	34.80	19	0	716	2250	0.2	2040	S-I	COATED
2110	8.0	14.03	4.62	0.247	1006.	48.98	32.89	13	1	702	2500	3.6	1240	S-I	COATED
2111	10.0	18.04	4.42	0.200	963.	46.87	40.45	18	2	649	2150	0.1	2600	S-I	COATED
2112	10.0	17.04	4.04	0.232	880.	42.84	34.93	16	1	674	2300	0.1	2660	S-I	COATED
2113	10.0	16.03	3.92	0.254	855.	41.63	31.93	16	1	671	2350	0.5	1740	S-I	COATED
2114	10.0	15.03	3.87	0.275	843.	41.02	29.51	18	2	256	2750	0.2	1620	S-I	COATED
2115	10.0	14.03	4.04	0.282	880.	42.84	28.76	17	1	649	3375	3.0	1020	S-I	COATED
2601	14.0	19.44	3.56	0.231	776.	37.80	35.41	48	48	688	3850	2.4	200	C-I	COATED
2602	14.0	24.30	3.47	0.190	756.	36.79	43.09	52	44	666	2550	1.2	122	C-I	COATED
2603	14.0	29.15	2.71	0.202	590.	28.73	40.36	43	41	599	2300	0.2	480	C-I	COATED
2604	14.0	34.02	0.27	1.766	58.	2.82	4.63	44	42	933	1050	0.1	30	C-I	COATED
2605	14.0	19.44	3.51	0.234	766.	37.29	34.93	52	44	688	2995	2.4	699	C-I	COATED
2606	14.0	24.30	3.16	0.208	689.	33.56	39.31	51	43	633	2800	1.1	695	C-I	COATED
2607	14.0	29.15	2.86	0.192	623.	30.34	42.63	52	42	616	2550	0.5	758	C-I	COATED
2608	14.0	31.59	1.77	0.286	385.	18.75	28.54	44	42	1066	1800	0.3	350	C-I	COATED
2609	14.0	34.02	0.66	0.706	145.	7.06	11.57	40	43	960	1200	0.1	16	C-I	COATED
2610	15.0	19.44	3.13	0.262	683.	33.26	31.16	50	40	669	4100	2.1	500	C-I	COATED
2611	15.0	24.30	3.23	0.204	704.	34.27	40.14	53	42	666	3450	1.1	150	C-I	COATED

THIS PAGE IS BEST QUALITY PRACTICABLE
FROM COPY FURNISHED TO DDC

TEST NO.	COMP RATIO	AIR FUEL	I-PWR KW	ISFC GM/WHR	IMEP KPA	ITQ NM	IEFF %	IGN AN	IGN DE	EGT K	HC PPM	CO %	NOX PPM	TYPE	CATALYST
2612	15.0	29.15	2.47	0.222	538.	26.21	36.82	52	42	613	2400	0.7	600	C-I	COATED
2613	15.0	31.59	2.04	0.248	445.	21.67	32.99	47	42	560	1900	0.5	345	C-I	COATED
2614	15.0	34.02	1.28	0.366	280.	13.61	22.31	40	42	1049	1500	0.2	180	C-I	COATED
2615	16.0	19.44	3.23	0.254	704.	34.27	32.10	51	41	669	2700	2.1	522	C-I	COATED
2616	16.0	24.30	3.15	0.208	687.	33.46	39.19	55	41	663	4650	2.1	665	C-I	COATED
2617	16.0	29.15	2.85	0.192	621.	30.24	42.49	53	41	630	3200	1.1	540	C-I	COATED
2618	16.0	31.59	2.04	0.248	445.	21.67	32.99	50	41	533	2550	0.6	400	C-I	COATED
2619	16.0	34.02	1.66	0.282	362.	17.64	28.92	49	41	1044	1700	0.4	349	C-I	COATED
2620	17.0	19.42	4.00	0.206	872.	42.43	39.71	52	40	655	4300	2.6	670	C-I	COATED
2621	17.0	24.30	3.70	0.177	807.	39.31	46.04	52	40	649	3250	1.7	699	C-I	COATED
2622	17.0	29.15	3.23	0.170	704.	34.27	48.15	52	40	644	3100	1.0	695	C-I	COATED
2623	17.0	31.59	2.80	0.180	611.	29.73	45.26	52	40	621	2450	0.5	755	C-I	COATED
2624	17.0	34.02	2.29	0.205	499.	24.29	39.83	52	40	1044	1750	0.2	712	C-I	COATED
2625	18.0	34.02	2.14	0.220	466.	22.68	37.18	52	40	1033	1800	0.2	710	C-I	COATED
2626	18.0	31.59	2.75	0.184	600.	29.23	44.50	52	40	1077	2800	0.6	715	C-I	COATED
2627	18.0	29.15	3.21	0.171	700.	34.07	47.87	52	40	574	4000	1.2	675	C-I	COATED
2628	18.0	24.30	3.58	0.184	781.	38.00	44.50	52	40	555	4600	0.1	675	C-I	COATED
2629	18.0	19.42	3.91	0.210	853.	41.53	38.86	52	40	644	6000	2.8	620	C-I	COATED
2630	14.0	19.44	4.27	0.192	932.	45.36	42.49	52	42	660	3200	2.3	850	C-I	NON COATED
2631	14.0	24.30	3.94	0.167	859.	41.83	48.99	52	42	655	2650	1.6	895	C-I	NON COATED
2632	14.0	29.15	3.42	0.160	745.	36.28	50.93	52	42	633	1850	0.6	905	C-I	NON COATED
2633	14.0	31.59	2.99	0.169	652.	31.75	48.33	52	42	577	1750	0.3	885	C-I	NON COATED
2634	14.0	34.02	1.93	0.244	420.	20.46	33.55	52	42	1033	750	0.1	625	C-I	NON COATED
2635	15.0	19.44	3.99	0.206	870.	42.33	39.65	52	42	666	4300	2.8	560	C-I	NON COATED
2637	15.0	24.30	3.69	0.178	803.	39.11	45.80	52	42	644	3450	1.6	670	C-I	NON COATED
2638	15.0	29.15	3.16	0.173	689.	33.56	47.16	52	42	610	2750	0.8	720	C-I	NON COATED

TEST NO.	COMP RATIC	AIR FUEL	I-PWR KW	ISFC GM/KWHR	IMEP KPA	ITQ NM	IEFF %	IGN AN	DE	EGT K	HC PPM	CO %	NOX PPM	TYPE	CATALYST
2639	15.0	31.59	2.63	0.192	574.	27.92	42.50	52	42	577	2450	0.4	715	C-I	NON COATED
2640	15.0	34.02	1.76	0.267	383.	18.65	30.57	52	42	1046	1505	0.2	610	C-I	NON COATED
2641	16.0	19.44	3.89	0.211	849.	41.32	38.71	52	42	655	4850	2.5	610	C-I	NON COATED
2643	16.0	29.15	2.85	0.192	621.	30.24	42.49	52	40	588	3550	1.1	501	C-I	NON COATED
2644	16.0	31.59	2.33	0.217	507.	24.69	37.59	52	40	549	2800	0.6	590	C-I	NON COATED
2645	16.0	34.02	1.61	0.291	352.	17.13	28.09	52	40	1044	2300	0.3	565	C-I	NON COATED
2646	16.0	24.30	3.32	0.198	725.	35.28	41.32	52	40	613	4550	1.9	510	C-I	NON COATED
2647	17.0	19.44	3.56	0.231	776.	37.80	35.41	52	38	655	7100	2.5	580	C-I	NON COATED
2648	17.0	24.30	3.42	0.192	745.	36.28	42.50	52	38	633	4350	2.4	710	C-I	NON COATED
2649	17.0	29.15	3.04	0.180	663.	32.25	45.32	52	38	599	3650	1.1	761	C-I	NON COATED
2650	17.0	31.59	2.71	0.187	590.	28.73	43.73	52	38	533	2850	0.6	724	C-I	NON COATED
2651	17.0	34.02	1.77	0.266	385.	18.75	30.74	52	38	1066	2100	0.3	635	C-I	NON COATED
2652	18.0	19.44	3.42	0.240	745.	36.28	33.99	52	38	644	6700	2.4	525	C-I	NON COATED
2653	18.0	24.30	3.37	0.195	735.	35.78	41.91	52	38	621	4550	2.1	582	C-I	NON COATED
2654	18.0	29.15	2.89	0.190	629.	30.64	43.05	52	38	577	3700	1.1	599	C-I	NON COATED
2655	18.0	31.59	2.47	0.205	538.	26.21	39.89	52	38	544	3300	0.8	538	C-I	NON COATED
2656	18.0	34.02	1.47	0.319	321.	15.62	25.61	52	39	1055	2550	0.4	545	C-I	NON COATED
2657	6.0	14.03	3.70	0.307	807.	39.31	26.40	21	7	713	2500	3.3	65	S-I	NON COATED
2658	6.0	15.03	3.80	0.280	828.	40.32	29.00	22	8	716	2000	2.0	180	S-I	NON COATED
2659	6.0	16.03	3.73	0.267	814.	39.61	30.39	20	9	744	1650	0.8	315	S-I	NON COATED
2660	6.0	17.04	3.65	0.257	795.	38.70	31.56	25	12	733	1200	0.1	355	S-I	NON COATED
2661	6.0	18.04	3.50	0.253	762.	37.09	32.02	22	7	716	800	0.0	500	S-I	NON COATED
2662	8.0	14.03	4.31	0.264	940.	45.76	30.73	18	5	691	3300	5.1	100	S-I	NON COATED
2663	8.0	15.03	4.27	0.249	932.	45.36	32.62	20	5	699	2800	2.7	210	S-I	NON COATED
2664	8.0	16.03	4.26	0.234	928.	45.15	34.64	20	5	710	2250	0.9	290	S-I	NON COATED
2665	8.0	17.04	4.18	0.224	911.	44.35	36.17	18	5	710	1400	0.0	400	S-I	NON COATED

TEST NO.	COMP RATIO	AIR FUEL	I-PWR KW	ISFC GM/WHR	IMEP KPA	ITQ NM	IEFF %	IGN AN	IGN DE	EGT K	HC PPM	CO %	NOX PPM	TYPE	CATALYST
2666	8.0	18.04	3.85	0.230	839.	40.82	35.24	23	8	699	1300	0.0	500	S-I NON COATED	
2667	10.0	14.03	4.37	0.261	952.	46.36	31.13	17	4	630	3250	6.0	50	S-I NON COATED	
2668	10.0	15.03	4.42	0.241	963.	46.87	33.71	16	1	633	2700	3.4	110	S-I NON COATED	
2669	10.0	16.03	4.45	0.224	969.	47.17	36.18	17	5	641	2300	1.8	170	S-I NON COATED	
2670	10.0	17.04	4.39	0.214	957.	46.57	37.97	18	4	646	2250	0.4	300	S-I NON COATED	
2671	10.0	18.04	4.32	0.205	942.	45.86	39.59	17	6	641	1550	0.0	310	S-I NON COATED	
2672	6.0	14.03	3.72	0.306	812.	39.51	26.53	21	8	721	3000	3.2	95	S-I COATED	PLATINUM
2673	6.0	15.03	3.74	0.284	816.	39.71	28.56	23	10	721	2550	2.1	215	S-I COATED	PLATINUM
2674	6.0	16.03	3.61	0.276	787.	38.30	29.38	26	13	727	2100	0.5	315	S-I COATED	PLATINUM
2675	6.0	17.04	3.56	0.263	776.	37.80	30.82	26	13	724	1450	0.1	390	S-I COATED	PLATINUM
2676	6.0	18.04	3.42	0.259	745.	36.28	31.32	27	13	708	1350	0.1	460	S-I COATED	PLATINUM
2677	8.0	14.03	4.27	0.265	932.	45.36	30.45	18	5	683	3900	4.8	95	S-I COATED	PLATINUM
2678	8.0	14.99	4.22	0.253	919.	44.75	32.11	20	4	694	3350	2.5	215	S-I COATED	PLATINUM
2679	8.0	16.03	4.18	0.238	911.	44.35	34.02	20	5	702	2900	0.9	355	S-I COATED	PLATINUM
2680	8.0	17.04	4.04	0.232	880.	42.84	34.93	20	7	699	2250	0.1	415	S-I COATED	PLATINUM
2681	8.0	18.04	3.87	0.229	843.	41.02	35.41	23	10	683	2000	0.1	450	S-I COATED	PLATINUM
2682	8.0	19.04	3.70	0.227	805.	39.21	35.72	21	9	669	2010	0.1	430	S-I COATED	PLATINUM
2683	8.0	20.05	3.51	0.227	766.	37.29	35.78	27	14	652	1850	0.1	700	S-I COATED	PLATINUM
2684	8.0	21.05	3.24	0.234	706.	34.37	34.62	33	8	598	2015	0.1	335	S-I COATED	PLATINUM
2685	8.0	22.05	2.75	0.264	598.	29.13	30.73	33	8	533	9999	99.9	9999	S-I COATED	PLATINUM
2686	10.0	14.03	4.26	0.268	928.	45.15	30.32	19	3	635	5150	5.4	105	S-I COATED	PLATINUM
2687	10.0	15.03	4.37	0.243	952.	46.36	33.35	16	5	644	4400	2.7	200	S-I COATED	PLATINUM
2688	10.0	16.03	4.27	0.233	932.	45.36	34.79	17	6	652	3500	1.1	290	S-I COATED	PLATINUM
2689	10.0	17.04	4.18	0.224	911.	44.35	36.17	18	8	655	3150	0.2	465	S-I COATED	PLATINUM
2690	10.0	18.04	4.08	0.217	890.	43.34	37.42	16	8	646	1500	0.7	620	S-I COATED	PLATINUM
2691	10.0	19.04	3.91	0.214	853.	41.53	37.83	18	9	630	2250	0.1	630	S-I COATED	PLATINUM

TEST NO.	COMP RATIO	AIR FUEL	I-PWR KW	ISFC GM/WHR	IMEP KPA	ITQ NM	IEFF %	IGN AN	IGN DE	EGT K	HC PPM	CO %	NOX PPM	TYPE	CATALYST
2692	14.0	19.44	3.56	0.231	776.	37.80	35.41	53	43	677	2200	1.8	100	C-I COATED	PLATINUM
2693	14.0	24.30	3.37	0.195	735.	35.78	41.91	53	43	669	1600	1.2	115	C-I COATED	PLATINUM
2694	14.0	29.15	2.79	0.196	609.	29.63	41.64	53	43	602	1500	0.3	130	C-I COATED	PLATINUM
2695	14.0	31.59	2.04	0.248	445.	21.67	32.99	53	45	549	1150	0.2	100	C-I COATED	PLATINUM
2696	14.0	34.02	0.71	0.659	155.	7.56	12.39	53	43	999	225	0.1	30	C-I COATED	PLATINUM
2697	15.0	19.44	3.66	0.225	797.	38.80	36.35	53	41	256	2750	3.0	93	C-I COATED	PLATINUM
2698	15.0	24.30	3.13	0.210	683.	33.26	38.95	53	41	666	2250	1.5	75	C-I COATED	PLATINUM
2699	15.0	29.15	2.75	0.199	600.	29.23	41.07	53	41	633	1600	0.9	155	C-I COATED	PLATINUM
2700	15.0	31.59	2.08	0.243	453.	22.07	33.60	53	43	544	1300	0.0	115	C-I COATED	PLATINUM
2701	15.0	34.02	0.77	0.610	168.	8.16	13.39	53	43	999	625	0.1	60	C-I COATED	PLATINUM
2702	16.0	19.44	3.54	0.232	772.	37.59	35.22	53	41	671	3100	2.3	115	C-I COATED	PLATINUM
2703	16.0	24.30	3.19	0.206	696.	33.87	39.66	53	41	660	2100	1.2	125	C-I COATED	PLATINUM
2704	16.0	29.15	2.66	0.205	580.	28.22	39.65	53	41	605	2150	0.1	110	C-I COATED	PLATINUM
2705	16.0	31.59	1.86	0.272	406.	19.75	30.07	52	42	1077	1700	0.5	80	C-I COATED	PLATINUM
2706	16.0	34.02	0.80	0.589	174.	8.47	13.88	53	41	988	700	0.1	35	C-I COATED	PLATINUM
2707	17.0	19.44	3.37	0.244	735.	35.78	33.52	53	40	655	4500	2.8	60	C-I COATED	PLATINUM
2708	17.0	24.30	2.75	0.239	600.	29.23	34.23	51	41	613	2500	1.4	80	C-I COATED	PLATINUM
2709	17.0	29.15	2.04	0.268	445.	21.67	30.45	51	41	552	2100	1.0	55	C-I COATED	PLATINUM
2710	17.0	31.59	1.16	0.436	253.	12.30	18.72	51	41	1010	880	0.1	32	C-I COATED	PLATINUM
2711	17.0	34.02	0.09	4.944	21.	1.01	1.65	51	41	938	820	0.0	10	C-I COATED	PLATINUM
2712	18.0	19.44	3.25	0.253	708.	34.47	32.29	53	40	652	5800	2.8	60	C-I COATED	PLATINUM
2713	18.0	24.30	2.99	0.220	652.	31.75	37.18	53	40	658	4000	2.0	85	C-I COATED	PLATINUM
2714	18.0	29.15	2.58	0.212	563.	27.42	38.52	53	41	610	2800	1.1	50	C-I COATED	PLATINUM
2715	18.0	31.59	2.04	0.248	445.	21.67	32.99	53	41	546	2300	0.6	25	C-I COATED	PLATINUM
2716	18.0	34.02	0.19	2.472	41.	2.02	3.31	53	41	1021	320	0.1	50	C-I COATED	PLATINUM
2717	6.0	18.04	3.37	0.263	735.	35.78	30.89	24	11	733	1100	0.0	710	S-I COATED	CERIUM

TEST NO.	COMP RATIO	AIR FUEL	I-PWR KW	ISFC GM/WHR	IMEP KPA	ITQ NM	IEFF %	IGN AN	IGN DE	EGT K	HC PPM	CO %	NOX PPM	TYPE	CATALYST
2718	6.0	17.04	3.51	0.267	764.	37.19	30.33	25	1	735	1450	0.2	590	S-I COATED	CERIUM
2719	6.0	16.03	3.58	0.278	781.	38.00	29.15	24	4	730	2100	1.2	475	S-I COATED	CERIUM
2720	6.0	15.03	3.65	0.291	795.	38.70	27.84	21	4	710	2700	3.2	320	S-I COATED	CERIUM
2721	6.0	14.03	3.69	0.309	803.	39.11	26.26	23	4	699	3200	5.4	215	S-I COATED	CERIUM
2722	8.0	18.04	3.78	0.234	824.	40.11	34.63	22	5	705	1500	0.0	730	S-I COATED	CERIUM
2723	8.0	17.04	3.94	0.238	859.	41.83	34.11	20	5	721	2200	0.2	600	S-I COATED	CERIUM
2724	8.0	16.03	3.98	0.250	868.	42.23	32.40	20	4	713	2700	2.0	620	S-I COATED	CERIUM
2725	8.0	15.03	4.01	0.265	874.	42.53	30.60	17	7	705	3150	3.4	230	S-I COATED	CERIUM
2726	8.0	14.03	4.07	0.280	886.	43.14	28.97	19	8	691	3600	6.1	80	S-I COATED	CERIUM
2727	10.0	18.04	4.13	0.214	901.	43.84	37.85	19	7	674	2200	0.1	490	S-I COATED	CERIUM
2728	10.0	17.04	4.19	0.224	913.	44.45	36.25	16	5	683	2750	0.7	330	S-I COATED	CERIUM
2729	10.0	16.03	4.19	0.238	913.	44.45	34.10	16	5	671	3250	2.8	175	S-I COATED	CERIUM
2730	10.0	15.03	4.20	0.253	915.	44.55	32.04	19	7	666	3650	3.8	120	S-I COATED	CERIUM
2731	10.0	14.03	4.20	0.271	915.	44.55	29.92	17	7	660	4450	6.0	80	S-I COATED	CERIUM
2732	14.0	19.44	2.80	0.293	611.	29.73	27.85	53	43	633	2800	2.4	80	C-I COATED	CERIUM
2733	14.0	24.30	2.66	0.247	580.	28.22	33.05	53	43	671	2200	1.2	100	C-I COATED	CERIUM
2734	14.0	29.15	2.18	0.251	476.	23.18	32.57	53	43	630	1800	0.5	110	C-I COATED	CERIUM
2735	14.0	31.59	1.72	0.294	375.	18.24	27.77	53	45	571	1400	0.2	35	C-I COATED	CERIUM
2736	14.0	34.02	0.79	0.596	172.	8.37	13.72	53	45	256	650	0.1	25	C-I COATED	CERIUM
2737	15.0	19.44	2.74	0.300	596.	29.03	27.19	53	41	677	2550	2.8	90	C-I COATED	CERIUM
2738	15.0	24.30	2.56	0.256	559.	27.21	31.87	53	42	655	1800	1.5	110	C-I COATED	CERIUM
2739	15.0	29.15	2.15	0.255	468.	22.78	32.01	53	42	671	1700	0.4	100	C-I COATED	CERIUM
2740	15.0	31.59	1.61	0.313	352.	17.13	26.08	53	43	533	1600	0.2	120	C-I COATED	CERIUM
2741	15.0	34.02	0.80	0.589	174.	8.47	13.88	53	44	1005	850	0.1	85	C-I COATED	CERIUM
2742	16.0	19.44	2.85	0.288	621.	30.24	28.32	53	42	671	2700	2.6	120	C-I COATED	CERIUM
2743	16.0	24.30	2.54	0.259	553.	26.91	31.52	53	42	644	1500	1.4	115	C-I COATED	CERIUM

TEST NO.	COMP RATIO	AIR FUEL	I-PWR KW	ISFC GM/KWHR	IMEP KPA	ITQ NM	IEFF %	IGN AN	IGN DE	EGT K	HC PPM	CO %	NOX PPM	TYPE	CATALYST
2744	16.0	29.15	2.09	0.262	456.	22.17	31.15	53	42	621	1700	0.5	125	C-I COATED	CERIUM
2745	16.0	31.59	1.49	0.339	325.	15.82	24.09	53	43	555	1550	0.2	100	C-I COATED	CERIUM
2746	16.0	34.02	0.76	0.618	166.	8.06	13.22	53	44	1019	880	0.1	65	C-I COATED	CERIUM
2747	17.0	19.44	2.66	0.309	580.	28.22	26.44	53	41	256	3750	2.6	80	C-I COATED	CERIUM
2748	17.0	24.30	2.33	0.232	507.	24.69	28.92	53	41	655	3000	1.6	50	C-I COATED	CERIUM
2749	17.0	29.15	1.82	0.300	398.	19.35	27.19	53	42	256	2000	0.7	90	C-I COATED	CERIUM
2750	17.0	31.59	1.42	0.355	311.	15.12	23.02	53	42	533	1500	0.3	70	C-I COATED	CERIUM
2751	17.0	34.02	0.66	0.705	145.	7.06	11.57	53	42	988	800	0.1	40	C-I COATED	CERIUM
2752	18.0	19.44	2.56	0.320	559.	27.21	25.49	53	41	666	3600	2.5	70	C-I COATED	CERIUM
2753	18.0	24.30	2.39	0.275	522.	25.40	29.75	53	41	644	2600	1.4	86	C-I COATED	CERIUM
2754	18.0	29.15	1.80	0.304	393.	19.15	26.91	53	41	577	1750	0.9	110	C-I COATED	CERIUM
2755	18.0	31.59	1.28	0.394	280.	13.61	20.71	53	41	1066	1400	0.2	100	C-I COATED	CERIUM
2756	18.0	34.02	0.28	1.648	62.	3.02	4.96	53	41	1013	900	0.1	85	C-I COATED	CERIUM